Self-Consolidating Concrete (SCC) and High-Volume Fly Ash Concrete (HVFAC) for Infrastructure Elements: Implementation

Report C - Implementation of HVFA Concrete from Laboratory Studies into Bridge Application

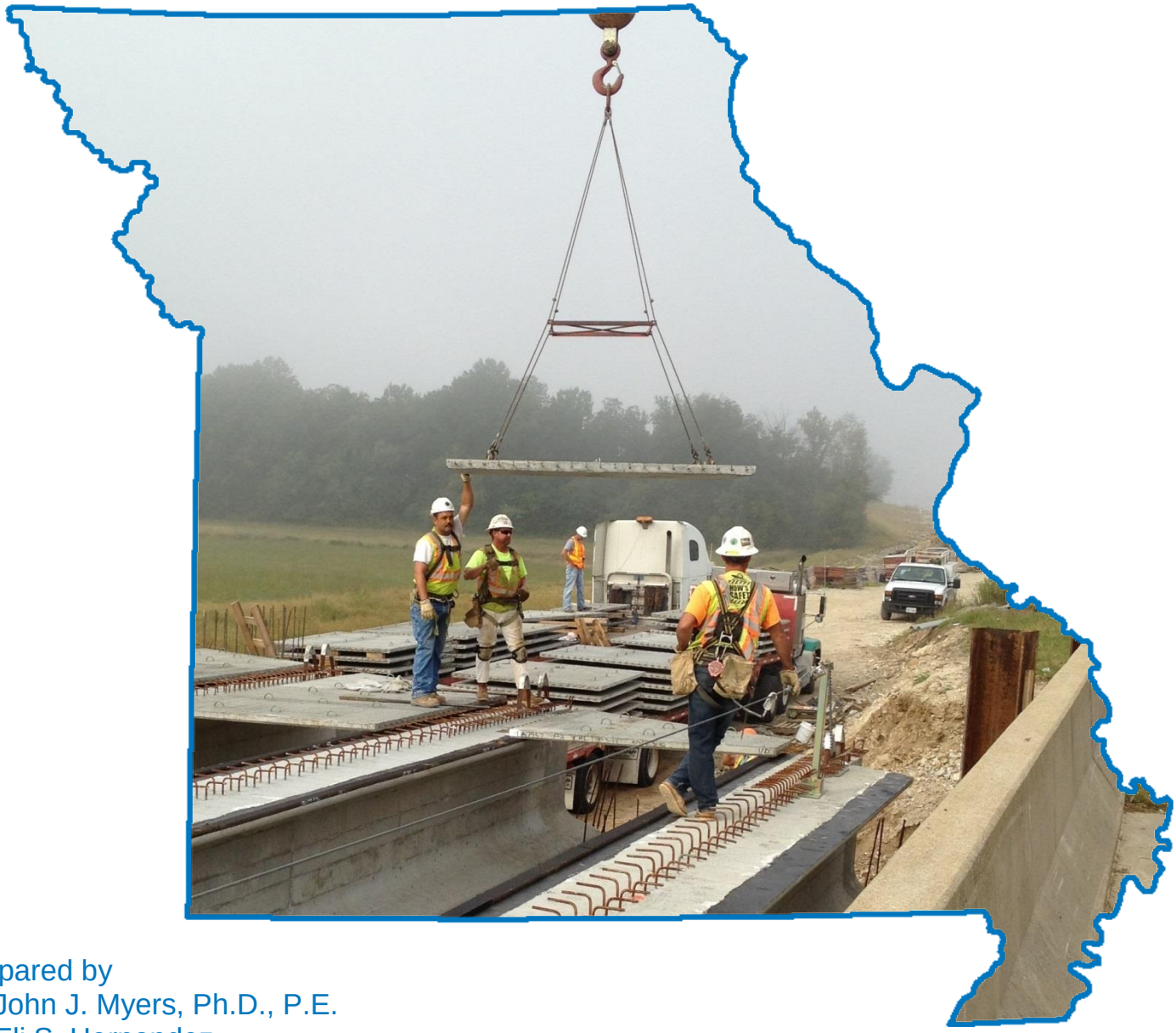

Prepared by

John J. Myers, Ph.D., P.E.
Eli S. Hernandez
Hayder Alghazali
Alexander Griffin
Kaylea Smith
Missouri University of Science & Technology

Final Report Prepared for Missouri Department of Transportation

June 2016 Project TR201236 Report cmr16-011C

TECHNICAL REPORT DOCUMENTATION PAGE

1. Report No.	2. Government Accession No.	3. Recipient's Catalog No.
cmr 16-011C		

4. Title and Subtitle
Self-Consolidating Concrete (SCC) and High-Volume Fly Ash Concrete (HVFAC) for Infrastructure Elements: Implementation. Report C, Implementation of HVFA Concrete from Laboratory Studies into Bridge Application

5. Report Date
March 2016
Published: June 2016

6. Performing Organization Code

7. Author(s)
John J. Myers, Ph.D., P.E. http://orcid.org/0000-0001-5269-8218, Eli S. Hernandez, Hayder Alghazali, Alexander Griffin, Kaylea Smith

8. Performing Organization Report No.

9. Performing Organization Name and Address
Missouri University of Science and Technology
Department of Civil, Architectural, and Environmental Engineering
325 Civil Engineering
Rolla, MO 65409

10. Work Unit No.

11. Contract or Grant No.
MoDOT project #TRyy1236
NUTC project # 00040350
USDOT contract # DTRT06-G-0014

12. Sponsoring Agency Name and Address
Missouri Department of Transportation (SPR) http://dx.doi.org/10.13039/100007251
Construction and Materials Division
P.O. Box 270
Jefferson City, MO 65102

Center for Transportation Infrastructure and Safety/NUTC program
Missouri University of Science and Technology
220 Engineering Research Lab
Rolla, MO 65409

13. Type of Report and Period Covered
Final report (October 2012-March 2016)

14. Sponsoring Agency Code

15. Supplementary Notes
Conducted in cooperation with the U.S. Department of Transportation, Federal Highway Administration. MoDOT research reports are available in the Innovation Library at http://www.modot.org/services/or/byDate.htm. This set of reports is available at https://library.modot.mo.gov/RDT/reports/TR201236/.

16. Abstract
This study was performed to examine the effects of cement replaced by high volumes of Class C fly-ash on durability characteristics of concrete up to 120 days. Specifically, this study investigates possibility of amending American Society for Testing and Materials (ASTM) to allow High Volume Fly-ash (HVFA) concrete to cure until later ages prior to testing instead of 28 days. Five mix designs were compared with varying fly-ash percentages from 0 to 70% (by total cementitious mass). No other additives were present in any of the five mix designs. Water to-cementitious ratio (w/cm) and total cementitious material remained constant as 0.40 and 750 pounds per cubic yard respectively. Both plastic concrete and hardened concrete properties were examined. The replacement of cement by fly-ash resulted in the concrete exhibiting adequate 28 day strength, stiffer moduli, lower chloride permeability, improved resistance to freezing and thawing, and improved abrasion resistance at 50% fly-ash replacement when compared to a baseline mix. At 70% flyash replacement, the concrete never reached equivalent properties to the other mixes. As the age and compressive strength of all mixes increased, so did the abrasion resistance and durability factor. Accelerated curing at 100°F (37.8°C), 130°F (54.4°C), and 160°F (71.1°C) proved to be detrimental to the concrete at all fly-ash levels, with higher temperatures causing increased damage. An increase in compressive strength was seen in the first few days prior to a decrease in compressive strength.

17. Key Words
Cast in place concrete; Cost effectiveness; Durability; High strength concrete; Mix design; Portland cement concrete; Precast concrete; Self compacting concrete

18. Distribution Statement
No restrictions. This document is available through the National Technical Information Service, Springfield, VA 22161.

19. Security Classif. (of this report)	20. Security Classif. (of this page)	21. No. of Pages	22. Price
Unclassified.	Unclassified.	160	

Form DOT F 1700.7 (8-72) Reproduction of completed page authorized

FINAL REPORT C

TRyy1236

Project Title: Self-Consolidating Concrete (SCC) and High-Volume Fly Ash Concrete (HVFAC) for Infrastructure Elements: Implementation

Report C: Implementation of HVFA Concrete from Laboratory Studies into Bridge Application

Prepared for
Missouri Department of Transportation
Construction and Materials

By

Dr. John J. Myers (Project Principal Investigator)
Eli S. Hernandez
Hayder Alghazali
Alexander Griffin
Kaylea Smith

Missouri University of Science and Technology, Rolla, Missouri

March 2016

ABSTRACT

This study was performed to examine the effects of cement replaced by high volumes of Class C fly ash on durability characteristics of concrete up to 120 days. Specifically, this study investigates the possibility of amending American Society for Testing and Materials (ASTM) to allow High Volume Fly Ash (HVFA) concrete to cure until later ages prior to testing instead of 28 days. Five mix designs were compared with varying fly ash percentages from 0 to 70% (by total cementitious mass). No other additives were present in any of the five mix designs. Water-to-cementitious ratio (w/cm) and total cementitious material remained constant as 0.40 and 750 pounds per cubic yard respectively.

Both plastic concrete and hardened concrete properties were examined. The replacement of cement by fly ash resulted in the concrete exhibiting adequate 28-day strength, stiffer moduli, lower chloride permeability, improved resistance to freezing and thawing, and improved abrasion resistance at 50% fly ash replacement when compared to a baseline mix. At 70% fly ash replacement, the concrete never reached equivalent properties to the other mixes. As the age and compressive strength of all mixes increased, so did the abrasion resistance and durability factor.

Accelerated curing at 100°F (37.8°C), 130°F (54.4°C), and 160°F (71.1°C) proved to be detrimental to the concrete at all fly ash levels, with higher temperatures causing increased damage. An increase in compressive strength was seen in the first few days prior to a decrease in compressive strength.

TABLE OF CONTENTS

LIST OF ILLUSTRATIONS

LIST OF TABLES

NOMENCLATURE

Symbol	Description
a	Depth of equivalent stress block (in.)
a_g	Maximum aggregate size (in.)
A_c	Area of concrete section (in.^{2})
A_{ps}	Area of prestressing steel (in.^{2})
A_s	Area of non-prestressing longitudinal steel (in.^{2})
A_v	Area of shear reinforcement (in.^{2})
b_w	Web thickness (in.)
b_v	Effective web width (in.)
c	Distance from extreme compressive fiber to neutral axis (in.)
c	Number of freeze-thaw cycles
DF	Durability factor
d_p	Depth from extreme compression fiber to centroid of prestressing tendons (in.)
d_s	Distance from extreme compression fiber to centroid of non-prestressed tensile reinforcement (in.)
d_v	Effective shear depth, taken as the perpendicular distance between resultants of tensile and compressive forces due to flexure (in.)
E_c	Modulus of elasticity of concrete (psi)
E_{ct}	Modulus of elasticity of concrete at transfer (psi)
E_p	Modulus of elasticity of prestressing steel (ksi)
E_s	Modulus of elasticity of non-prestressing steel (ksi)
f'_c	Specified design concrete compressive strength (ksi)
f'_{ci}	Compressive strength of concrete at release (psi)

f_{cgp}	Concrete stress at centroid of prestressing steel due to prestressing force after elastic losses and member self-weight (ksi)
f_{pc}	Compressive stress at the centroid of the concrete section due to the effective prestress force (psi)
f_{po}	Locked in difference in strain between the prestressing steel and the surrounding concrete multiplied by the modulus of elasticity of the prestressing steel (ksi)
f_{pt}	Stress in prestressing strands immediately after transfer (ksi)
f_r	Modulus of rupture of concrete (psi)
f_y	Specified yield strength of shear reinforcement (ksi)
f_{pe}	Effective stress in the prestressing steel after losses (ksi)
f_{py}	Yield stress of prestressing steel (ksi)
h	Total depth of member (in.)
H	Relative humidity (%)
h_c	Total depth of composite member (in.)
I_c	Gross moment of inertia of composite section (in.^{4})
I_g	Gross moment of inertia of girder (in.^{4})
k_f	Factor for strength of concrete at release
K_{df}	Transformed section coefficient that accounts for time dependent interaction between concrete and bonded steel for time period between deck placement and final time
k_{hc}	Humidity factor for creep
k_{hs}	Humidity factor for shrinkage
K_{id}	Transformed section coefficient that accounts for time dependent interaction between concrete and bonded steel for time period between transfer and deck placement
K_L	Factor for type of prestressing steel

k_s	Factor accounting for V/S of concrete section
k_{td}	Time development factor
M_{cr}	Flexural cracking moment (k-ft)
M_{cr}	Flexural cracking moment due to applied loads (k-ft)
M_{fl}	Nominal moment capacity as noted in Kani (1967) (k-ft)
MAS	Maximum Aggregate Size
M_{max}	Maximum applied moment at section due to externally applied loads (k-ft)
M(t)	Maturity index (expressed in degree-days or degree-hours)
M_u	Factored moment at section (k-ft)
n	fundamental transverse frequency at 0 cycles
n	frequency of freeze-thaw cycles (1/T)
N_u	Factored axial force at section (kips)
P_c	Relative dynamic modulus at c freeze-thaw cycles
P_e	Effective prestress force (ksi)
P_Δ	Prestress force lost due to long term prestress losses before deck placement (kips)
Q	activation energy divided by the gas constant expressed in Kelvin degrees (°K)
r_u	Relative strength of member
s	Center to center spacing of shear reinforcement (in.)
s_x	Cracking spacing parameter (in.)
s_{xe}	Equivalent value of s_x taking into account the MAS
T	Time of one-pulse wave in micro seconds at c freeze-thaw cycles
T	Average concrete temperature during the interval Δt
T_a	Average temperature of the concrete during a time interval

T_0	Datum temperature
t	Age of specimen (days)
t_d	Age of concrete at deck placement (days)
te	Equivalent age over a time interval (DT) at a specified temperature in days or hrs
t_f	Age of concrete at final time (days)
t_i	Age of concrete at transfer (days)
V/S	Volume to surface ratio (in.)
V_c	Nominal concrete shear resistance (kips)
V_{ci}	Nominal shear resistance when diagonal cracking results from applied shear and moment (kips)
V_{cw}	Nominal shear resistance when diagonal cracking results from high principle stresses in the web (kips)
V_d	Applied shear force at section due to unfactored dead load (kips)
V_i	Factored shear force at section due to externally applied loads (kips)
V_n	Nominal shear resistance (kips)
V_p	Component of prestressing force in the direction of shear force (kips)
V_s	Nominal shear reinforcement resistance (kips)
V_u	Factored shear force at section (kips)
w	AASHTO unit weight of concrete (k/ft^3)
w/cm	Water to cement ratio
w_c	ACI unit weight of concrete (lb/ft^3)
α	Angle of inclination of shear reinforcement to longitudinal reinforcement (degree)
β	Factor indicating ability of diagonally cracked concrete to transmit tension

ε_{bdf}	Concrete shrinkage strain of girder between time of deck placement and final time
ε_{bid}	Concrete shrinkage strain of girder between time of transfer and deck placement
ε_{ddf}	Concrete shrinkage strain of deck between placement and final time
ε_s	Net longitudinal strain at centroid of longitudinal reinforcement
Δf_{cd}	Change in concrete stress at centroid of prestressing strands due to shrinkage of deck concrete (ksi)
Δf_{cdf}	Change in concrete stress at centroid of prestressing strands due to long term losses between transfer and deck placement combined with deck weight and superimposed loads (ksi)
Δf_{pCD}	Prestress losses due to creep of CIP deck concrete (ksi)
Δf_{pCR}	Prestress losses due to creep of girder concrete (ksi)
Δf_{pES}	Elastic shortening prestress losses (ksi)
Δf_{pR1}	Prestress losses due to relaxation of tendons before placement of CIP deck (ksi)
Δf_{pR2}	Prestress losses due to relaxation of tendons after placement of CIP deck (ksi)
Δf_{pSD}	Prestress losses due to shrinkage of concrete after placement of CIP deck (ksi)
Δf_{pSR}	Prestress losses due to shrinkage of concrete before placement of CIP deck (ksi)
Δf_{pSR}	Prestress gain due to shrinkage of CIP deck (ksi)
ΔT	time interval (expressed in days or hours)
ϕ	Shear resistance factor
μ	Concrete mixture plastic viscosity
λ	Reduction factor for lightweight concrete
θ	Angle of inclination of diagonal compressive stress (degrees)

τ_0	Concrete mixture yield stress
AASHTO	American Association of State Highway and Transportation Officials
ACI	American Concrete Institute
ASTM	American Society for Testing and Materials
CA	Coarse aggregate
CC	Conventional concrete
CIP	Cast in place
CR	Creep
DOT	Department of Transportation
EPG 751	Engineering Policy Guide section 751 from the Missouri Department of Transportation
FA	Fine aggregate
FEA	Finite element analysis
FEM	Finite element model
HS-SCC	High strength self-consolidating concrete
HSC	High strength concrete
HRWR	High range water reducer
HRWRA	High range water reducing admixture
LRFD	Load and resistance factored design
MoDOT	Missouri Department of Transportation
MOE	Modulus of elasticity
MOR	Modulus of rupture
MS	Mild steel shear reinforcement
NCHRP	National Cooperative Highway Research Program

NU	Nebraska University
PC/PS	Precast prestressed concrete
QC/QA	Quality control/quality assurance
R2K	Response 2000
RC	Reinforced concrete
SCC	Self-consolidating concrete
SERL	Structural Engineering Research Laboratory
SH	Shrinkage
T1	First test conducted on each girder, with shear reinforcement
T2	Second test conducted on each girder, without shear reinforcement
TG1	Test girder 1, consisting of WWR shear reinforcement
TG2	Test girder 2, consisting of MS shear reinforcement
WWR	Welded wire mesh shear reinforcement.

1. INTRODUCTION

1.1. BACKGROUND

The production of Portland cement generates roughly one pound of carbon dioxide per every pound of cement produced that exits to the atmosphere (Malhorta, 2010). This is an issue because concrete, aside from water, is the most consumed material in the world and Portland cement is a key component. With that being said, sustainability is a concern. By introducing pozzolanic material (slag, fly ash, silica fume, etc.) as a replacement for cement in concrete, the emission of CO_2 can be controlled. However, a reduction of carbon emissions is not the only benefit to cement replacement. Introducing pozzolans to a concrete mixture can improve durability and workability, reduce early heat of hydration, and often times increase later age strength. Aside from these characteristics, using Supplementary Cementitious Materials (SCM) in concrete mixtures can prove to be financially beneficial as well. Introducing SCM can produce direct savings in cost of materials and sustainability resulting in longer life span of the structure. As well as direct savings, eventually every nation will have to consider indirect savings such as resource preservation and reduced pollution through emissions and landfill space. As of 2005, U.S. coal-fired power plants reported producing 71.1 million tons of fly ash, of which 29.1 (40%) million tons were reused in various applications (Mehta and Monteiro, 2006). If the nearly 42 million tons of unused fly ash had been recycled, it would have reduced the need for approximately 27,500 acre-ft. (33,900,000 m^3) of landfill space. Similarly, in 2012, the American Coal Ash Association's (ACAA) 2012 Coal Combustion Production & Use Survey Report showed there was 52.1 million tons of fly ash produced and 46% was recycled in concrete products alone Figure 1.1.

Many researchers have investigated the effects of incorporating fly ash into concrete mixtures. Substitution of cement by fly ash has many advantages and disadvantages. By replacing the cement with fly ash, the concrete may see benefits such as increased workability, increased long-term strength and sometimes increased durability characteristics. Alternatively, introducing fly ash in proportions greater than 50%, some disadvantages may occur. These disadvantages include delayed setting time, decreased rate of strength gain and some durability issues.

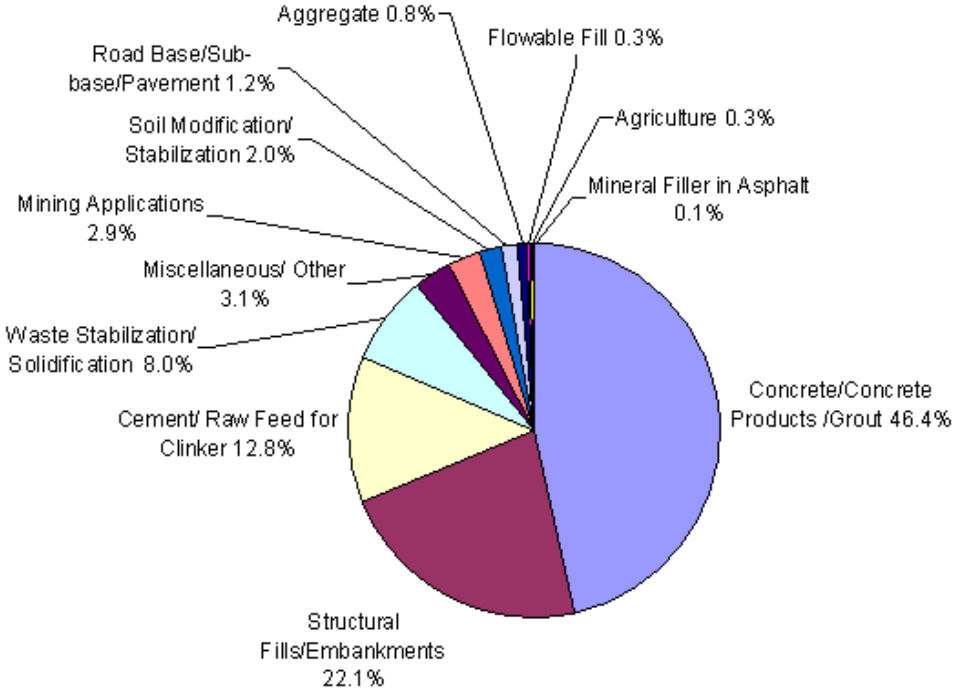

Figure 1.1. Allocation of Recycled Fly Ash (ACAA, 2012)

There is significant documented works on the effect of fly ash on durability characteristics at 28 days, but limited works at later ages (56, 90, 120 days) and no reported works on the applicability of specified American Society for Testing Methods (ASTM) specification test ages for high volume fly ash (HVFA) concretes. There are many reasons for investigation of the effect of fly ash replacement on durability characteristics especially in the Midwest. For bridge decks in Missouri specifically, durability is an important factor. Missouri undergoes a number of freeze-thaw (F&T) cycles each year which is an issue within itself. Furthermore, when the roads freeze over, MoDOT places de-icing salts which may also cause durability related issues. Along with freeze-thaw and permeability concerns, abrasion (of many forms) is a common problem

1.2. RESEARCH OBJECTIVES

It may be considered highly desirable to replace cement by fly ash in percentages greater than 50 for environmental sustainability and fiscal reasons. However, when replacing at high levels, disadvantages may occur. The purpose of this study is to examine the effects of fly ash on strength and durability at a replacement rate of cement

up to 70% at later ages of testing. The emphasis of this study is to determine the appropriate age at which to test HVFA concrete for each durability investigation. Once each characteristic is assessed, recommendations are made to amend ASTM standards to allow later age testing according to the durability aspect in question. Properties that are assessed in this study include, slump, air content, density, temperature, compressive strength, modulus of elasticity, abrasion resistance, freeze-thaw durability, and chloride ion penetration resistance.

1.3. SCOPE OF RESEARCH

This study reviews the effect of HVFA on concrete properties at testing ages of 28 days and beyond. Fresh properties assessed are slump, air content, temperature and density. Hardened properties included abrasion resistance, durability factor by freezing and thawing, and chloride ion penetration resistance. Accelerated curing temperatures (100°F (37.8°C), 130°F (54.4°C), and 160°F (71.1°C)) are also assessed to examine the possibility of obtaining properties at 70% similar to properties of a conventional mix at 28 days.

1.4. REPORT ORGANIZATION

This report is organized into five sections. Section 1 is an introduction to this study related to the effect of using HVAF on concrete properties, the research objective, and the scope of this research.

Section 2 presents a literature review that includes the following subject areas: production, classification and physical attributes of fly ash, effects of fly ash on fresh and hardened concrete properties, a review of the maturity method, effects of accelerated curing on hardened and durability concrete properties, and a brief description of the Bridge A7957 implementation project.

The experimental work is described in Section 3. This discussion includes the experimental design, equipment and materials employed, and test procedures used at the Missouri University of Science and Technology (Missouri S&T) Butler-Carlton Hall Structural Engineering Research Laboratory (SERL).

Section 4 includes test results and discussion. The conclusions obtained in this study, as well as recommendations and future research, are presented in Section 5. Appendices A through D are located at the end of this report, which include supplemental details and information.

2. LITERATURE REVIEW

2.1. FLY ASH

A pozzolan is a siliceous or aluminous material that reacts with Calcium Hydroxide in the presence of water to form compounds similar to that of calcium silicate hydrate (C-S-H). Pozzolans are widely used as supplementary cementitious materials (SCM). Fly ash, in particular, is the most commonly used SCM for concrete applications. Fly ash is used in about 60% of ready mixed concrete (PCA 2000). Various fly ash classes are known to drastically improve durability characteristics such as freeze- thaw resistance, permeability, abrasion resistance, and chloride/chemical penetration of concrete, while others enhance strength and other mechanical properties.

2.1.1. Production

ACI Committee 116 defines fly ash as "the finely divided residue resulting from the combustion of ground or powdered coal, which is transported from the firebox through the boiler by flue gases." Simply put, fly ash is the by-product of coal-fired power plants. By using fly ash in concrete the material is diverted from the waste stream (500 million tons of Fly ash produced a year in the world) and reduces the energy investment in producing virgin materials. Fly ash emits far less CO_2 than cement does (1:8.7 CO_2/ton) (PCA 1988).

2.1.2. Classification

Fly ash has two prominently used classifications, Class C and Class F. The burning of lignite or sub-bituminous coal produces Class C fly ash. Class F fly ash is produced from burning anthracite and bituminous coal. Table 2.1 shows the requirements in composition in Class C and F fly ash. Fly ash is mostly comprised of silicon dioxide (SiO_2), aluminum oxide (Al_2O_3) and iron oxide (Fe_2O_3). Loss on ignition refers to the carbon content. Minor constituents in the chemical make-up are magnesium, sulfur, sodium, potassium, and carbon. Crystalline compounds are present in small amounts. More than 5 percent carbon in a fly ash meant for use as a mineral admixture in concrete is considered undesirable because the cellular particles of carbon tend to increase both the

water requirement for a given consistency and the admixture requirement for air entrainment. Variations in the carbon content of fly ash are a major problem in controlling the quality of sintered fly ash aggregate. ASTM 618 (AASHTO M-295) is the specification for fly ash. Class F and Class C fly ashes are commonly used as pozzolanic admixtures for general purpose concrete (MRS Proceedings 1989). Class C fly ash is readily available in the Midwest.

Table 2.1. Chemical Composition Requirements (ASTM C618-12, FHWA 2007)

Property	Class C (%)	Class F (%)
SiO_2, Al_2O_3, Fe_2O_3, min	50	70
SO_3, max	5	5
Moisture content, max	3	3
Loss on Ignition, max	6	6

Class F materials are generally low-calcium (less than 10% CaO) fly ashes with carbon contents usually less than 5%, but some may be as high as 10%. Class C materials are often high-calcium (10% to 30% CaO) fly ashes with carbon contents less than 2%. Many Class C ashes when exposed to water will hydrate and harden in less than 45 minutes. Some fly ashes meet both Class F and Class C classifications.

Class F fly ash is often used at dosages of 15% to 25% by mass of cementitious. Dosage varies with the reactivity of the ash and the desired effects on the concrete (Helmuth, 1987 and ACI 232, 1996). Class C fly ash is more commonly used in concrete applications due to its self-cementing characteristics. Self-cementing meaning it will harden and gain strength over time. Class F fly ash, on the other hand, often needs an activator.

2.1.3. Physical Attributes

During combustion, the coal's mineral impurities (such as clay, feldspar, quartz, and shale) fuse in suspension and are carried away from the combustion chamber by the

exhaust gases. While the fused material is carried away, it cools and solidifies into spherical glassy particles called fly ash (Figure 2.1a). The dirty appearance in Figure 2.1b is due to the deposition of alkali sulfates on the surface of the glassy spherical fly ash particles (Mehta and Monteiro, 2006).

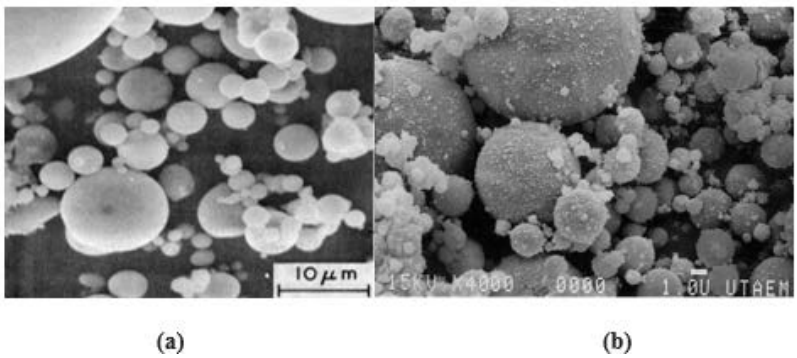

Figure 2.1. Fly Ash Under Magnifications (a) Scanning Electron Micrographs of Typical Class F Fly Ash: Spherical Glassy Particles; (b) Fly Ash at 4000x Magnification (Mehta and Monteiro, 2006)

Fly ash particles are grey or tan and are mainly solid spheres but some are hollow cenospheres. Also present are plerospheres, which are spheres containing smaller spheres.

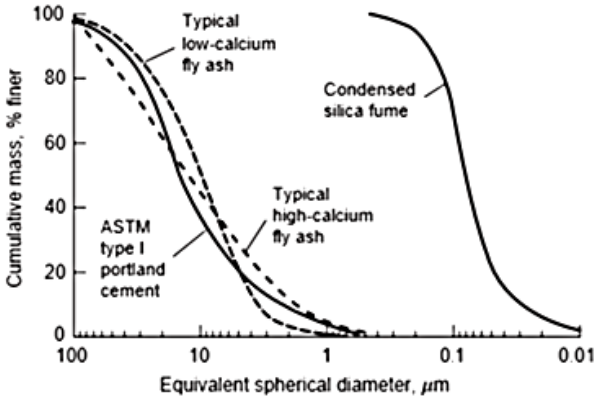

Figure 2.2. Size Comparison of Particles (Mehta and Monteiro, 2006)

Fifty percent by mass of fly ash particles are less than 20 μm (7.87 * 10-4 in) however; particle size distribution studies show that the particles in a typical fly ash sample vary from < 1 μm (3.94 * 10-5 in) to nearly 100 μm (3.94 * 10-3 in) in diameter.

Particles larger than 45 μm (1.77 * 10-3 in) can cause hydration issues leading to problems with the concrete. Figure 2.2 compares particle size distribution with Portland cement and silica fume. The particle size distribution, morphology, and surface characteristics of the fly ash selected for use as a mineral admixture exercise a considerable influence on the water requirement and workability of fresh concrete, and rate of strength development in hardened concrete.

2.2. EFFECT OF FLY ASH ON FRESH CONCRETE PROPERTIES

When cement is substituted in a concrete mixture, the properties of the concrete will change. This section discusses those changes present prior to hardening.

2.2.1. Heat of Hydration

One benefit of including SCM in concrete mixes is the little amount of heat produced early upon hydration. Cement starts hydration almost immediately after contact with water. This is, however, not the case with HVFA concrete. Fly ash retards the hydration of the concrete. This means the placing temperature will also be lower than conventional concrete. Fly ash retards the hydration of the concrete mix (Figure 2.3, Mehta and Monteiro, 2006) producing low heat early. However, the high calcium fly ash mix surpasses the conventional mix approximately 17 hours. In another study, Langan et al., (2002), the effects of fly ash replacement and water-to-cementitious (w/cm) ratio was compared. In this study, fly ash actually increased the heat of hydration in the first few minutes at lower w/cm ratios, but the hydration in the dormant period was reduced drastically. Also, as the w/c ratio increased, the retardation increased as well. Once the dormant period had been completed, an accelerated hydration period was observed.

In this same study, they reported that at 72 hrs, the mix with 20% fly ash and w/c=0.35 produced 59.1 kcal/kg (107.2 Btu/lb_m) when using Type 10 Portland cement. With the hydration of Portland cement however, the majority of hydration occurs within 1-3 days, and Neville (2003) reports at 72 hrs that Type I produced 68.1 kcal/kg (124.6 Btu/lb_m), Type III 83.1 kcal/kg (150.8 Btu/lb_m), and Type IV 46.6 kcal/kg (21.1 Btu/lb_m). This shows, depending on type of cement used, the incorporation of fly ash reduced heat at 72 hrs.

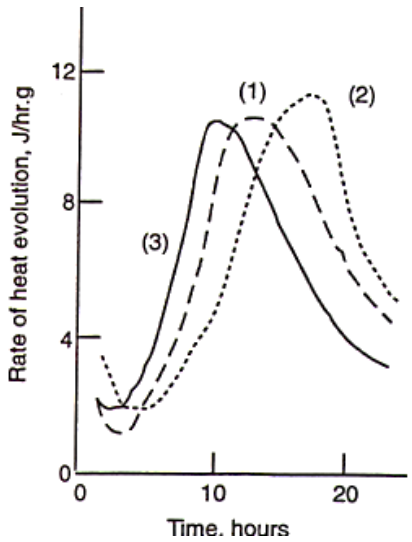

Conversion: 1 J/h-g = 0.4299 Btu/h-lb. (Adapted from Uchikawa, 1986)

Figure 2.3. Rate of Heat Evolution at 20°C (1) 40% Ordinary Fly Ash; (2) 40% High Calcium Fly Ash; (3) No Fly Ash (Mehta and Monteiro, 2006)

Pozzolans are also used in applications where mass concreting is necessary or applications of high-strength concrete where high cementitious contents are used to develop higher strength levels. In many mass concrete applications, temperatures rise drastically during heat of hydration. As the interior concrete rises in temperature, the outer concrete may be cooling and contracting; if the temperature varies too much within the structure, the material can crack. If assumed that the maximum temperature of the mass is reached within 72 hours of placement, it is said that the use of fly ash offers the possibility of reducing the temperature rise almost in direct proportion to the amount of Portland cement replaced by the admixture. This phenomenon occurs because, under normal conditions, the fly ash will not fully react for several days (PCA Durability, 2000).

The first successful attempt of fly ash replacement in mass concreting was performed in 1948 during the construction of the Hungry Horse Dam in Montana. In the production of this dam more than 3 Million cubic yards of concrete was placed. More recently, fly ash was used in concrete for the Dworshak Dam, Idaho, which is a 7-million yd^3 (0.26-million ft^3) concrete structure. There is an added benefit to low heat of hydration of fly ash. Sometimes, the heat during hydration can cause thermal cracking.

With the use of fly ash, the heat is reduced in turn reducing thermal cracking and allowing for a more durable concrete structure (Mehta and Monteiro, 2006).

Myers and Carrasquillo (1998) showed that use of Class C fly ash at replacement levels to Portland cement of 35% was effective at controlling high temperature development in high-strength concrete (HSC) and also contributed to later-age strength development. The effectiveness in controlling temperature development in HSC was shown in the Louetta Road Overpass in Houston, Texas and the North Concho River Overpass in San Angelo, Texas.

2.2.2. Workability and Water Demand

One of the largest governing factors of concrete mix proportioning is generally workability. Workability is typically defined as the ease in which the concrete can be mixed, placed, handled, compacted and finished. A common procedure to measure the workability of fresh concrete is the slump test (ASTM C143-12). Mineral admixtures (such as fly ash) are used in concrete because they tend to enhance cohesiveness and workability of freshly mixed concrete. The finer the material, in this case fly ash, the less amount of material needed to enhance cohesiveness and workability of the fresh concrete. It also assists in the particle packing modeling of concrete mixes. The improvements in cohesiveness, packing, and finish are particularly valuable in lean concrete mixtures or those made with aggregates that are deficient in fine particles.

For a given consistency, many high surface area admixtures, such as pumicite, rich husk ash, and silica fume increase water demand. However, fly ash reduces the water requirement. The lower water demand means for the same slump, HVFA concrete requires less water allowing for a lower w/c ratio. It is suggested with HVFAC mixes to start with a 0.4 w/c ratio when determining mix design (Upadhyaya, 2009). Inversely, if the water cementitious ratio is held constant, the slump will increase with increasing cement replacement. This is due to the small size and glassy texture allowing fly ash to act as ball bearings. Fly ash can also increase the consistency at given water content when used as a fine aggregate partial replacement. The result of addition of fly ash is similar to the result of adding super plasticizer (Mehta and Monteiro, 2006).

Many researchers have found that replacement by fly ash; less water was required for a given slump than conventional mixes. The reduction of water increases as the percent replacement of fly ash increases. Brown (1952) conducted several studies replacing cement and fine aggregate at levels of 10-40% by volume. He found that at every 10% addition of Class C fly ash replacement there was a change in workability of the same magnitude as increasing the water content by 3-4%. In the case of the South Saskatchewan River Dam in Canada, lignite fly ash was used as replacement for fine aggregate. The results consisted of lower w/cm ratio although the workability and cohesiveness of the mix was improved.

Tattersall and Banfill's (1983) research reported the applicability of the Bingham model to reveal rheological properties. It was concluded that incorporating fly ash decreases the yield stress (τ_o) and the plastic viscosity (μ) until a minimum is reached.

2.2.3. Air Content

There have been no findings of a correlation between replacement of cement with fly ash and the percent of air entrapped in the concrete mix. Some researchers report the fly ash acts as filler within the mix (Goto and Roy, 1981). This may lead to a reduction in entrapped air.

2.2.4. Other Considerations

A mix that bleeds excessively is generally harsh and not cohesive. The incorporation of fine materials, such as fly ash, decreases bleeding. The fine particles of fly ash can fill spaces between cement grains, thereby producing denser pastes by contributing to the packing effect. This also densifies the interfacial transition zone between cement paste and aggregate reducing the effect of bleeding (Figure 2.4). The addition of the fine material reduces the size and volume of voids in the mix improving resistance to segregation and bleeding. Also, fly ash requires less water thereby reducing bleeding as well. A study performed by Gebler and Klieger (1986) showed that concretes with Class C fly ash showed less bleeding than concretes with Class F fly ash. Reduction of segregation and bleeding by the use of mineral admixture is of considerable importance when concrete is pumped.

Incompatibility of mineral and chemical admixtures is a common problem in mix proportioning. Fly ash has shown some incompatibilities when incorporated with other admixtures as well. There is a natural delay in hydration and set time when fly ash is introduced into a concrete mix. Cold weather may further delay the pozzalonic activity and retard hydration and set even more.

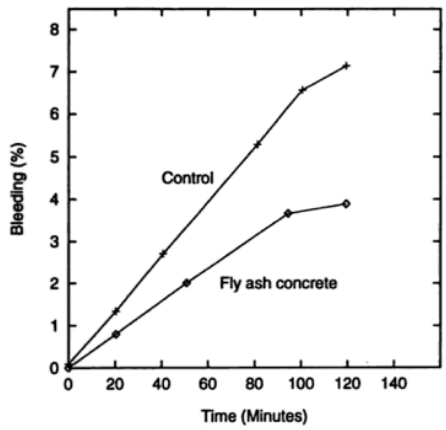

Figure 2.4. Relative Bleeding of Control (Mehta and Monteiro, 2006)

Class C fly ash has higher calcium content than Class F. This can cause issues with air entrainment. The calcium and magnesium in the fly ash may precipitate with the surfactants in the air entraining additives. Issues with water-reducers (WR) have also been noted. Purdue (2) performed an experiment on the type of water-reducer used in HVFAC and how it affected the concrete. The addition of polycarboxylate type WR to high C_3A (> 9%) and low alkali (< 0.7%) content fly ash resulted in stiffening related problems. WR used with low (< 8%) C_3A content and high (> 3.1%) sulfate content fly ash resulted in severe retardation of set. Inversely, low sulfate (< 2.8%) content fly ash resulted in rapid acceleration of set.

Aside from the physical advantages of replacing cement with fly ash, there are financial benefits as well. Using a byproduct of the burning of coal instead of producing a new material (cement) provides up-front savings. Other advantages include material diverted from land-fills, less water used in mixing concrete, decrease in CO_2 emissions and long term maintenance reduction.

2.3. EFFECT OF FLY ASH ON HARDENED CONCRETE PROPERTIES

Section 2.2 discussed how substituting fly ash for cement affected the fresh properties of concrete. In this section, previous experiments will be investigated to gather information about how this substitution affects hardened properties as well.

2.3.1. Compressive Strength

One of the most generic indicators of a concrete quality is its compressive strength. With the introduction of fly ash, the compressive strength of concrete may suffer early on. The delayed and slow pozzolanic reaction within the fly ash reduces the early strength of concrete. Later strength gain doesn't suffer however in HVFA. Strength gain process is delayed because it is a secondary reaction that takes place between the silica in the fly ash and the calcium hydroxide from the hydration of the cement (Knutsson, 2010). However, at some point, the compressive strength of HVFAC may exceed that of conventional concrete. C_3A is the product of cement hydration that attributes to early strength and C_2S contributes to late strength. With replacement of cement, there is less C_3A and in turn lower early strength (Khayat, 2014). Increasing the fineness of the fly ash will help the hydration and provide an increase in strength gain (Knutsson 2010). Generally, particles of less than 10 μm ($3.94*10^{-4}$ in) contribute to early strength of concrete up to 28 days; particles of 10 to 45 μm ($3.94*10^{-4}$ to $1.77 * 10^{-3}$ in) contribute to later strength, and particles coarser than 45 μm ($1.77 * 10^{-3}$ in) are difficult to hydrate. Also, low-calcium fly ash tends to contribute little to early strength due to its lower reactivity than high-calcium fly ash. Production of the fly ash has a lot to do with its reactivity. In cold weather, the strength gain in fly ash concretes can be more adversely affected than the strength gains in non-fly ash concrete. Strength gain can be increased by the addition of other admixtures. The addition of calcium hydroxide helps to maintain the hydration at a faster rate. Gypsum can be added to the mix to balance out the lack of sulfates present in a high volume fly ash mix. Typically, fly ash contains a very low amount of sulfates. Low amounts of sulfate lead to delayed hydration. It can also lead to an overall reduction in the magnitude of hydration peak, which, in turn, leads to a reduction in early strength. Gypsum helps balance the sulfate giving more desirable results (Sustainable Sources, 2014).

In another study (Mohamed, 2011) the effect of fly ash and silica fume cement replacement on compressive strength was analyzed. In this study however, compressive strength of concrete with 0% replacement was not measured for comparison. Water-cement ratio was held constant at 0.42. The results show that there is an optimum percent replacement for the maximum compressive strength. Figure 2.5 reveals this as 30%. This correlates reasoning as to why, until recently, 30% is the maximum replacement level by some codes. Blomberg (2003) recommends a maximum replacement of 25% unless other additives are also included. Compressive strength was also dependent upon the amount of cement. Cement hydration is the primary factor for strength gain, therefore the correlation between amount of cement and strength gain makes sense. Aside from cement content, the compressive strength increased with an increase in fly ash up to 30% then again decreased. Mohamed also found that the compressive strength also increased as the length of moist curing increased. In applications where compressive strength is not an issue, replacement levels greater than 30% are beneficial for durability aspects.

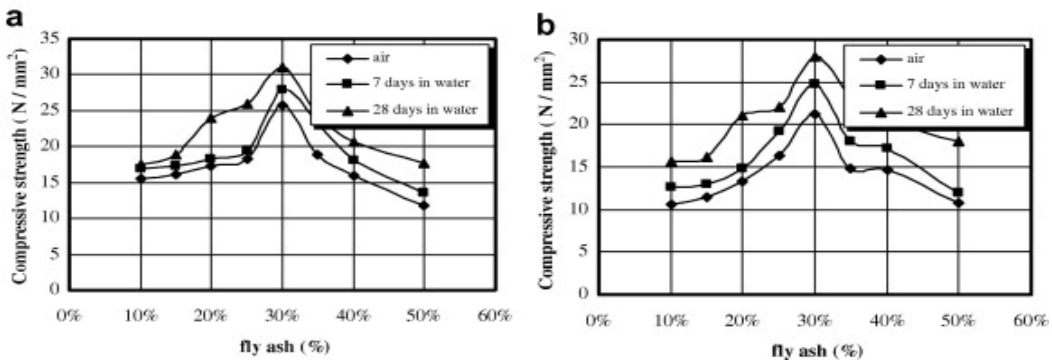

Conversion: 1 kg/m^3= 1 lb./ft^3

Figure 2.5. Compressive Strength for Type I: (a) Cement Content = 550 kg/m3; (b) Cement Content = 450 kg/m^3. (Mohamed 2011)

2.3.2. Modulus of Elasticity

In previous work (Pitroda and Umrigar, 2013) the higher volume Class C fly ash had increased modulus of elasticity. It was proposed that this increase could be due to unreacted particles acting as fine aggregates to contribute to the rigidity of the concrete.

ACI states the modulus of elasticity (MOE) is a function of compressive strength [Equation (2.1)].

$$E_c = 57{,}000\sqrt{f_c'} \tag{2.1}$$

Where: f'_c is the compressive strength of concrete, and E_c is the modulus of elasticity for the concrete.

This equation shows that as the compressive strength increases so will the modulus. This would suggest that when the compressive strength of the HVFAC mixtures exceeds that of the control mixes, and then the MOE would also exceed that of the control concrete mixtures.

There are many contradictory results in the field of fly ash and MOE. In a study performed by Missouri University of Science and Technology (Missouri S&T) (Volz et al. 2012), when the HVFAC mix had not outperformed the control mix in terms of compressive strength, in some instances, it still outperformed in terms of MOE at 28 days. In other research, it was concluded that the fly ash replacement did not affect the MOE. However, it was found that the modulus of the early concrete with fly ash was lower than concrete without. The oldest testing age was 56 days (Blomberg, 2003). In this study, two control mixes were examined. The mix with lower cement content exhibited a greater MOE. When the paste content is decreased the modulus of the aggregate used becomes more dominant than the modulus of the paste. If a higher modulus is desired, it is suggested to use a durable aggregate. These findings may propose that fly ash mixtures may have higher MOE due to a smaller amount of cement.

2.4. EFFECT OF FLY ASH ON DURABILITY CHARACTERISTICS

Portland Cement Association (PCA, 2000) defines durability, as ’is the ability to last a long time without significant deterioration.’ When a material is durable it helps the environment by conserving resources and reducing wastes and the environmental impacts of repair and replacement. The longer a material lasts the more construction and demolition waste can be diverted from going to landfills. The production of new building materials depletes natural resources and can produce air and water pollution (Myers and Carrasquillo, 1998).

There are many durability categories that concrete is tested for (Figure 2.6). Abrasion resistance, permeability, and freeze/thaw are the durability items discussed in this report. All of these properties can be tested for in the lab. For increased sustainability and some increased durability properties, fly ash has been widely used in mix design of concrete. However, fly ash may not improve these properties proportionally to the replacement rate.

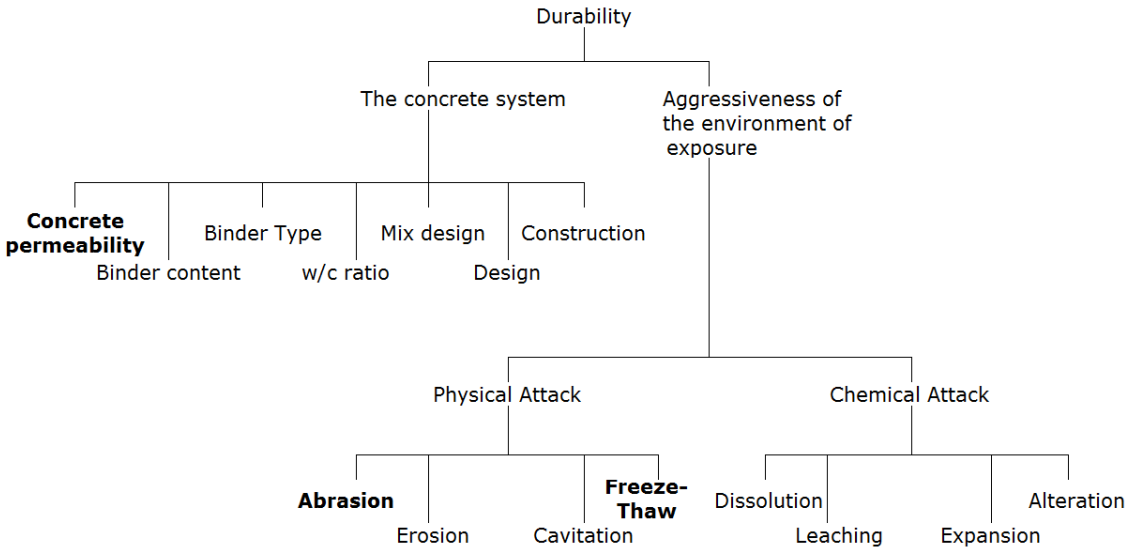

Figure 2.6. Factors Affecting Durability (Adapted from PCA, 2008)

2.4.1. Abrasion Resistance

Abrasion is a sub form of wear. It implies the steady systematic loss of surface material by some mechanical means or load. The load may be in the form of direct compression or pure shear, but generally both these actions will apply simultaneously, such as occurs in rubbing, scratching, scraping, gouging etc. Some common sources of abrasion are friction between vehicle tires and concrete pavement road surfaces and by water flows over exposed dam or bridge footings. This abrasion wear can lead to a decrease in member thickness, which can cause cracking, failure of the member, or corrosion of rebar. Abrasion can be measured by mass loss and depth of wear. If the depth is less than 1 mm (0.0394 in.) this is considered shallow abrasion. If the wear

exceeds 5 mm (0.197 in.), then it is considered deep abrasion. Intermediate abrasion is any value in between the two (Papenfus, 2002).

Although compressive strength is the most apparent factor affecting abrasion (Hadchti and Carrasquillo) resistance, incorporation of SCM can increase the resistance as well. Naik and Singh (1991) tested 40%, 50%, and 60% Class C fly ash mixes and compared them against a control mix. After testing according to ASTM C944, using the depth of wear as the measurement for comparison, the study reported the 50% fly ash mix had a shallower wear depth than the conventional mix. In another test (Atis, 2002) the BSI 1993 –British Standards Institute "Method for determination of aggregate abrasion value," was the procedure used. This test is similar to ASTM C944. The measurement used to compare concrete mixes was the mass loss upon abrasion. A conventional mix, 50% and 70% fly ash mixes were used. At each level of fly ash replacement, two different compressive strengths were engineered. The results suggested again that the compressive strength was the most influential factor. Also, the results show that at higher strengths higher levels of replacement showed increased resistance. However, at lower compressive strength, the opposite is true.

Missouri University of Science and Technology (Missouri S&T) (Report E, 2012) also did a study on the abrasion resistance of concrete with 50% and 70% cement replacement by fly ash. In this study ASTM C944 was followed with slight modifications. The conventional specimens were not moist cured after demolding. Once the 28-day compressive strength was reached, the fly ash specimens were moist cured for 10 weeks. The mass loss was measured after each of the three 2-minutes abrasion cycles. This study also agrees with the previous researchers that compressive strength was the most influential variable. Compressive strength at 28 days of the conventional mix was 5,400 psi (37.2 MPa) and it performed the best in terms of mass loss (Figure 2.7) and depth of wear (Figure 2.8). However, the 70% fly ash mix had lower compressive strength [3,100 psi (21.4 MPa)] than the 30% mix [3,500 psi (24.1 MPa)] and it outperformed in terms of mass loss and depth of wear.

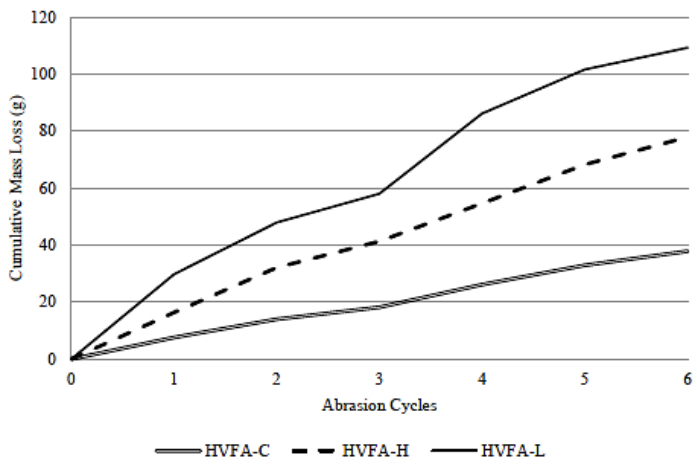

Conversion: 1lb. = 453.6 g

Figure 2.7. High Volume Fly Ash (HVFA) Mass Loss Results (Volz et al. 2012)

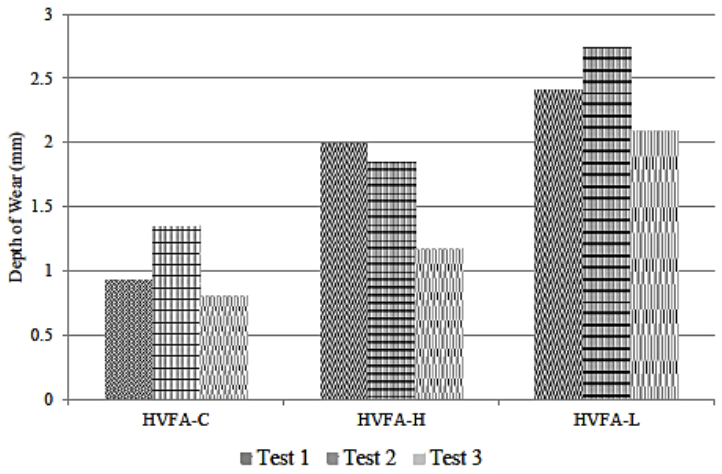

Figure 2.8. Depth of Wear Results (Volz et al. 2012)

Naik and Singh (1991) used methods provided by ASTM C779 B when testing for abrasion resistance. At 28 days all mixes (conventional, 50% and 70%) had achieved structural strength [4500 psi (31.0 MPa)] and none failed the abrasion test [< 3mm (0.118 inches] depth of wear in 30 minutes. However, when the time increased to 60 min, the 50% and 70% mixes had a depth of wear in excess of 3mm (0.118 inches). All mixes performed well at 91 days. When comparing depth of wear to compressive strength, mixes performed equivalently at all replacement rates (Naik and Singh 1991, Myers and Carrasquillo 1998).

In a study performed by Tikalsky and Carrasquillo (1998), Class C fly ash exhibited superior abrasion resistance compared to either plain Portland cement concrete or concrete containing Class F fly ash.

Ukita et al. (1989) showed that at a 30% cement replacement with a Class F fly ash, the abrasion resistance of fly ash concrete was lower relative to plain Portland cement concrete. Barrow et al. (1989) measured abrasion resistance of concrete made with fly ash having cement replacement between 0 and 35% by volume. They concluded that the concrete incorporating either Class C or Class F fly ash attained abrasion resistance equivalent to that of no-fly ash concrete. Recently Bilodeau and Malhotra (2000) determined abrasion resistance of high-volume Class F fly ash concretes. Their test result shows higher resistance to abrasion for no-fly ash concrete as compared with high-volume fly ash concretes.

Langan et al. (1990) studied the influence of compressive strength on durability of concrete containing fly ash at a 50% cement replacement by weight. The authors concluded that the compressive strength does not seem to have a significant effect on abrasion resistance of concrete.

2.4.2. Chloride Ion Penetration

When discussing durability to chemical attack, permeability plays a fundamental role in the deterioration of concrete and corrosion of reinforcement from destructive chemical actions. “Permeability is most important because it controls rate of entry of moisture that may contain aggressive chemicals,” (Krivenko et al., 2006). Among these actions is attack by acidic or sulfate solution. One chemical that is detrimental to concrete is de-icing salt. Chloride ions from de-icing salts can penetrate by transport in water, diffusion in water, or absorption. Only the free chloride ions can damage the concrete (Neville, 2003). Shamsai (2012) stated that the water-cement ratio is an important factor in controlling permeability. As the water-cement ratio increased so did the porosity.

One way to combat chloride ion penetration is with the incorporation of Class C fly ash. Fly ash will react with the Calcium hydroxide (CH) to form C-S-H. Also, the addition of SiO_2 from the fly ash reacts with the cement and forms a more stable and

dense form of C-S-H (Knutsson, 2010). Dhir (1999) agrees that fly ash densifies the hydration products. Many researchers agree that the fly ash binds the chloride ions (Dhir 1999, Myers and Carrasquillo 1998, Haque et al., 1993). Dhir (1999) states this is because the active alumina (Al_2O_3), more prevalent in fly ash, binds the chloride ions. He found that the optimum replacement rate was 30% (Class of fly ash not specified). These reactions decrease permeability in the long run and increase resistance to chemical attacks. At early ages, however, the fly ash mixes showed higher permeability possibly due to the delayed reaction of the fly ash. The pozzolanic reaction of fly ash causes pore refinement. Pore size is not the only concern, but connectivity is the main factor (Mindess et. al., 2003). It's been suggested the pozzolanic reaction breaks the interconnected pore system in turn decreasing permeability also causing an increase in chemical durability of the concrete. Resistance to chemical attack is important especially in areas where de-icing salt is used and in reinforced or prestressed concrete.

A study performed on permeability of concrete piping with and without fly ash, in the 1950s by R. E. Davis at the University of California, showed considerably lower permeability at age 6 months. However, at 28 days, the concrete containing 30% low-calcium fly ash had higher permeability. This can be attributed to the slower reaction rate of fly ash than cement at early stages which agree with Dhir (1999). Another benefit to consider is the low heat of hydration as discussed in section 2.2.1. Because fly ash decreases the heat of the fresh concrete, there is reduced possibility of thermal cracking in turn reducing possible ingress of aggressive chemicals (Myers and Carrasquillo 1998).

Research (Mehta and Monteiro 2006) has confirmed that, with cement pastes containing 10 to 30 percent of a low-calcium fly ash, significant pore refinement occurred during the 28 to 90-day curing period. This drastic refinement resulted in a large reduction of the permeability.

Volz et al. (2012) also performed a study using ASTM C1543. Some of the results did not perform as expected. The conventional mix showed a typical chloride profile, highest chloride content was at the surface and it decreased with depth and also gave results that showed negligible corrosion risk. Both HVFA high and low cementitious mixes did not perform according to typical chloride profile. These mixes showed low chloride content at the surface and relatively high concentrations at 0.25 in (6.35 mm)

depth. However, at 1.5 in (38.1 mm), the desired 0.03% was reached. The results may suggest that the HVFA concrete had high capillary action but low diffusion. The air entrained HVFAC mix showed a profile similar to that of the conventional mix. Despite the non-prolific results, all HVFAC mixes outperformed the conventional concrete (Figure 2.9).

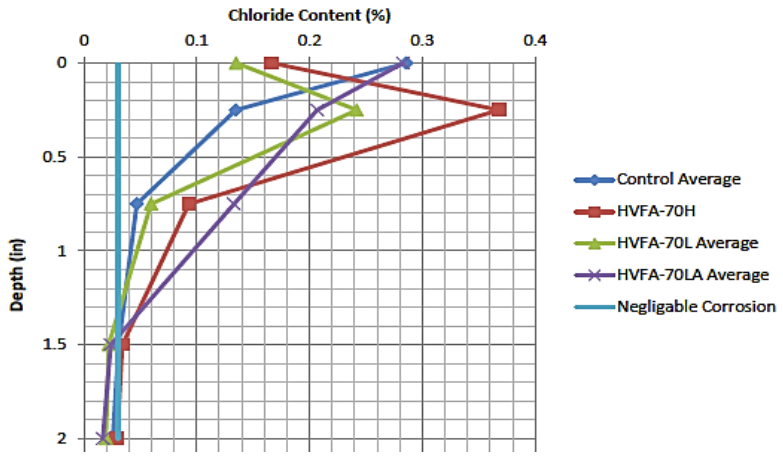

Figure 2.9. Averaged Chloride Profile for HVFA Mixes (Volz et al. 2012)

2.4.3. Freeze and Thaw Resistance

Concrete generally contains some unused water in capillary pores; space not filled by hydration products, CH and C-S-H. When this water freezes, it expands 9%. Therefore, if saturation levels are greater than 91% the frozen water will have nowhere to go and thus the internal hydrostatic pressures exerted will crack the concrete. The cracks created will cause a reduction of Modulus of Elasticity (MOE) and also a reduction of Modulus of Rupture (MOR). To eliminate this phenomenon, air-entraining admixtures are used. When concrete is air entrained, spherical bubbles are formed. These entrained air bubbles provide a relief system for the hydrostatic pressure. Air bubbles provide a void system for freezing water to expand into the bubbles causing less freeze and thaw damaged to the concrete.

A visual representation is shown in Figure 2.10. Research shows roughly that less than 4% air content exhibits less than great durability except in HSC. After 4% air content is reached, there is little increase in durability for an increase in air content. As a rule of thumb, concrete losses 5% in strength per % of air content so there is little

advantage in going above 4 to 5% in total air content. Durability is measured by a durability factor (DF) that includes the ratio of modulus of elasticity (E) after # of cycles to E initial. Different entities have different standards for the minimum rating of durability. Mindess, Young, and Darwin (2003) suggests that there are not hard limits on whether or not a concrete will fail based upon freeze-thaw data, only proposing that concrete with a DF of more than 60 will perform adequately. However, Missouri Department of Transportation (MoDOT) specifies the lower limit as 75 when conducted in accordance with AASHTO T 161, Procedure B.

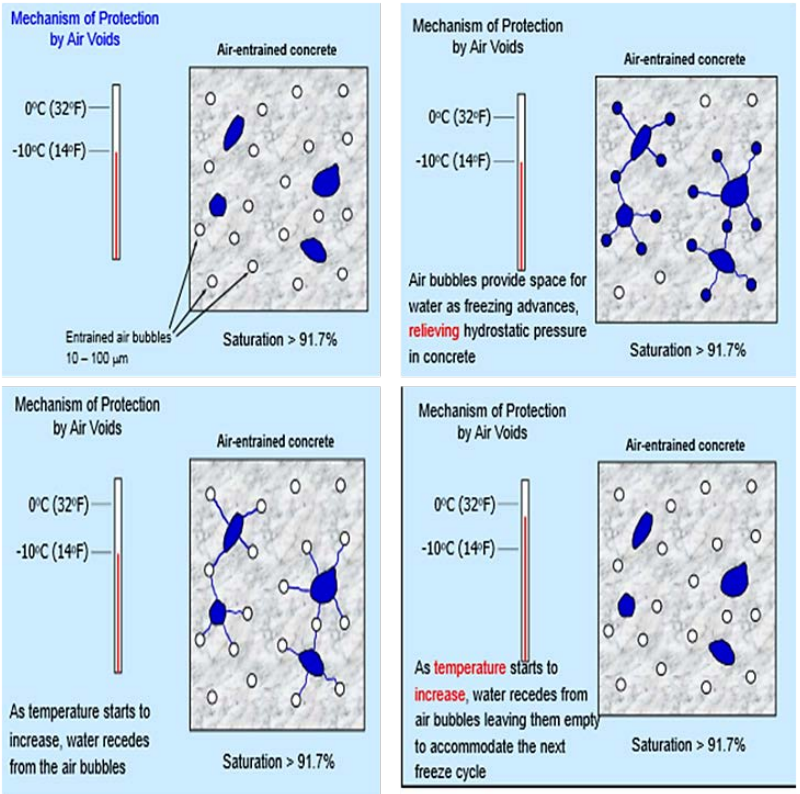

Figure 2.10. Process of Air Entrained Relief (Khayat 2014)

Some may say that fly ash increases concrete resistance to freeze and thaw (Headwaters Resources, 2015); however, some would disagree (Naik and Singh, 1994). Because Class C fly ash increases long-term strength, it may be better to withstand the freeze thaw forces than a conventional concrete at later ages as well. Naik and Ramme (1991) performed a study where cement was replaced by fly ash at 45%. Freeze and thaw durability was evaluated for air entrained and non-air entrained. They found the air

entrained outperformed the non-air entrained HVFAC. In another study (Naik and Singh 1994), it was reported that 0% and 30% replacement levels performed identically. However, when replacement was greater than 30%, the durability factor dropped significantly. As the percent replacement increased, not only did the DF decrease, but the mass loss significantly increased as well. These mixes even had adequate air content (> 4%). Although the fly ash mixes did not perform as well as the other mixes, all mixes passed ASTM requirement of DF equal to or greater than 60.

Volz et al. (2012) conducted a study on durability testing. Within these tests, freeze and thaw resistance of concrete was tested on mixes that contained 0 and 70% fly ash. There were three mix designs investigated at 70% replacement: 70H, 70L, 70LA. H, L, and LA refer to high cement content, low cement content, and incorporation of air entrainment admixture respectively. The testing was completed in accordance to ASTM C 666, Procedure A. The results showed that the 70% replacement level with high cement content performed the worst. This finding concurs with (Sustainable Sources, 2014) in the fact that there is a maximum replacement level to get adequate results. The high carbon content of fly ash at this level requires more air entraining admixture to be provided and that can be hard to attain because the admixture is absorbed by the carbon. For this mix, in particular, there was no air entrainment added. Although the 70H mixture did not perform well, the 70L and 70LA mixtures both out-performed, in terms of DF, the conventional mix (Table 2.2).

The results do correlate with other findings, however, only the 70L mix exceeded the minimum DF set by MoDOT of 75. The reason for this is a result of the limestone used as course aggregate. Typically air entrained (70LA) concrete would perform better, but with high replacement and therefore carbon content, the air void system can be hard to maintain.

Another issue with using fly ash is the fact that it contributes to the packing effect, which in turn reduces air voids. In a companion study performed at Missouri S&T (Volz et al. 2012) it was found that the incorporation of fly ash increased the DF and at 70% they encountered a higher DF than 50%. Both mixes exceeded 75.

Table 2.2. Average Durability Factors for HVFA Mixes

Bath ID	Durability Factor
Control	21.6
HVFA-70H	2.1
HVFA-70L	81.8
HVFA-70LA	68.5

Note: Adapted from Volz et al. 2012

2.5. MATURITY METHOD

Using the maturity method to predict the estimated in place strength of concrete can prove to be very beneficial. Knowing the strength of the concrete at specific ages can allow for scheduling of important construction activities. These activities include but are not limited to removal of formwork and reshoring; post-tensioning of tendons; termination of cold weather protection; and opening of roadways to traffic (ASTM C1074-11). This can prove to have a financial benefit as well. In the construction industry, standard practice relies on the concrete to have gained 70% of its 28-day compressive strength before any load is applied to a structural element (Upadhyaya, 2009). Maturity method is not limited to traditional curing practices. By using this method, the concrete strength can be predicted for laboratory specimens cured under non-standard temperature conditions as well. There are some limitations to using this practice however. The concrete must be cured in an environment where hydration can occur. This method does not take into account the effect of early age heat generation on long-term strength and must be accompanied by another means of indication of concrete strength.

Rohne and Izevbekhai (2009) used maturity method in Minnesota to predict when the interchange known as “Unweave the Weave,” could open for traffic. Minnesota Department of Transportation (MnDOT) used this method on several projects to study the advantage and disadvantages of using maturity meters in a field setting. This project was one of the first to be observed. The goal was to reduce excessive initial cure periods. Results showed that the maturity curves were sensitive to small amounts of cement content changes such as 10 lb./yd^3 (0.37 lb./ft^3). Another interesting observation was the datum temperature. ASTM C1074-11 suggests a datum temperature of 32°F (0°C). This

project showed that value is too high and the concrete continued to gain strength well below this recommendation. In other research performed by Myers (2000) on HPC bridge decks, it was found the maturity method did in fact adequately (±10%) represent the strength of the concrete. There was only a 4.1% variance, on the conservative side, of the predicted strength and the tested 28-day strength.

Traditional methods of concrete strength estimation are destructive and inconvenient. Methods of making test specimens may not truly represent the way concrete is placed in the field. The length of the curing period is not the only important piece to strength gain. The internal temperature plays a role as well. When placing vast amounts of concrete, the difference in internal and external temperature may vary greatly. Data loggers become useful in this situation. Using the maturity method provides a means of accessing the strength at more frequent time intervals than traditional practices translating into a higher level of quality assurance (Myers, 2000).

Maturity is the time temperature history of the concrete mixture. The warmer the concrete, the faster it will gain strength (Mohsen, 2004). Not only does the ambient air temperature affect this strength gain, but also the exothermic reactions from hydration. Therefore, since the strength gain depends on time temperature history, if the history is known, then the strength can be estimated. Using this method in the field only requires monitoring the temperature-time history of the in place concrete once the relationship between strength and maturity has been developed in the laboratory. The maturity index acquired in the field from the temperature history can be translated into strength (Myers, 2000).

2.6. EFFECTS OF ACCELERATED CURING ON CONCRETE

Curing of concrete is a process intended to enhance the hydration of the cement in concrete. A proper environment is necessary to control the temperature and moisture diffusion within the concrete. These items must be considered for desired properties to progress. Research has shown that HVFA concrete is more susceptible to method of curing than its counterpart (Myers and Carrasquillo, 1998). There are many forms of curing. Common types include moist curing (100% RH), ambient air curing, steam

curing, and accelerated temperature curing. In this report, moist curing and acceleration curing by ovens will be investigated.

2.6.1. Compressive Strength

It has been discovered that curing concrete at higher temperatures, greater than 68°F (20°C), can improve early strength, but long-term strength suffers (Myers and Carrasquillo, 1998). However, this may not be the trend when discussing fly ash concrete (Malhorta 1994). If not careful, curing at high temperatures can be detrimental to conventional concrete (Maltais and Marchand 1997, Kjellsen et. al., 1990). Kaur (2013) reported that curing at 248°F (120°C) has the biggest impact on the conventional mix and 35% fly ash mix at early ages. All specimens at 28 and 56 days showed a decrease in compressive strength.

Gjorv et al. (1990) discusses the phenomenon of quick hydration products forming and blocking grains of cement particles from hydrating further. Yazıcı et al. (2005) reported in "Effects of Steam Curing on Class C high-volume fly ash mixtures," that steam curing is only beneficial when interested in increasing the 1-day compressive strength (Figure 2.11). Yazıcı tested concrete up to 90 day cured in water, steam, and lab air and reported a decrease in compressive strength when steam cured compared to standard cure in the majority of mixes past 7 days (Figure 2.12).

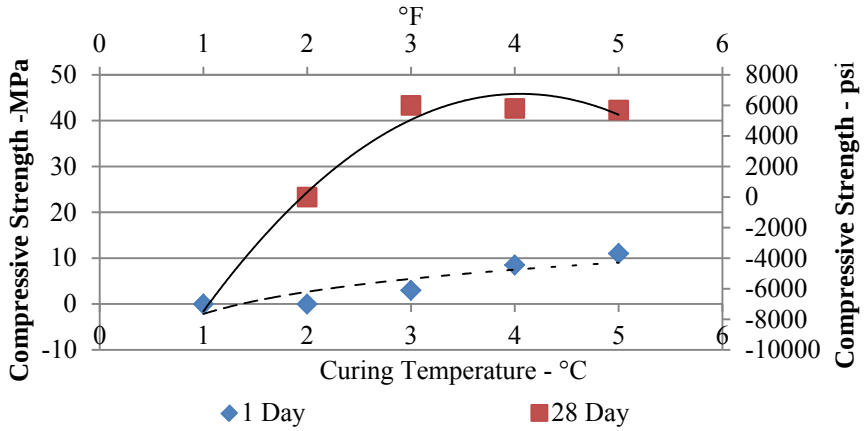

Figure 2.11. Compressive Strength vs. Curing Temperature (Adapted from Verbeck and Helmuth, 1968)

It was also noted that steam curing affected 10-20% mixes. Steam curing can be an issue with low lime fly ash mixes within the range of 50-131°F (10-55 °C); it may actually retard the set (Ma et al., 1995).

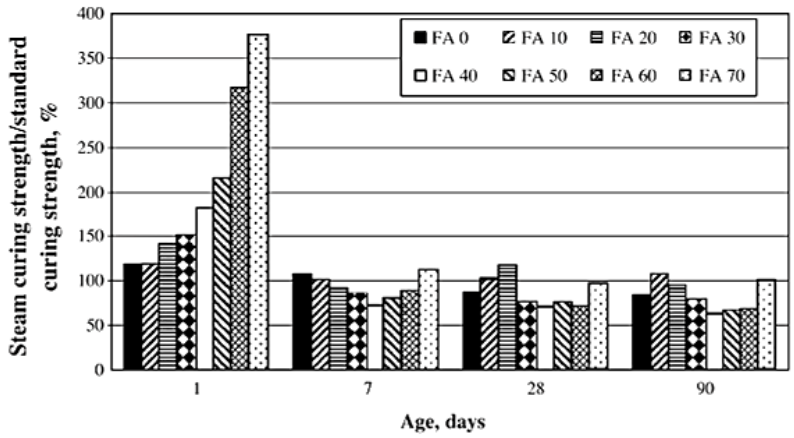

Figure 2.12. Relative Compressive Strength (Ma et al., 1995)

Mehta and Monteiro's (2006) research showed a higher compressive strength at 7-day of cores of high-volume fly ash cured under high temperature than laboratory-cured cylinders. High temperatures can be harmful to Portland cement, however, the high proportion of fly ash benefitted from this high temperature exposure. The high temperatures acted as a thermal activator to accelerate the pozzolanic reaction. An example was the pressure tunnel of Kurobegowa Power Station in Japan, where the concrete is located in hot base rock (212 to 320°F [100 to 160°C]), the use of 25% fly ash as a cement replacement in the concrete mixture showed a favorable effect on the strength.

Other research, performed by Ozyildirim (1998), agreed with the aforementioned thermal activation of pozzolanic reaction. Ozyildirim analyzed the effect of temperature curing on concrete with fly ash, silica fume, and slag. The two properties tested for were compressive strength and permeability. The researcher tested at 1, 7, 28, and 365 days. Two batches were made. The first batch used high range water reducer (HRWR) while the second only used water reducer. Ozyildirim used two fly ash mixes with 20% replacement. One mix had the same amount (100%) of cement (100/0/20/0) as the control mix and the other mix only had 85% (85/0/20/0) cement of the control mix. The 100%

cement fly ash (20%) mix showed higher compressive strength than the control mix, post 1 day, at all temperature curing levels (41, 50, 73.4, 100°F [5, 10, 23, 38 °C]). However, the mix with only 85% cement content of control and 20% fly ash and HRWR only exceeded the control compressive strength at 1 year when cured at 50°F (10°C) up to 28 days then cured at 73.4°F (23°C). The 85/0/20/0 mix with basic water reducer never exceeded the compressive strength of the control mix at any temperature. Overall, the results showed that the compressive strength of the control mix was not as variable as pozzolan mixes. One year compressive strengths for the fly ash mixtures were higher when initially cured at low temperature for 28 days then cured at higher temperatures.

2.6.2. Modulus of Elasticity

Kjellsen et al. (1990) also investigated the effects of curing at higher temperatures. The results agree with (Ozyildirim 1998) in respect to cement not being able to completely hydrate due to the blockage of hydration products. Kjellsen proposed that these areas of dense hydration products leave larger pores in surrounding areas resulting in a denser pore structure throughout the concrete. It was reported that the increase in pores causes a decrease in modulus of elasticity and leaves the concrete more susceptible to cracking when introduced to structural stresses.

2.6.3. Durability Characteristics

There has been little research performed directly investigating the effect of temperature curing on abrasion resistance. As discussed in section 2.4.1, compressive strength is one of the more influential factors in abrasion resistance. However, contradictory results have been noted when it comes to accelerated curing.

Naik and Singh found that at all replacement rates curing at 73.4°F (23°C), the abrasion resistance increased with increasing amounts of fly ash. However, at temperatures greater than 73.4°F (23°C), the opposite is true. In another study (Barrow et al, 1989), concrete with replacement rates of 25% and 50% performed worse at three different curing temperatures (50, 74.5, 100°F [10, 23.8, 37.7°C]). The authors purposed the reason for this is in part to improper curing of the concrete. Atis (2002) showed that at

compressive strengths greater than 5,800 psi, 70% replacement performed greater than 50%. However, it was established that the curing method had no effect on the results.

In 1998, Hadchti and Carrasquillo investigated temperature curing with low relative humidity. It was found that there was a decrease in abrasion resistance when cured at higher temperatures and lower RH.

In the same study previously mentioned by Ozyildirim (1998), the permeability of fly ash, silica fume, and slag was investigated and compared to a conventional mix. Both fly ash mixes (100/0/20/0 and 85/0/20/0) had lower permeability than the conventional mix, when HRWR was used, except at the lower temperatures [50°F and 73.4°F (10°C and 23°C)] when only cured for 28 days. The permeability of every mix decreased as the temperature increased and also as the duration of the temperature increased. By 1 year, the fly ash mixes all reached low to moderate ranges according to ASTM C1202. Just like the compressive strength, the pozzolan mixes varied more in terms effectiveness of the temperature curing on the permeability than the control mix.

In addition to the decrease of modulus of elasticity due to coarser pore structure, the permeability of the concrete suffers also according to Kjellsen (1990). Kjellsen's (1990) results agree with results gathered by Goto and Roy (1981). In this study, it was found that the pore size when cured at 140°F (60°C) was significantly larger than when cured at 81°F (27°C). Due to increasing pore size and coarse pore structure when cured at elevated temperatures, Campbell and Detwiler (1993) believe the curing process is more detrimental than w/cm ratio.

In another study (Acquaye, 2006) the effect of fly ash and temperature curing on chloride ion penetration were assessed at 28 and 91 days. The results indicate that the mix with 18% fly ash has a higher resistance to penetration at both 28 and 91 days at all curing temperatures [73, 160, 180 °F (27.8, 71.1, 82.2°C)] when compared to the mix without fly ash. For the conventional mix, curing at 73°F significantly outperformed both of the other temperatures validating results found by previous mentioned researchers. For the fly ash mix, results at 160°F (71.1°C) and 180°F (82.2°C) were almost identical at both ages and outperformed the fly ash mix cured at 73°F (22.8°C). However, the fly ash mix cured at 73°F (22.8°C) very nearly performed as well as the other two at 91 days

(Figure 2.13). This suggests that the phenomenon of elevated curing causing a coarser pore structure due to lack of hydration holds more truth when discussing mixes without fly ash.

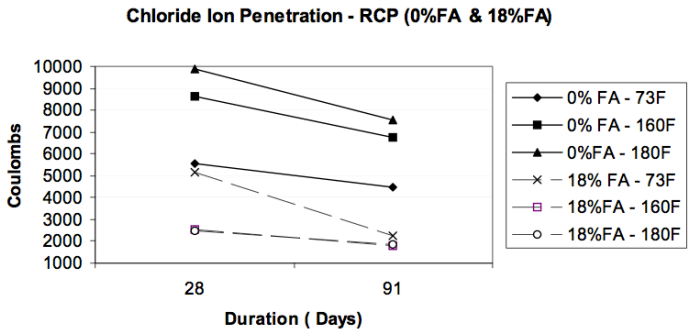

Conversion: 1°C=5/9(°F-32)

Figure 2.13. Chloride Ion Penetration at 28 and 91 Days (Acquaye, 2006)

Little information was found on the effect of accelerated curing methods on the performance during freeze and thaw cycles. One source (Tanesi et al., 2004) used four different curing regimes and then tested the specimens according to ASTM C666-Procedure A. They found that the specimens cured in the air actually had a higher DF than the other specimens. The specimens steam cured at 140°F (60°C) for 48 hours was lower than the air cured but higher than the steam cured at 194°F (90°C). And the 140°F (60°C) was also slightly higher than the specimens cured at 194°F (90°C) after 15 days for 48 hours.

2.7. BRIDGE A7957

Bridge A7957 is located on highway 50, west of Linn, Osage County, Missouri (Myers et al. 2014). Within this structure, four different types of concrete mixtures were implemented and studied. The four concrete types included conventional concrete (CC), HVFAC, normal strength self-consolidating concrete (NS-SCC) and high-strength self-consolidating concrete (HS-SCC). A longitudinal view of Bridge A7957 is shown in Figure 2.14.

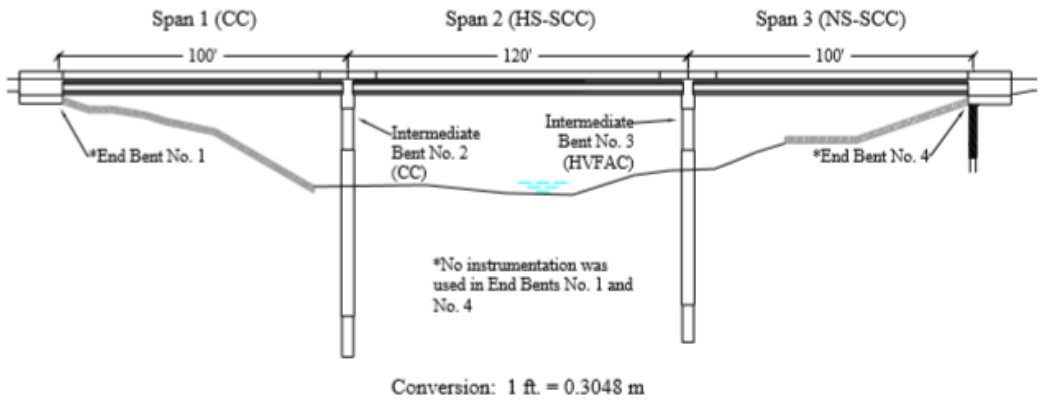

Figure 2.14. Bridge A7957 Elevation View

The HVFAC mix design used was based off MoDOT's B mix with 50% fly ash replacement. The mix had a design w/cm of 0.33 and air of 6.0%. For this mixture, the target compressive strength was 3,000 psi (20.7 MPa). Each intermediate bent (Bent No. 2 and 3) were cast in two units, the web walls and columns then the pier caps. Both bents were instrumented with temperature sensors to record their temperature- time histories respectively.

Table 2.3. Intermediate Bents Hydration Rates

	Bent 2		Bent 3		Percent
Location	°F/cwt	°C/cwt	°F/cwt	°C/cwt	Reduction
North Column	11.47	6.37	8.67	4.82	24.4
South Column	11.77	6.54	8.63	4.79	26.7
North Web Wall	9.77	5.43	5.93	3.29	39.3
South Web Wall	9.71	5.39	6.31	3.51	35.0
Top Pier Cap	7.68	4.86	4.37	2.43	43.1
Middle Pier Cap	12.32	6.85	N/A*	N/A*	N/A*
Bottom Pier Cap	9.11	5.06	6.51	3.61	28.6

Note: * DAS failed to record the last part of the data for this sensor location

Sensors were located in each column and web wall of each bent (north and south) and the top, middle, and bottom of each pier cap. For each location the hydration rate was

calculated (Table 2.3) using Equation (2.2). The reduction process was calculated based off Bent No. 2.

$$R = \frac{Peak\ Temperature - Initial\ Temperature}{100\ lbs.\ cementitious\ material\ per\ yd^3} \tag{2.2}$$

The results showed there was a significant reduction in heat generation within the intermediate bents with the fly ash replacement. Overall, there was a 20-40% reduction in heat generation from conventional concrete to 50% HVFA concrete.

3. LABORATORY INVESTIGATION

3.1. EXPERIMENTAL DESIGN

This section provides information on the mix design and plan for experimental design.

3.1.1. Preliminary Study

Before durability testing could be performed, the mix designs under investigation needed to be solidified. The goal was to have all mixes (CC-70% HVFA) have a compressive strength greater than 4,000 psi (27.58 MPa) at 28 days without varying the water to cement ratio or cementitious content and keeping slump as constant as possible. For deck or substructure applications, 4,000 psi (27.58 MPa) is the minimum value for structural concrete. Typical water to cementitious (w/cm) ratio of 0.4 was chosen. In this study, sand to coarse aggregate ratio was kept constant for the mixes of 50% HVFAC and above. Through trial and error, mixes were evaluated and slump was observed. As the amount of fly ash increased from 0 to 70%, the slump level also increased. The mix design proportions are illustrated in Table 3.1.

Table 3.1. Mix Design Breakdown

Mix ID	**CC**	**35**	**50**	**60**	**70**
CA (lb./yd^3)	1706	1736	1614	1607	1600
FA (lb./yd^3)	1210	1500	1268	1262	1258
cement (lb./yd^3)	750	488	375	300	225
Fly Ash (lb./yd^3)	0	262	375	450	525
water (lb./yd^3)	300	300	300	300	300
w/c	0.40	0.40	0.40	0.40	0.40
Total CM	750	750	750	750	750
Ratio (Sand/Stone)	0.71	0.86	0.79	0.79	0.79
Total Agg	2916	3236	2882	2869	2858

Conversion: 1 lb. = 453.6g, 1 cy= 27 ft^3

The lowest slump achieved at 70% fly ash was 7 in. (177.8 mm); therefore, a range of 7in ± 1 in. was targeted and obtained from all mixes. To achieve this, the mixes with higher percent of fly ash had lower fine/coarse aggregate ratio.

3.1.2. Main Study

Once the mix designs were determined, the main study (i.e. Mechanical Property Tests, Durability, and Maturity) was undertaken. Table 3.2 breaks down each test and how many specimens were fabricated.

Table 3.2. Testing Matrix (Phase I and Phase II)

Phase	Investigation Parameter	Physical or Mechanical Test	Specimen Size (in.)	No. of Replicate Specimens (per mix)	Age of test (days)
I-Control Study	Strength	f'c/MOE	4x8 cyl.	21	3,7,14,28, 56,90,120
	Durability	Abrasion	3.5x6x16	4	28,56,90,120
		Chloride Content	3.5x18x18	4	
		Freeze-Thaw	3.5x4x16	4	
	Maturity	Thermocouples	4x8 cyl.	2	0-28
II-Accelerated Curing	Strength	f'c/MOE	4x8 cyl.	18	3,7,14,28
	Durability	Abrasion	3.5x6x16	6	14,28
		Chloride Content	3.5x18x18	6	
		Freeze-Thaw	3.5x4x16	12	

Conversion: 1 in. = 25.4 mm

Table 3.2 shows how the main study was broken into two different phases, the control phase and the accelerated curing phase. All specimens were demolded at age between 24hr to 48 hr. During the control phase, abrasion and ponding specimens were cured for 14 days in the moist cure room (69°F and 100% Relative humidity) then cured in the lab at ambient temperature. All cylinders were continuously moist cured

throughout the control phase and freeze-thaw specimens were cured in a limewater tank at engineering research laboratory (ERL).

Phase two specimens were demolded after 24-48 hours. Three temperatures were chosen for accelerated curing. Specimens were cured for 48 hours, after demolding, in three different ovens (100°F (37.8°C), 130°F (54.4°C), and 160°F (71.1°C)). After the 48-hour oven-curing period, the specimens were placed in the lab where they sat until age of testing. Phase one aimed to show HVFAC at later ages can perform similar to that of the control mix at 28 days. Durability specimens were tested at 28, 56, 90, 120 days from casting date. Cylinders were tested for compressive strength and modulus of elasticity at 3, 7, 14 days in addition to the later ages. Phase two investigated the possibility of getting similar results from the HVFAC to that of control mix at early ages by accelerating the curing process by curing at higher temperatures.

Throughout this study, each concrete mixture was referred to by using the nomenclature presented in Table 3.3.

Table 3.3. Mix ID Descriptions

	Mix ID	Description
Phase I	CC	Conventional Concrete
	X%	High Volume Fly Ash
Phase II	XT100	Cured at 100°F
	XT130	Cured at 130°F
	XT160	Cured at 160°F
*Where X= 35, 50, 60, 70 (fly ash replacement)		

3.2. EQUIPMENT

In this section, each piece of equipment used during the course of this research will be discussed. All equipment was property of Missouri University of Science and Technology (Missouri S&T) and was set up and used at the Center for Infrastructure Engineering Studies (CIES) Engineering Research Lab (ERL).

3.2.1. Fresh Concrete Mixing

A 6-ft^3 (0.222 yd^3), variable speed, mixer was used to mix all the concrete in the material research laboratory (Figure 3.1).

Figure 3.1. Concrete Mixer (Capacity: 6 ft^3)

3.2.2. Mixing and Casting of Mortar Cubes

A small and large Humboldt variable speed mixer (Figure 3.2 and Figure 3.3) was used to mix mortar cubes in accordance to ASTM C109-13 based on mortar mix design specified in Appendix A1 of ASTM C1074-11. Mortar cubes were cast in steel and plastic molds of 2.0 x 2.0 x 2.0 in. (50.8 x 50.8 x 50.8 mm) as shown in Figure 3.4. The mortar samples were fabricated to measure the temperature time history of mortar.

Figure 3.2. Small Humboldt Variable Speed

Figure 3.3. Large Humboldt Mixer

Figure 3.4. Plastic Cube Molds

3.2.3. Slump of Fresh Concrete

The slump of each fresh concrete mix was measured using a standard ASTM C143-12 slump cone. Fresh concrete was placed in 3 layers and consolidated with a 5/8-inch (15 7/8 mm) diameter rod and measured with a measuring tape. This equipment is pictured in Figure 3.5.

3.2.4. Unit Weight and Air Content of Fresh Concrete

A Type B Hogentogler pressure meter was used to find the air content of each fresh concrete mixture. The fresh concrete was placed in two layers and consolidated by a 5/8-inch (15 7/8 mm) diameter rod as pictured in Figure 3.6.

Figure 3.5. Slump Test Equipment

3.2.5. Temperature of Fresh Concrete

A digital thermometer (Figure 3.7) was used to determine the fresh concrete temperature. This thermometer can read from 0 to 392 °F and -17 to 200 °C.

Figure 3.6. Type B Hogentogler Pressure Meter

Conversion: 1 in. = 25.4 mm

Figure 3.7. Acurite Digital Thermometer

3.2.6. Formwork

All durability specimen formwork (Figure 3.8) was constructed using lumber. Cylinders were cast in plastic 4x8 in. (101.8x203.2 mm) molds (Figure 3.9).

Figure 3.8. Formwork for Durability Specimens

Figure 3.9. Cylinder Molds

3.2.7. Curing Equipment

All concrete specimens, excluding freeze-thaw specimens, were cured in the moist cure room in Butler Carlton Hall at Missouri S&T. The moist cure room contains a mister ensuring 95% relative humidity at all times. The freeze-thaw specimens were submerged in a limewater tank at ERL until age of testing. Mortar cubes were cured in water baths at three different temperatures based on mix design (Figures 3.10-3.12).

Figure 3.10. Room Temperature Water Bath

Figure 3.11. Hot Temperature Water Bath Tank

Figure 3.12. Cold Temperature Water Bath

3.2.8. Ovens

Two large ovens manufactured by Shel Lab (grey oven) in combination with one large oven (green oven) manufactured by Grieve (Figure 3.13).

Figure 3.13. Curing Ovens

3.2.9. Neoprene Pads

Neoprene pads were used in accordance to ASTM 1231-14 (Table 3.4). Neoprene pads are only permitted for a certain number of uses permitted by ASTM 1231-14.

Table 3.4. Neoprene Pad Requirements (ASTM 1231-14)

Compressive Strength,[A] MPa [psi]	Shore A Durometer Hardness	Qualification Tests Required	Maximum Reuses
Less than 10 [1 500]		Not permitted	
10 to 40 [1 500 to 6 000]	50	None	100
17 to 50 [2 500 to 7 000]	60	None	100
28 to 50 [4 000 to 7 000]	70	None	100
50 to 80 [7 000 to 12 000]	70	Required	50
Greater than 80 [12 000]		Not permitted	

3.2.10. Tinius Olsen Universal Machine

A servo controlled universal Tinius Olsen 200 kips (1,378.95 MPa) load frame was used to determine the Compressive Strength (concrete cylinders and mortar cubes, Figure 3.14) in accordance to ASTM C39-14. The same machine was used to determine the Modulus of Elasticity (MOE) in accordance to ASTM C469-14. All data was collected by the data acquisition system. For the modulus test, the concrete specimen was held in an apparatus that contained an LVDT, which measured axial strain during the test (Figure 3.15).

Figure 3.14. Tinius Olsen Universal Machine

Figure 3.15. Modulus Ring

3.2.11. Abrasion Resistance

Resistance to abrasion was measured based on ASTM C944-12. A drill press in hi bay lab at Missouri S&T with a rotary cutter (Figure 3.16) attached was used to test the specimens using a 44lb (19.96 kg) load (Figure 3.17).

Figure 3.16. Test Girder Delivery Process at Missouri S&T

Figure 3.17. Abrasion Testing Setup

3.2.12. Freeze-Thaw Resistance

Freeze-thaw (F&T) specimens underwent freeze-thaw cycles in the 17 slot Humboldt Freeze-thaw chamber in ERL (Figure 3.18). Every 36 cycles, each specimen was removed from the chamber once thawed and weighed. The Proceq Ultrasonic Pulse Velocity (UPV) meter (Figure 3.19) was used to measure the pulse velocity of each specimen.

Figure 3.18. Humboldt Freeze-Thaw Chamber

Figure 3.19. Proceq Ultrasonic Pulse Velocity Meter

3.2.13. Chloride Content

A drill press was used to drill for concrete powder samples prior to and after 3-month ponding of specimens. The powder samples were then analyzed with a Rapid Chloride Test meter from Germann Instruments for chloride content (Figure 3.20).

Figure 3.20. Rapid Chloride Test (RCT) Meter

3.2.14. Maturity Meter

Thermocouple wires were slid into the center of two concrete cylinders per mix design and paired with a Humboldt 4-channel maturity meter to gather temperature history to calculate maturity for each mix (Figure 3.21).

Figure 3.21. Humboldt Concrete Maturity Meter

3.3. MATERIALS

This section provides the materials used for the experimental study.

3.3.1. Portland Cement

Type I/II Portland Cement (Quikrete Cement Manufacture) was purchased from Lowe's Home Improvement store in Rolla, Missouri for purposes of this study.

3.3.2. Fly Ash

ASTM Class C fly ash was donated from Osage County Concrete in Linn, Missouri for use in this research project (Table 3.5).

Table 3.5. Chemical Composition Class C Fly Ash*

Item	AASHTO_M296	ASTM C618-12	Actual
Fineness (+325 Mosh)	34	34	15.2
Fineness Variation	5	5	0.6
Moisture Content	3	3	0.08
Density (g/cm3)			2.7
Density Variation	5, max	5, max	0.96
Loss on Ignition	5, max	6, max	0.12
Soundness	0.8	0.8	0.03
S.A.I. 7 days	75, min	75, min	98.7
S.A.I. 28 days	75, min	75, min	101.9
Water Req. % Control	105	105	94.2
SiO_2, Al_2O_3, Fe_2O_3 (Total)	50, min	50, min	35.17, 21.07, 6.58 (62.82)
Sulfur Trioxide SO_3	5, max	5, max	1.43
Calcium Oxide C_aO	-	-	26.46
Magnesium Oxide	-	-	0.22
Sodium Oxide Na_2O	-	-	1.91
Potassium Oxide K_2O	-	-	0.44
Available Alkali as Na_2O	1.5, max	-	1.31

*Note: Supplier: Headwater, source: Thomas Hill, MO

3.3.3. Aggregate

Fine aggregate used for all concrete batching was local, rounded, Missouri River sand. Coarse aggregate (Potosi dolomite) used was known to have a high durability factor and was obtained from Illinois for Phase I. However, due to limited storage space, aggregate was changed for Phase II. Coarse aggregate similar to the Illinois dolomite was obtained from Weber Quarry in New Melle, Missouri. Sieve analyses for coarse and fine aggregate are shown below in Figures 3.22-3.24, respectively. All aggregate properties are listed in Table 3.6.

Table 3.6. Aggregate Properties

Property	Coarse (Missouri Dolomite)	Coarse (Illinois Dolomite)	Fine (Missouri River Sand)
Nominal Maximum Size	3/4”	½”	⅜”
Specific Gravity	2.65	2.67	2.56
Absorption (%)	0.93	0.95	0.49
Bulk Density-Loose (lb./ft^3)	100.9	103.6	49.84
Bulk Density-Compacted (lb./ft^3)	112.2	115.1	52.64

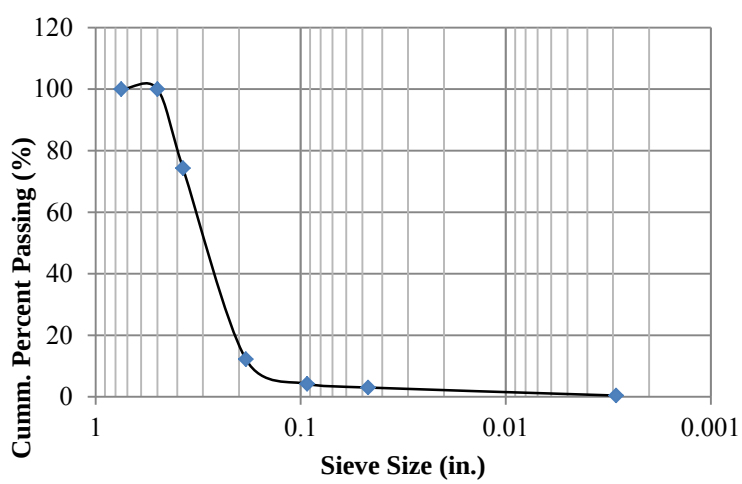

Conversion: 1 in. =25.4 mm

Figure 3.22. Coarse Aggregate Gradation - Missouri

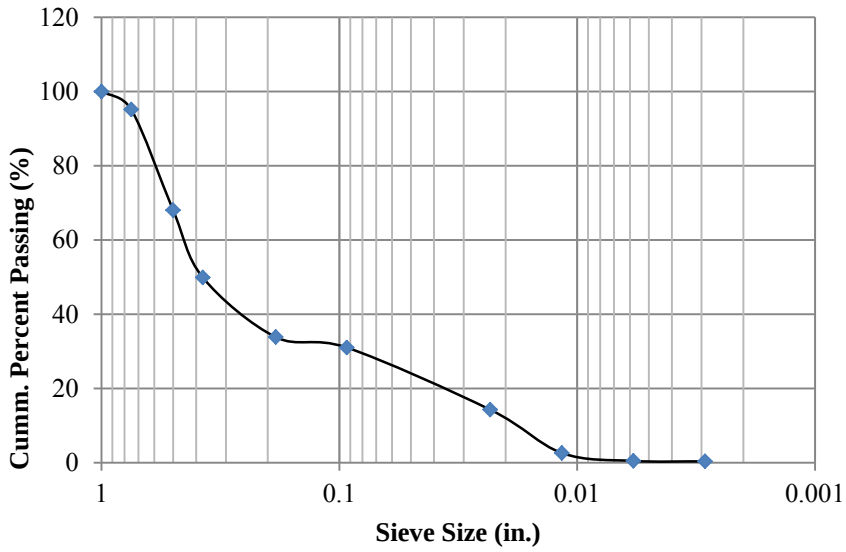

Conversion: 1 in. =25.4 mm

Figure 3.23. Coarse Aggregate Gradation - Illinois

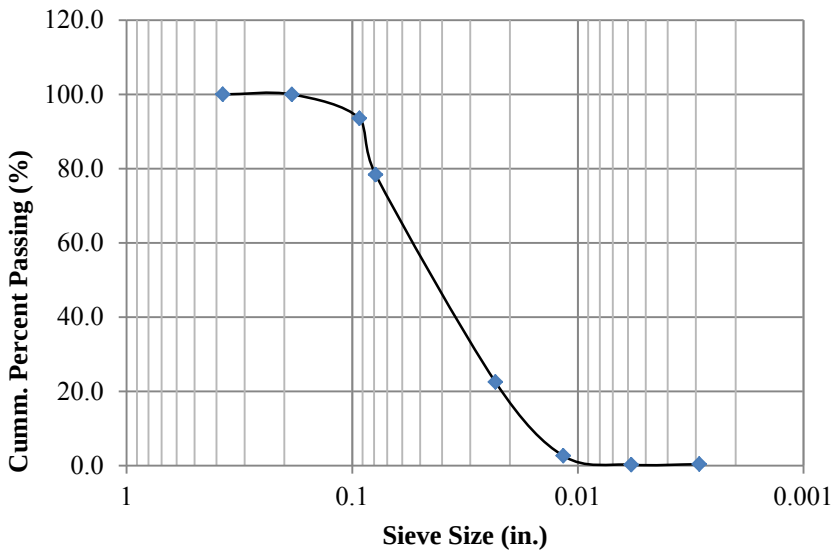

Conversion: 1 in. = 25.4 mm

Figure 3.24. Fine Aggregate Gradation

3.3.4. Mixing Water

Potable tap water from a hose in materials lab located in Butler-Carlton Hall at Missouri S&T was used for mixing of concrete.

3.4. TEST PROCEDURES

Test procedures for fresh and hardened concrete properties are discussed in this section. Any deviation from common practices will be noted.

3.4.1. Aggregate Moisture Content

Surface moisture content (SMC) and total moisture content (TMC) were obtained following ASTM C70-13. These values were then used to adjust the mix design before batching.

3.4.2. Mixing of Fresh Concrete

Mixing of fresh concrete followed ASTM C192-14; however, there were a couple modifications. Before mixing, the mixer was damped with water so the actual mixing water wouldn't be absorbed drawing it from the mix. Once this water was added, the mixer was started on a low speed and drained. The mixer was then set to a speed of 12 and the total amount of coarse aggregate was added the mixer. Next, the entire amount of sand was added to the mixer as well. This was mixed until the aggregates appeared well blended. Half of the water was then added. Finally, all cementitious material was added along with the remaining amount of water. The mixer then rested for the three minutes specified by ASTM C192-13 followed by more mixing until the mix appeared homogenous (2-3 min). Batching occurred on multiple days for each mix due to the capacity limitation of the 6.0 cubic foot mixer. Design weights for each mix are shown below in Table 3.7.

Table 3.7. Mix Design

Material (lb./yd^3)	CC	35	50	60	70
Coarse Aggregate	1706	1736	1400	1836	1836
Fine Aggregate	1210	1500	1400	1400	1400
Cement	750	488	375	300	225
Fly ash	0	263	375	450	525
Water	300	300	300	300	300
w/cm	0.40	0.40	0.40	0.40	0.40

Conversion: 1 lb. = 453.6g, 1 cy= 27 ft^3

Ponding and abrasion specimens were poured together in three batches. Freeze-thaw specimens were poured on another day. All batch weights were adjusted on mixing day to account for any differences (e.g. sand and crushed stone moisture contents). Phase II was completed following the same procedure months after Phase II batching had been completed.

3.4.3. Mortar Cubes

Cube molds were sealed with Vaseline to prevent leakage from the paste. Design weights were based on ASTM C1074-11 Appendix A 1.1.2. Each mortar mix was also adjusted for moisture content of the sand; typically, 18 cubes were batched at once (Table 3.8). Batching of mortar cubes for use in the maturity method followed ASTM C109-13. For each mix, 54 cubes were molded. After molding of cubes, 18 cubes for each mix were placed in their respective water baths (Table 3.9).

Table 3.8. Batch Weights for Mortar Cubes (18 cubes)

	CC	35%	50%	60%	70%
Fine Agg. (lb.)	13.2	13.5	14.2	14.2	14.2
Cement (lb.)	5.8	3.8	2.9	2.3	1.7
Fly ash (lb.)	0.0	2.0	2.9	3.5	4.1
Water (lb.)	2.37	2.37	2.38	2.38	2.38

Conversion: 1 lb.= 453.6g

Compressive Strength of the mortar cubes was tested using universal testing machine (UTM) at a load rate of 200 lb./sec (90.72 kg/sec), which is within the acceptable range provided by ASTM C109-13. Before each test, the faces of the cube were sanded and the testing planes were brushed off from any debris. Using ASTM C1074-11 Appendix A1.1.4, three cubes were tested when their compressive strength was approximately 583 psi (4MPa) and then three more cubes were tested at each successive test equal to twice the age of the previous test. Based on the strength gain curves the k-value was found using A1.1.8.2. From here, the datum temperatures were determined by A1.2 for each mix design.

Table 3.9. Mortar Water Bath Temperatures (°F)

	Bath 1	Bath 2	Bath 3
CC	46.2	66.2	106.0
35	46.2	66.2	106.0
50	66.2	78.4	106.0
60	66.2	78.4	106.0
70	66.2	78.4	106.0

Conversion: °C= (°F-32)/1.8

3.4.4. Temperature of Fresh Concrete

Using the Acurite thermometer, the temperature of each fresh concrete mix was measured following ASTM C1064 by placing the thermometer into the wheel barrow of fresh concrete. When temperature was stabilized, it was recorded.

3.4.5. Slump of Fresh Concrete

Slump was determined according to ASTM C143-12 immediately after mixing.

3.4.6. Unit Weight and Air Content

Unit weight was calculated in accordance with ASTM C138-14. Once the air content container was weighed for empty weight, concrete was placed in the air content container in two layers and rodded 25 times each. The top was struck off with a metal trowel and wiped down for any spillage. The container was then weighed on the floor scale in pounds. Air content was measured using a Type B vertical air chamber pressure meter following ASTM C231-14. The same concrete sample was used for air content following unit weight measurement.

3.4.7. Compressive Strength of Concrete Cylinders

Cylinders (4-inch diameter) were cast in accordance with ASTM C192-14 in order to perform compressive strength tests. Compressive strength was determined in accordance to ASTM C39-14. Neoprene pads were used to cap cylinders during testing.

3.4.8. Modulus of Elasticity of Concrete Cylinder

Cylinders for modulus of elasticity were prepared as in 3.4.7. ASTM C469-14 was followed to determine modulus of elasticity. Neoprene pads were used to cap cylinders during testing. Tests were run on three replicate cylinders. The first gave the compressive strength. The second two cylinders were run to 40% of that compressive strength three times apiece. The second and third run on each cylinder was recorded and the average is specified as the modulus. During Phase II-Accelerated curing, the cylinders were sensitive to 40% loading, so in some cases only 25-35% of peak load was used for Modulus loading.

3.4.9. Abrasion Resistance

Abrasion specimens were 3.5 x 6 x 16 in. (88 x 152.3 x 406.4 mm) in size and cast in accordance with ASTM C192-13. Instead of rodding the specimens, a battery power operator was used to vibrate specimens. All specimens were finished with a steel trowel minutes within casting. Specimens were cured in the moist cure room for 14 days before lab curing until age of test. ASTM C944-12 was the test method used for abrasion testing at 28, 56, 90, and 120 days. For Phase II, specimens were cured in the oven from hour 24 to hour 72 and tested at 14 and 28 days. A double load of 44lb (19.96 kg) was used to abrade the specimens. The specimens were abraded three times for 2 minutes each time. Between each 2-minute session, the specimen was brushed off and weighed. This process was repeated two more times on different locations of the specimen (Figure 3.25).

Figure 3.25. Post-Test Abrasion Specimen

3.4.10. Chloride Ion Penetration

Chloride specimens were cast according to ASTM C192-13 with dimensions of 12 x 12 x 4 in. (304.8 x 304.8 x 101.6 mm) and only one specimen cast per mix design. Specimens were vibrated instead of rodded. Each specimen was cured for 14 days in the moist cure room after demolding. After the completion of moist cure, the specimens were set downstairs until age of testing (temperature 70 °F and 45% relative humidity). One specimen was ponded with 3% NaCl solution at four different ages (28, 56, 90 and 120 days) for Phase I. Phase II specimens were placed in the oven at 24 hours after casting and removed after 48 hours of curing. The specimens were then ponded at 14 and 28 days. Sampling (Figure 3.26) of powder for chloride concentration was in conformance with ASTM C1543-10. Each block was sampled after 3 months of ponding.

At least $3.3 * 10^{-3}$lb (1.5g) samples were taken at the intervals within those listed in ASTM C1543-10 (Table 3.10).

Figure 3.26. Chloride Ion Penetration Specimen

Table 3.10. Ponding Sample Interval

Sampling Intervals (in)	
ASTM Range	Sample Range
0.39-0.79	3/8-3/4
0.98-1.38	1.0-1.4
1.57-1.97	1.6-2.0
2.17-2.56	2.2-2.5

Conversion: 1in=25.4mm

The equipment was calibrated before each use and the calibration results were used to find the chloride content once the mV was found using the RCT meter. Findings will be classified using the ranking proposed by Broomfield (2007) (Table 3.11).

Table 3.11. Correlation between %Cl by Mass of Concrete and Corrosion Risk

% Chloride by mass of concrete	Corrosion Risk
<0.03	Negligible
0.03-0.06	Low
0.06-0.14	Moderate
>0.14	High

Adapted from Broomfield, 2007

3.4.11. Freeze-Thaw Resistance

Freeze-thaw specimens were cast according to ASTM C192-13 except specimens were vibrated by a handheld battery operated vibrator instead of being rodded. Prisms were 3.5 x 4 x 16 in. (88 x 101.6 x 406.4 mm) and cured in limewater bath until age of testing for Phase I. For phase II, specimens were cured in the ovens starting at 24 hours for a length of 48 hours then lab cured. ASTM C666-03 procedure A was the test method performed. This method specifies test should end on a thaw cycle. However, tests ended on a freeze cycle and allowed to thaw in the chambers. Ultrasonic pulse velocity (UPV) was measured after each set of 36 freeze-thaw cycles. These values were used to calculate the durability factor (DF) using Section 9 of ASTM C666-03. Examples of a set of specimens are shown in Figure 3.27.

(a) Before (b) After

Figure 3.27. 60-Cycle Freeze-Thaw Specimens

Once the specimens reached the specified number of 300 total cycles, or when the relative dynamic modulus (RDM) reduced to 40%, the test was considered completed. Testing could also be terminated if the specimens deteriorated and testing could no longer continue. Once finished, the RDM of elasticity was calculated using Equation (3.1).

$$\boldsymbol{P_c = \frac{n_1^2}{n^2} x100} \tag{3.1}$$

Where P_c is the RDM at c cycles of freezing and thawing; n_1 is the frequency (1/T); T is the time of one-pulse wave in micro seconds at c cycles of freezing and thawing; and n is the fundamental transverse frequency at 0 cycles of freezing and thawing. The durability factor is then calculated using Equation (3.2).

$$\boldsymbol{DF = \frac{PN}{M}} \tag{3.2}$$

Where P is the RDM at N cycles (%), N is the number of cycles at which P reaches the specified minimum value for discontinuity the test or the specified number of cycles at which the exposure is to be terminated, whichever is less, and M is the specified number of cycles at which the exposure is to be terminated.

3.4.12. Maturity Method

ASTM C1074-11 detailed the process for maturity of the concrete. Thermocouple wires were placed in two cylinders from each mix. The temperature was recorded every 30 minutes for the first 48 and then each hour after. Recordings were taken for 28 days and all temperature data was recorded. Once the cylinders cured for 28 days, the wires were cut and the cylinders were then used for other testing (compressive strength). Using the data from mortar cube testing, the datum temperature (T_0) was determined by A1.1.8.2 of ASTM C1074-11. Using the Nurse –Saul maturity function, the maturity index (M) can be calculated with Equation (3.3).

$$\boldsymbol{M(t) = \sum_{0}^{t} (T - T_0)\Delta t} \tag{3.3}$$

Where M(t) is the maturity index (expressed in degree-days or degree-hours); Δt is the time interval (expressed in days or hours); T is the average concrete temperature during the interval Δt; and T_0 is the datum temperature. ASTM C1074-11 states the datum temperature can be taken as 50°F (10°C). For this experiment, a datum temperature was obtained.

At the testing of each cylinder for compressive strength (3, 7, 14, 28 days) the maturity is evaluated by Eq. (3.3). This data along with the compressive strength is plotted. A best-fit curve is also plotted and used to estimate the in-place concrete strength of the respective concrete mixture. Using this strength-maturity relationship, as desired, an estimate of in-place strength can be gathered using the temperature history of the concrete at that time (Kaburu, 2015).

The maturity method may be useful for estimating concrete strength when cured at different temperatures by also using Equation (3.4)

$$\boldsymbol{t_e = e^{-Q(\frac{1}{T_a}-\frac{1}{T_s})}\Delta t} \tag{3.4}$$

Where t_e is the equivalent age over a time interval (Δt) at a specified temperature (T_s) in days or hrs. T_a is the average temperature of the concrete during Δt. Q is the activation energy divided by the gas constant. All temperatures and Q are in Kelvin.

3.4.13. Accelerated Curing

To accelerate the curing of each mix, three different ovens were set at 100°F (37.8°C), 130°F (54.4°C), and 160°F (71.1°C). Specimens were demolded at 24 hours and immediately placed into the oven. Afterwards, they were stored in the material lab under control conditions (room temperature and humidity). Oven curing occurred for 48 hours then specimens were removed and finished curing in the basement until ages of tests.

4. RESULTS AND DISCUSSION

4.1. FRESH CONCRETE TESTS

Fresh concrete tests included slump, air content, and temperature. Table 4.1 shows a summary of the fresh concrete properties. In this table, the values are averaged from pours for Phase I and Phase II.

Table 4.1. Fresh Concrete Properties

Mix ID	CC	35	50	60	70
Slump (in)	7	7 3/4	7 1/2	7 3/4	7
Room Temp (°F)	71.2	70.4	59.8	70.8	72.2
Concrete Temp (°F)	71.1	71.3	62.8	71.6	73.0
Air Content (%)	2.3	2.2	1.6	1.3	1.6
Mass (lb.)	36.5	37.1	37.2	37.3	37.3
Density (lb./ft^3)	139.1	141.6	142.0	142.4	142.4

Conversion: 1°C=5/9(°F-32)

4.1.1. Slump Tests

To ensure consistency and comparison between mixes, a target slump of 7 ± 1 in. was targeted for all mixes and water-to-cementitious (w/cm) ratio was held at 0.40 across the mixes. As the amount of fly ash increases, so does the slump. When keeping the amount of water consistent, the slump tends to increase. The proportion of fines and coarse aggregate was adjusted to curb this effect. When cement was replaced at 70%, it was difficult to lower the slump below 7 inches (177.8 mm). Table 4.1 shows the slump for each mix and each phase. The value listed in the table was the average of the slumps for Phase I and Phase II.

4.1.2. Unit Weight and Air Content

The density across all mix designs was consistent with a value of around 142 lb./ft^3 (2.272 g/cm^3). This density value is close to the typical value of 145 lb./ft^3 (2.32 g/cm^3) in normal weight concrete. Since the same aggregate and paste materials were

used in all mix designs, it makes sense that the density value was approximately the same for all of the mixtures. As expected, the air content was also relatively similar between the mixes. The control mix and the 35% HVFAC mixes had the highest percent of measured entrapped air at 2.2% and 2.3 %, respectively. As the percent fly ash increased, generally, the percent air decreased. This is due in part to the fact that fly ash fills gaps refining the pore structure. Naturally, this reduces entrapped air.

4.2. HARDENED CONCRETE PROPERTIES

Hardened properties investigated in both phases included compressive strength and modulus of elasticity. The maturity method was also employed during Phase I to estimate concrete strength at different ages and temperatures.

4.2.1. Compressive Strength

As the percent of fly ash increased, the compressive strength gain was delayed further. Mohamed (2011) discovered the optimum replacement level to be 30%. In that study, the compressive strength increased up to 30% replacement by fly ash. After the optimum 30% was reached, there was a decline in strength at levels greater than 30%. However, in this study, 50% was found to be the optimum replacement level (Figure 4.1).

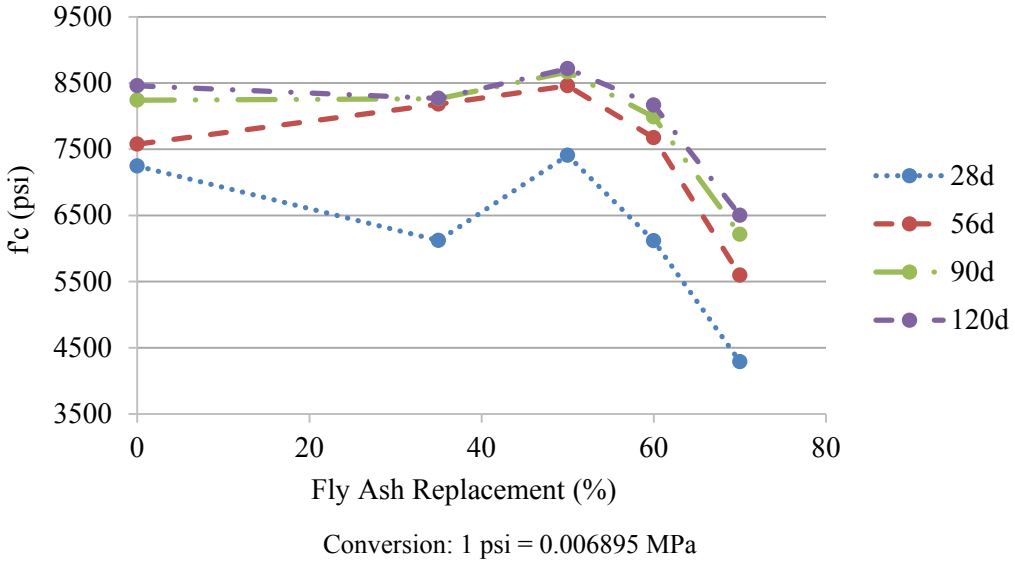

Figure 4.1. Compressive Strength vs. Percent of Fly Ash

Strengths were similar up to 50% and then a decline in compressive strength was seen at levels greater than 50% replacement. Figures 4.1 and 4.2 show that mixes at all levels continue to gain compressive strength throughout the entire 120-day period. However, the conventional concrete gains little compressive strength past 28 days while the fly ash gains the most compressive strength between 28 and 56 days. Past 56 days little compressive strength is gained.

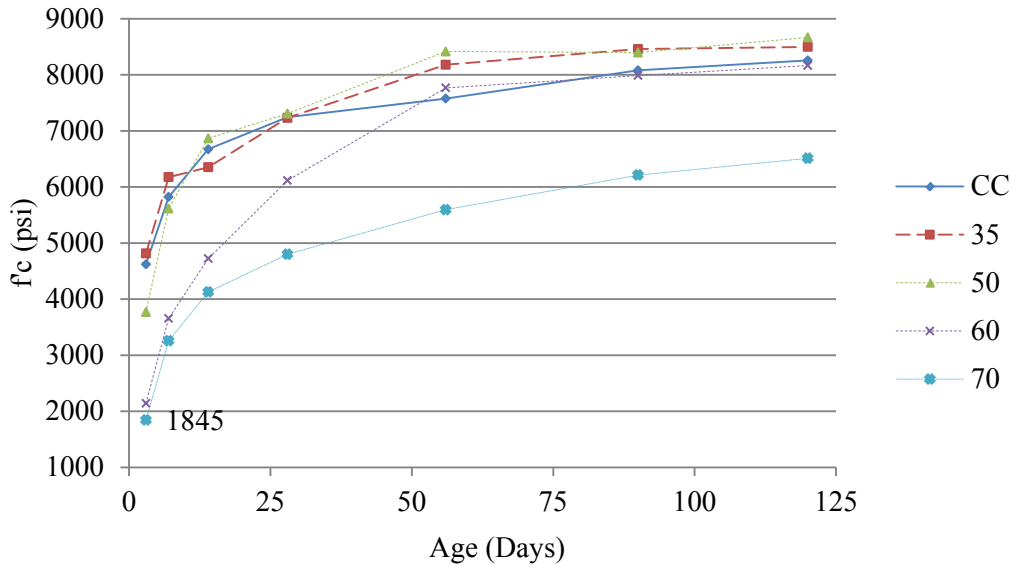

Conversion: 1 psi = 0.006895 MPa

Figure 4.2. Concrete Compressive Strength Gain-Phase I

The greatest compressive strength gains result from the 50% mix between 3 and 7 days. After 7 days, the conventional, 35% and 50% perform very similar until 56 days where the 35% and 50% mixes gain more compressive strength than the conventional mix (Figure 4.2). This further displays the delayed hydration in HVFA concrete. After 28 days the conventional mix levels out while the HVFAC mixes are still gaining compressive strength. The 60% HVFAC becomes equivalent to that of the control mix around 60 days. Although the 35% and 50% exceed the conventional mix and the 60% mix becomes equivalent to the conventional mix, the 70% HVFAC fails to ever gain greater compressive strength than the conventional mix. In fact, the 70% HVFAC never gains compressive strength equivalent to that of the conventional mix at 28 days where as

the 60% gains equivalent compressive strength at 56 days and the 35% and 50% showed similar 28 day compressive strengths to that of the conventional mix.

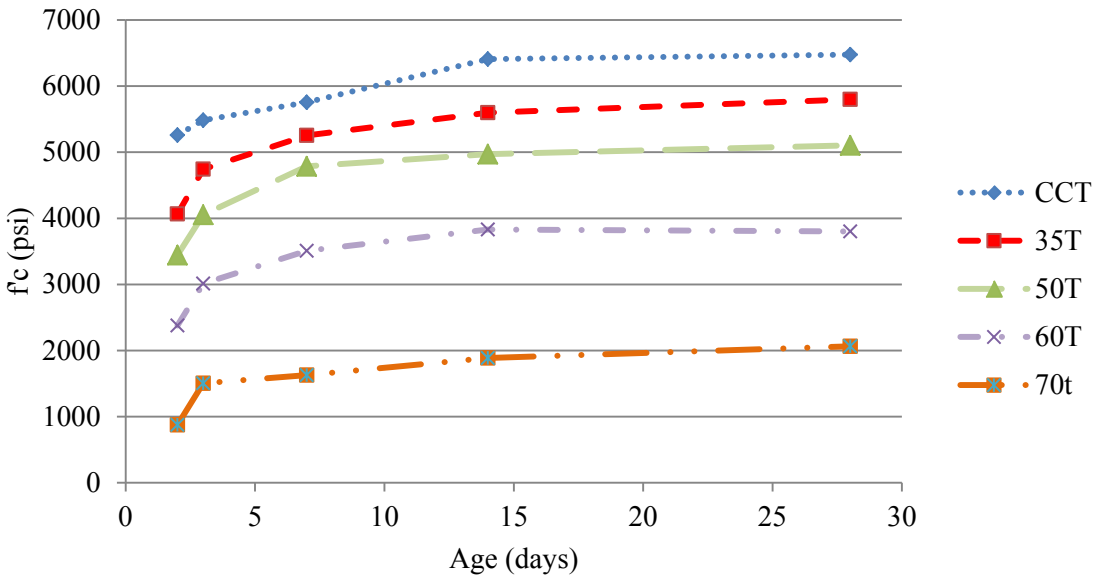

Conversion: 1 psi = 0.006895 MPa

Figure 4.3. Compressive Strength at 100°F (37.8°C)

Phase II consisted of the same concrete mixes as Phase I. However, these mixes were cured in an oven for 48 hours after demolding. Three temperatures were selected: 100°F (37.8°C), 130°F (54.4°C), and 160°F (71.1°C). Myers and Carrasquillo (1998) discovered the largest increase in compressive strength from accelerated curing occurs in the first couple of days and curing above a temperature rise of 68°F (20°C) may result in a decrease in later-age compressive strength due to micro cracks that can form in the transition zones reducing compressive strength potential. In Phase II, there is generally a significant increase in compressive strength between day 2 and 3 in all mixes at all curing temperatures (Figures 4.3-4.5). As the curing temperature increases, the rate of compressive strength gain decreases. Within Phase II between days 3 and 7, at 100°F (37.8°C) there is a slight increase in compressive strength before topping out post 14 days. The conventional and 35% mix at 160°F (54.4°C) also continues to see an increase in compressive strength between 3 and 7 days. Specimens cured above 100°F (37.8°C) level out prior to the 14-day mark (Figure 4.3). In fact, at 160°F (71.1°C), the

compressive strength remained constant after 3 days (Figure 4.5). Curing regime seemed to affect the 70% HVFAC mix the greatest at all temperatures of curing. It is suspected this is due to the increased delay in hydration at such high replacement levels. Free water demand was unavailable within the concrete during curing; therefore, sufficient hydration did not occur in the short time frame given.

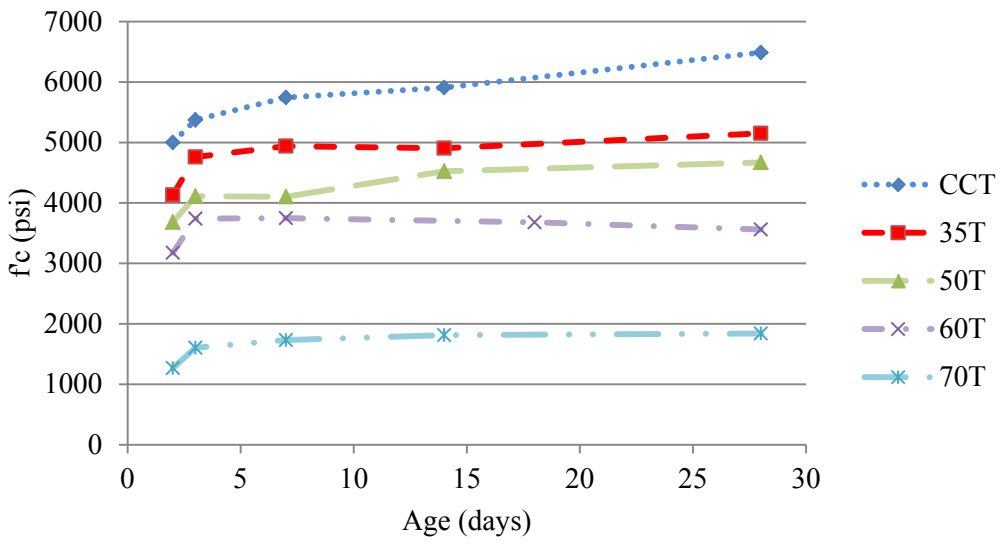

Conversion: 1 psi = 0.006895 MPa

Figure 4.4. Compressive Strength at 130°F (54.4°C)

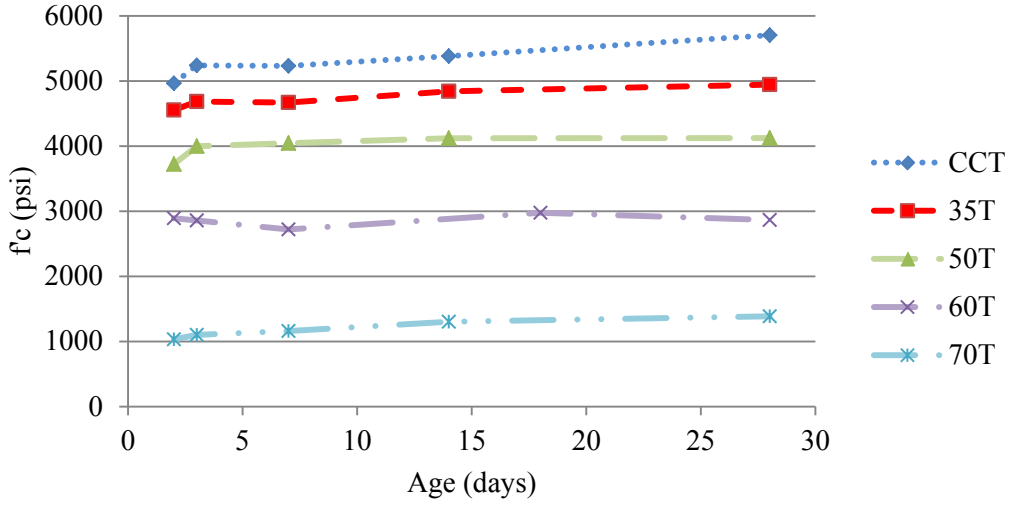

Conversion: 1 psi = 0.006895 MPa

Figure 4.5. Compressive Strength at 160°F (71.1°C)

Figure 4.6 displays compressive strength for each mix as a percentage of the compressive strength from Phase II moist cure regime for 3 and 7 days. Figure 4.7 shows the same ratio for 14 and 28 days. Phase II specimens did not perform very consistently especially early on. At 3 days and each curing temperature, there was an increase in compressive strength from conventional curing (Except 70% HVFAC). However, there was no increase in compressive strength compared to conventional curing methods post 3 days. In fact, there was a decrease in compressive strength which increased as the curing temperature increased.

Curing at 100°F (37.8°C) seemed to be the least detrimental to strength gain at early and later-ages. Although specimens were cured at 100°F (37.8°C), they did not achieve similar strengths to that as the conventional method; these specimens had the largest compressive strengths when compared at all fly ash replacement level and ages of concrete in Phase II.

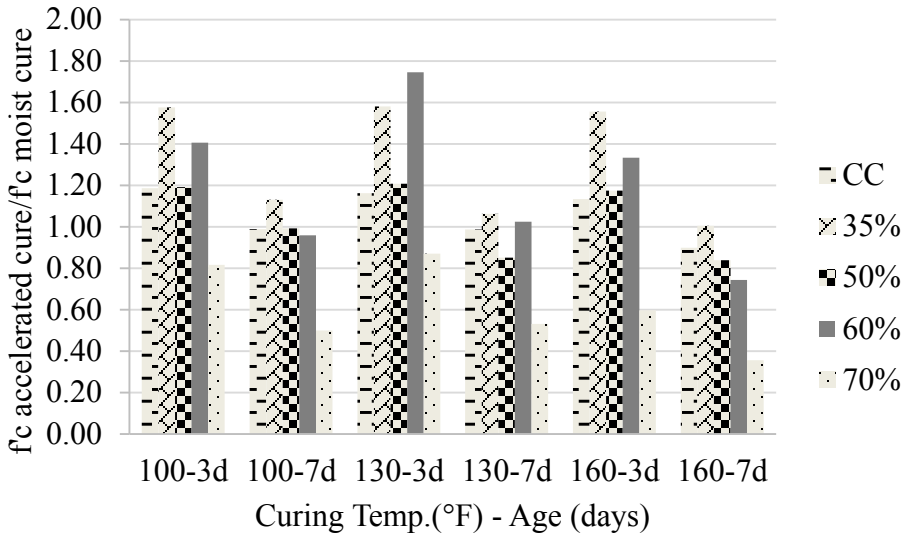

Conversion: 1°C=5/9(°F-32)

Figure 4.6. Normalized Compressive Strength in Phase II-3 and 7-day

The accelerated curing mostly affected the early ages of 3 and 7 days. Of those two ages, 3 days was the most influenced. At 3 days of age, all mix designs exhibited over a 1% increase in compressive strength for all three temperatures. The most drastic increase (> 35% fly ash) is seen at 3 days for the 35%-60% fly ash mixes with 60%

showing above a 70% increase when cured at 130°F (54.4°C). At 7 days in age, only the 35% fly ash mix nearly matches the control. By 14 days in age there is a reduction in compressive strength of all mixes except 35% and 50% fly ash cured at 100°F (37.8°C). HVFAC with 70% replacement is drastically affected at all ages and curing temperatures further suggesting that at high volumes of replacement, the concrete is more sensitive to curing regimes. The 35% mix seemed to respond the most consistently to the curing method having the highest percent at most ages and curing temperatures. Overall, the mixes seem to perform best in term of compressive strength (i.e. exhibit strength gain) when cured at 100°F (37.8°C). Accelerated curing was proposed in order to gain 28 day properties at 14 days. Although specimens performed well early on, Figure 4.7 displays that this goal was not achieved in terms of compressive strength. As mentioned in Section 2.6.1, Gjorv et al. (1990) speaks of the phenomenon that occurs when cement hydrates too quickly. The quick hydration of cement particles blocks the rest of the concrete from hydrating. In terms of HVFAC, the delayed reaction of fly ash hydration in combination with accelerated drying removing the water and the cement particle blocking hydration products, this method of curing can be very detrimental. Furthermore, Yazıcı et al. (2005) goes on to say that accelerated curing is only beneficial if interested in compressive strength gain at 1 day.

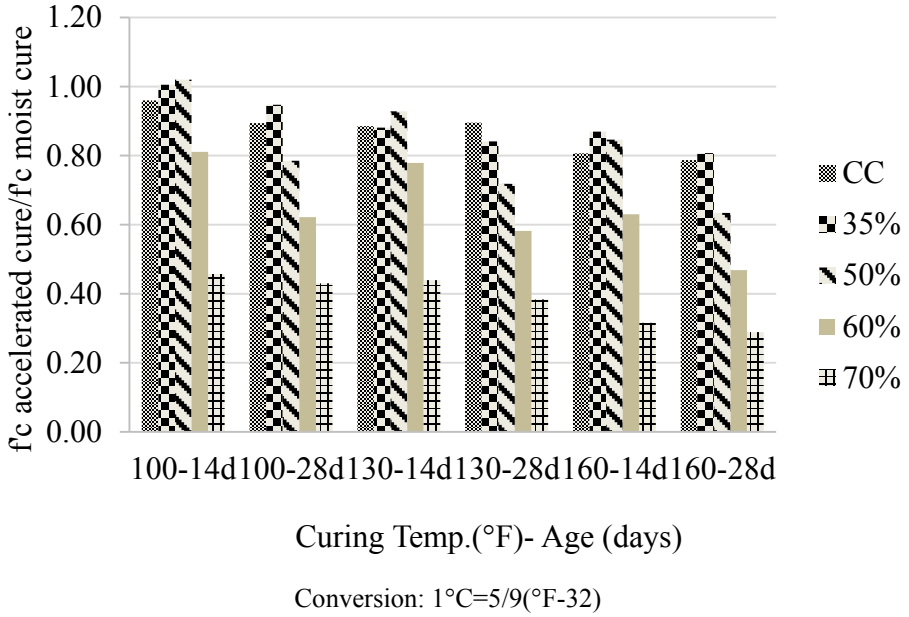

Figure 4.7. Normalized Compressive Strength in Phase II-14 and 28-day

4.2.2. Modulus of Elasticity

There is a strong correlation between compressive strength and modulus of elasticity (MOE) of concrete (Figure 4.8). As the ACI equation suggests [Equation (2.1)], the findings were linear at every replacement level once adequate compressive strength was gained. At 7 days however, when the 60% and 70% had gained only 1,000 psi (6.89 MPa), the MOE was lower than what the equation predicted. Between the range of 3,500 psi (24.13 MPa) and 6,000 psi (41.37 MPa), the higher fly ash levels actually exceed the conventional mix in terms of MOE. Although, at 7,500 psi (51.7 MPa), 50% and beyond plateau while the conventional mix continues to gain stiffness.

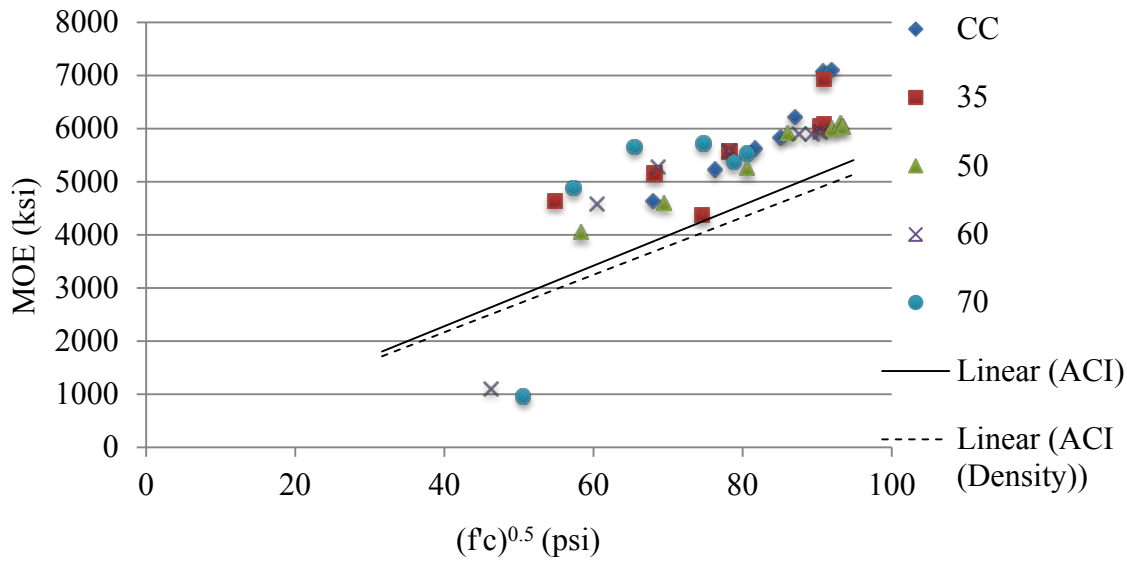

Conversion: 1 psi = 0.006895 MPa

Figure 4.8. Compiled MOE vs. Compressive Strength (Phase I)

Figure 4.9 conveys MOE as a function of compressive strength using the conventional mix as the baseline value and normalizing the HVFAC results. MOE for each mix with fly ash was divided by the MOE of the conventional mix to directly compare the results. When comparing MOE at different ages, the conventional mix consistently had higher stiffness than the other mixes but not by a significant amount. Up to 50% HVFA the MOE was within 20% of the conventional mix. Although the HVFAC mixes do not outperform the conventional mix at specific compressive strengths, each mix exceeded the predicted ACI value once it reached 2,500 psi (17.24 MPa) in terms of

compressive strength. Results convey that as the HVFA concrete is allowed to gain strength it will also gain appropriate stiffness.

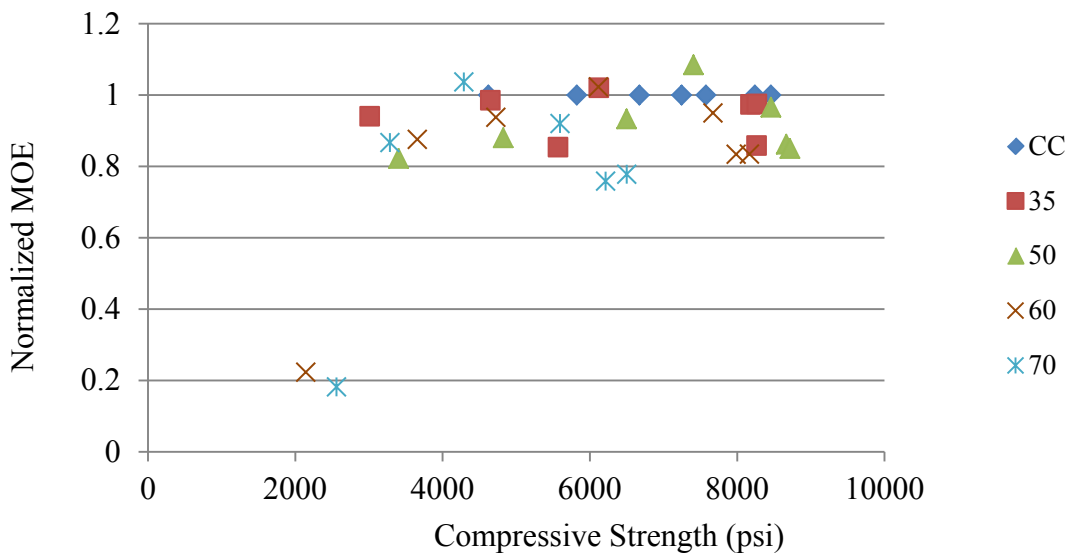

Conversion: 1 psi = 0.006895 MPa

Figure 4.9. Normalized MOE vs. Compressive Strength

The MOE for the conventional concrete and the HVFA concrete is presented in Figures 4.10 and 4.11. Setting the y-intercept to zero in Figure 4.10 yields an R^2 value equal to 0.8382 displaying a linear correlation.

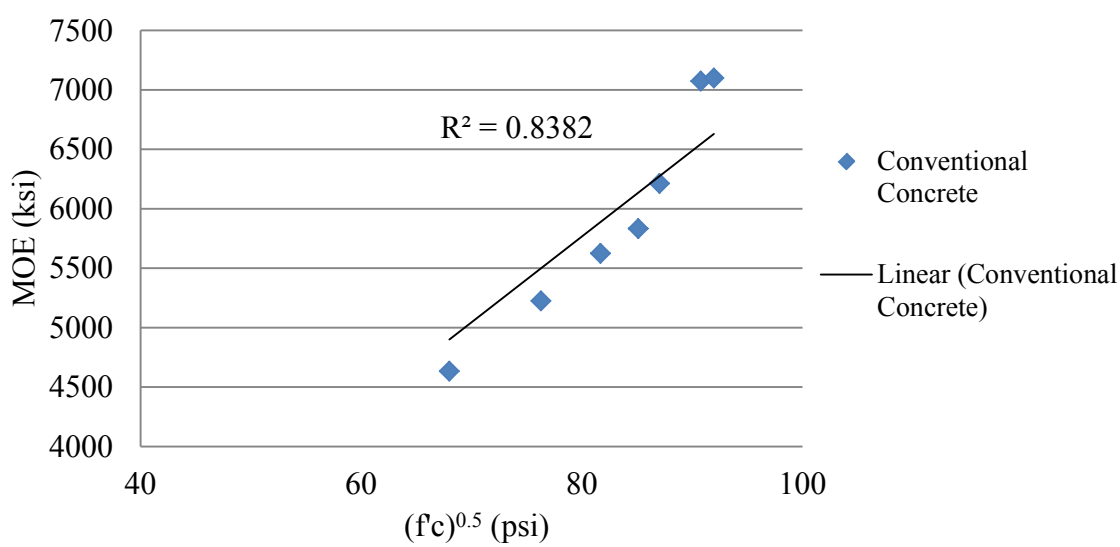

Conversion: 1 psi = 0.006895 MPa

Figure 4.10. MOE vs. Compressive Strength (Phase I) - Conventional Concrete

The HVFAC data (Figure 4.11) yields an R^2 value equal to 0.8537 (not displayed) using a polynomial trend line. However, when fitting the data with a linear trend line, the R^2 value drops to 0.4808 including all the HVFAC data. Furthermore, if you do not include the 70% HVFAC data points, the R^2 value increases to 0.6975. An important observation to consider is the number of data points. There are only 20 data points shown in this figure. Relative to the amount of previous research on HVFAC, this value is low. This could be the explanation for lower correlations to linear trends.

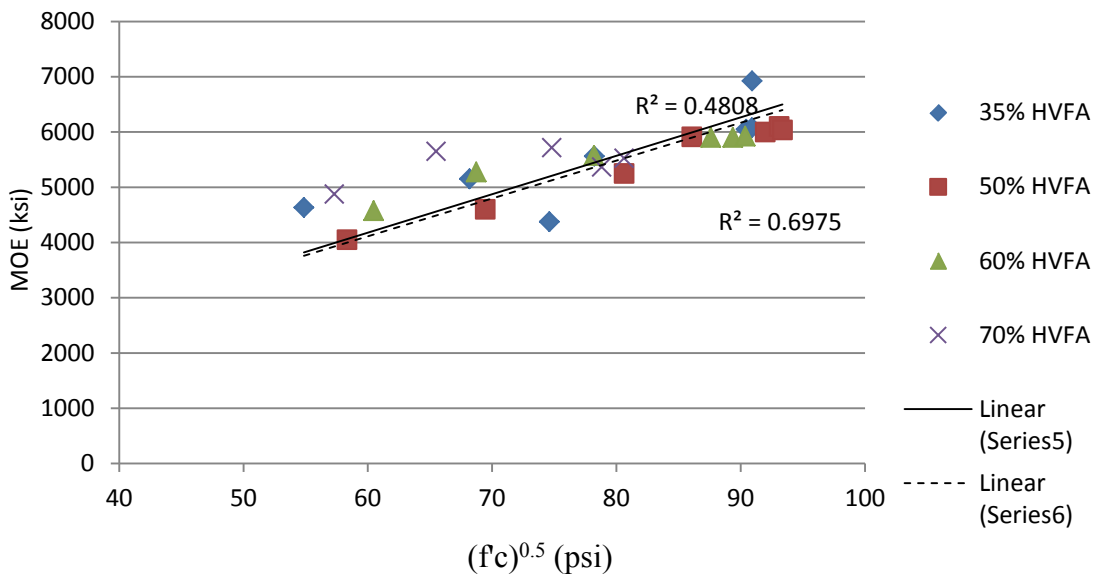

Conversion: 1 psi = 0.006895 MPa

Figure 4.11. MOE vs. Compressive Strength (Phase I) - HVFA Concrete

Figure 4.12 represents MOE values from this research and previous studies. Included are conventional mixes and HVFA mixes MOE values from this research. The results presented in this report fall in line with previous findings. From this figure it is concluded that there is no significant separation between MOE values for HVFAC and conventional concrete. Again, the majority of the data falls above the ACI equations based on compressive strength. Listed in Table 4.2 is a summary of all the linear curve fit equations.

Table 4.2. Linear Fit Equations

Figure	Linear Fit Equation	
4.10	y=72.079x	
4.11	y=68.516x	w/o 70%
4.11	y=69.618x	with 70%
4.12	y=70.211x	

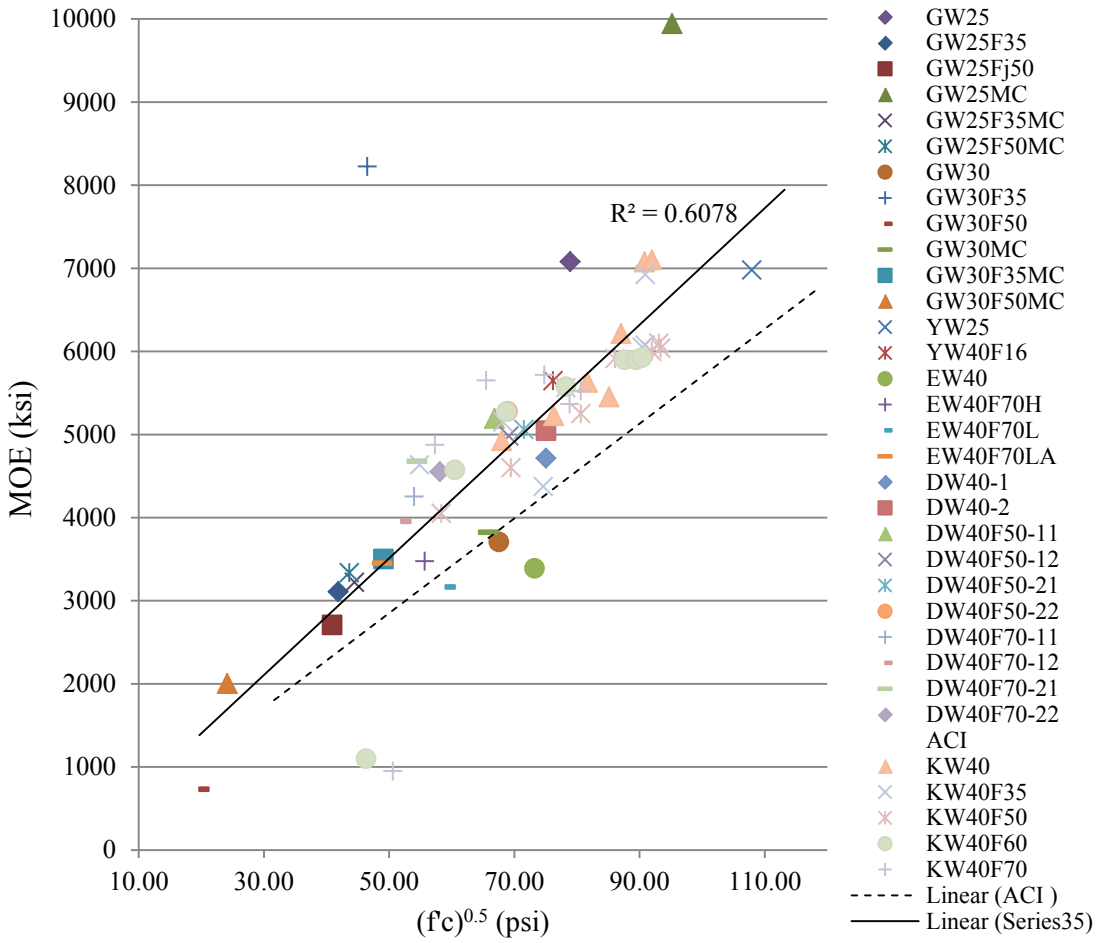

Conversion: 1 ksi = 6.895 MPa

Figure 4.12. Modulus of Elasticity Database

Figure 4.13 plots the MOE versus amount of fly ash (%). This figure is similar to Figure 4.1 for compressive strength. At early ages (28 and 56 days) the MOE is very similar for all mixes. Figure 4.2 displayed that HVFAC compressive strengths were lower at 28 and 56 days yet HVFAC exhibits higher relative stiffness to compressive strength

concluding that the fly ash mixes perform better than the conventional mix when it comes to MOE development per unit strength.

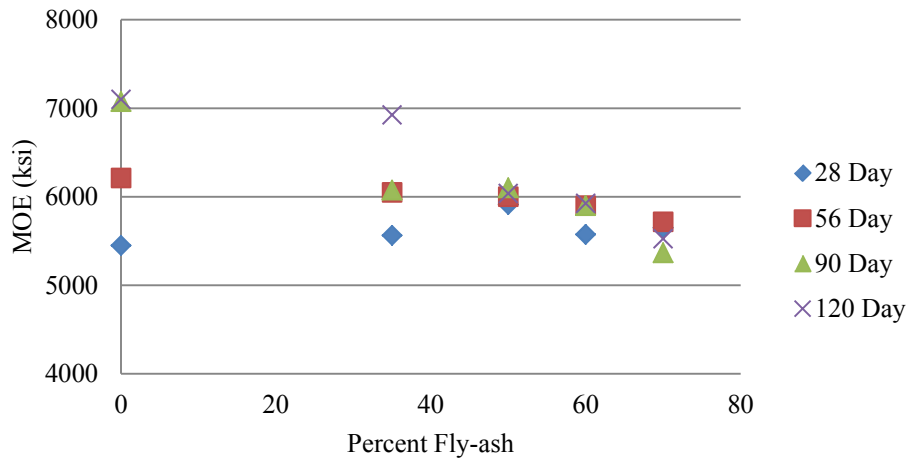

Conversion: 1 ksi = 6.895 MPa

Figure 4.13. MOE vs. Percentage of Fly Ash

As the percent fly ash increases however, the MOE decreases but not significantly. Unlike the compressive strength, 70% HVFAC performs similarly to other mixes in terms of MOE at all ages. At 0 and 35% replacement levels, the stiffness continues to increase as the concrete ages. However, at levels greater than 35% this is not true. Replacement levels at 50% and above show a reduced rate in stiffness gain per unit compressive strength with age. These concrete mixes do not gain stiffness as they age. Their stiffness at 28 days is the stiffness expected at 120 days as well.

4.2.3. Maturity Method

Using ASTM C1074-11, the maturity method was implemented with the 5 mix designs in Phase I of this research. First, mortar cubes were tested to determine the datum temperatures (T_o) for each mix (Table 4.3). ASTM C1074-11 suggests using a datum temperature of 32°F (0°C) for conventional concrete. However, other researchers propose that value is too high (Rohne and Izevbekhai, 2009). As Table 4.3 indicates a value of 32°F (0°C) for conventional concrete is in fact too high, but a conservative approximation.

Table 4.3. Datum Temperatures

Mix ID	T_o(°C)	T_o(°F)
CC	-1.2	29.9
35	4.2	39.5
50	4.9	40.8
60	5.4	41.7
70	5.4	41.6

After determining datum temperatures, the maturity index can be computed using the temperature history (Figure 4.14) from the moist cured cylinders [64.4°F (18°C)]. Temperature history data was gathered by using a 4-Channel James Meter manufactured by Humboldt. Temperatures were recorded at every half hour up to 48 hours and every hour afterward. The meter was disconnected on the 28th day.

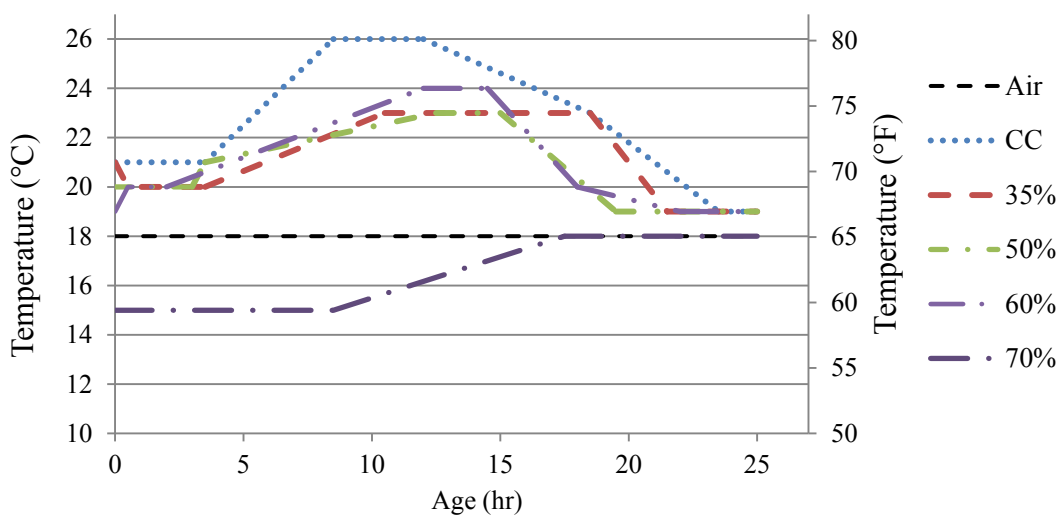

Figure 4.14. Temperature-Time History

The maturity index is the area under each temperature-time history curve. Using the temperature history and the Nurse-Saul's Equation (3.3), the maturity can also be found. Once the maturity index is calculated for each mix, it is plotted against the compressive strength from lab testing for concrete strength estimation (Figure 4.15).

Figure 4.15 allows for estimation of compressive strength at any time the maturity index is known from the temperature-time history. Using the temperature data from the in-place concrete the maturity index is computed again using Equation (3.3). Next, the maturity index of respective mix from laboratory testing (best fit curve) can be used to estimate the compressive strength. Many construction practices are dependent upon the concrete compressive strength for release of their cast-in-place (CIP) formwork to increase construction productivity.

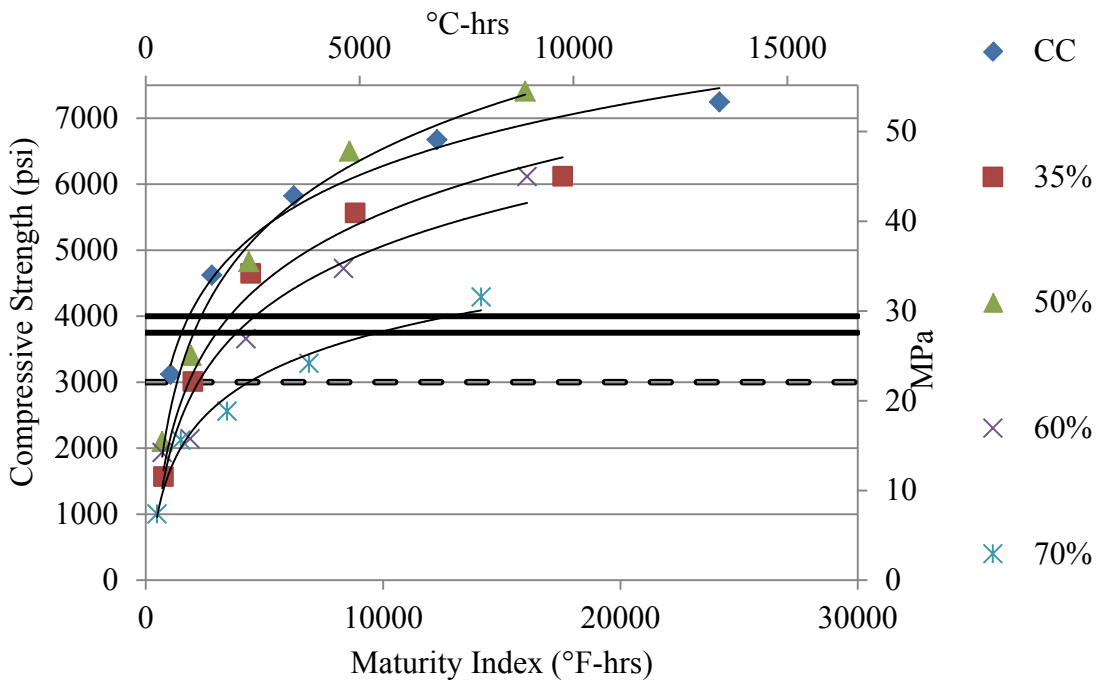

Figure 4.15. Compressive Strength vs. Maturity Index

Using the maturity method can help determine the appropriate times for construction activities such as the removal formwork, post-tensioning, opening roadway to traffic, etc. When considering Bridge A7957 the target strength for the HVFAC was 3,000 psi (20.68 MPa) and the conventional mix 4,000 psi (27.58 MPa). Listed below in Table 4.4 is the required 28-day strength (f'_c) and required strength for formwork removal (f_c) set forth by MoDOT for specific class of concrete. These markers are also plotted on Figure 4.15. The class of concrete is defined in Table 4.5.

Table 4.4. MoDOT Requirements for Structural Concrete

MoDOT Class of Concrete	Cement Factor (lb/cyd)	f'_c (psi)	f_c (psi)	E_c (ksi)
B	525	3000	1200	3156
B-1	610	4000	1600	3644

Conversion: 1,000 psi=6.895 MPa. Adapted from MoDOT (2013)

Table 4.5. Class of Concrete Description

Application	MoDOT Class of Concrete
Integral End Bents (Below lower construction joint)	B
Semi-Deep Abutments (Below construction joint under slab)	B
Intermediate Bents	B (*)
Intermediate Bent Columns, End Bents (Below construction joint at bottom of slab in Cont. Conc. Slab Bridges)	B-1
Footings	B
Drilled Shafts	B-2
Cast-In-Place Pile	B-1

(*) In special cases when a stronger concrete is necessary for design, Class B-1 may be considered for intermediate bents (caps, columns, tie beams, web beams, collision walls and/or footings). Adapted from MoDOT, 2013

Bridge A7957 has one HVFAC intermediate bent (B*) and one Conventional intermediate bent (B*). The HVFA bent is considered a MoDOT Class B with a required compressive strength of 3,000 psi (20.68 MPa). Conversely, the conventional bent is classified as a MoDOT Class B-1 with a required compressive strength 4,000 psi (27.58 MPa). Through analysis of Figure 4.15, the age at which each mix reaches a certain compressive strength is estimated in Table 4.6.

The mix designs in this research have relatively high cementitious levels (750 lb./yd^3). This was to ensure all level of fly ash replacement gained sufficient compressive

strength for all durability and structural purposes. Although all mixes meet the 4,000 psi (27.58 MPa) mark at some point, the 70% mix has a drastic increase in age before the target compressive strength is attained. In fact, it takes 70% HVFAC 92.5% longer to gain 4,000 psi than the conventional mix and 69.9% than 60% HVFAC. In addition, the 70% HVFAC take 4 times longer to attain 3,000 psi (20.68 MPa) than the conventional to attain 4,000 psi (27.58 MPa).

Table 4.6. Age (h) of Concrete at Specified Compressive Strengths

Compressive strength (psi)	CC	35%	50%	60%	70%
1200	5.5	17.3	15.8	20.4	30.2
1600	7.2	22.8	20.1	28.5	48.9
3000	19.3	67.4	48.7	86.3	211.6
3500	29.7	94.0	65.9	126.1	363.8
4000	45.4	134.3	88.8	183.4	607.9
4500	68.1	187.0	119.3	265.8	-
5000	101.9	262.9	160.0	385.3	-

Moist cured at 64.4°F (18°C). Conversion: 1,000 psi=6.895 MPa

Without the maturity method destructive techniques are used to determine the concrete compressive strength. Using Table 4.6 time of formwork removal and opening to traffic can be estimated. Before any load is applied, 70% of 28-day compressive strength must be gained (Upadhyaya, 2009). Based on this, load could be applied to the conventional concrete before 24 hours whereas load cannot be applied to 70% HVFAC concrete until 2 days have passed. It is clear to see the delay in the construction time line using HVFAC may cause. Time prior to removal of formwork for 50% HVFAC is three times that of conventional concrete. Based on this method, 70% HVFAC would be unreasonable to use.

The maturity method can also be used to estimate concrete compressive strength at different curing temperatures using Equation (3.4). First, the activation energy divided

by the gas constant (Q) was computed from the mortar cube compressive strength data. Using the average temperature (T_a) of the lab cured concrete and the curing temperature (T_s) in question; the equivalent age can be computed. Following this procedure sample values of age according to formwork removal for MoDOT Class B concrete were calculated at various temperatures (Figure 4.16) based on common temperatures experienced in Missouri throughout the year (Missouri Climate, 2015).

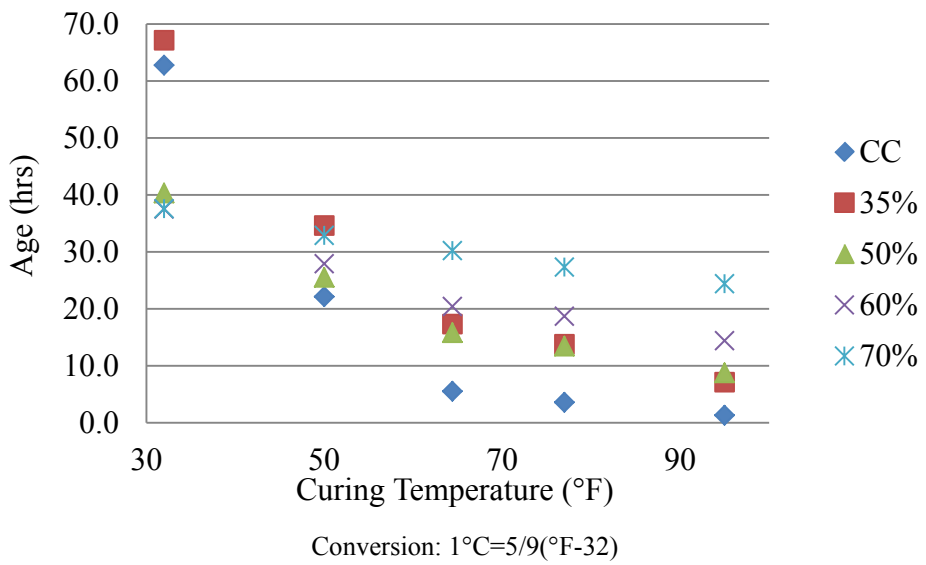

Figure 4.16. Required Age for Formwork Removal [1,200 psi (8.27 MPa)]

Generally, as the temperature increases the age required to meet strength requirements for formwork removal decreases. The effect of temperature on conventional concrete considerable compared to HVFAC. Based on this data using HVFAC below 65°F (18°C) is not recommended as the construction schedule may be delayed significantly. Using 70% HVFAC is not reasonable in applications where time is an important factor. Above 60°F (16°C) 35% and 50% HVFAC perform similarly with 50% HVFAC gaining compressive strength slightly quicker. The rate at which the age drops with temperature increase decreases with the 60% HVFAC whereas 50% HVFAC continues to linearly decrease with temperature. Another concern is hot weather concreting with conventional concrete. There is a concern of flash set with this conventional concrete mix when placed above 80°F (27°C). Temperatures between 60°F (16°C) and 80°F (27°C), depending on construction schedule, the optimum concrete may

be the conventional mix or 35% to 50% HVFAC. Considering temperatures above 80°F (27°C) the optimum mix is 60% HVFAC.

4.3. DURABILITY CHARACTERISTICS

Durability experiments included in this study consist of the following; Abrasion resistance, freeze-thaw resistance and permeability by ponding test.

4.3.1. Abrasion Resistance

Resistance to wear was compared among HVFAC mixes in terms of mass loss (g) following ASTM C944-12. Three sets of three two-minute abrasion periods were performed for testing. Although there were three periods of abrasion completed, the final results omit the first period on each set. For a complete collection of findings consult Appendix B.

During Phase I there was little standard deviation (< 1.06) in mass loss between any layers. Phase II, however, had high standard deviation (> 5) between the layers. As a result, both phase results omit the first layer for consistency. ASTM C944-12 states that the variation between two properly conducted tests by the same operator on similar samples should not differ from each other by more than 36% [for 44 lb. (19.96 kg)]. The first trial was omitted. The rest of the trials were below a 36% variation. Phase I specimens performed more consistently with 80% of the trials resulting in less than 36% variation. Similar to Phase II when trial one was omitted in Phase I all values fell below 36% variation from trial 2 to trial 3. It is speculated that this high variation in trial one is due in part to the accelerated curing process (Phase II). When oven dried at low relative humidity, water leaves the surface of the concrete specimen at a higher rate than the interior of the specimen. This causes a very dry and soft surface on Phase II specimens meaning the surface (layer 1) may lose more mass, which is what occurred. Another cause may be the phenomenon of cement hydrating and blocking further hydration previously mentioned (Gjorv, 1990). The results agree those found by Hadchti and Carrasquillo (1998); abrasion resistance suffered when cured at higher temperatures and lower relative humidity. Furthermore, to be able to compare Phase I with Phase II, as mentioned the first layer is also omitted in Phase I results for comparison.

Table 4.7 shows the average (of three trials) mass loss for Phase I. As the age of the specimen increased the mass loss decreased. The general trend was consistent with Hadchti and Carrasquillo (1998) in the fact that as the compressive strength increased (compressive strength increased with age), so did the abrasion resistance (Figure 4.17).

Table 4.7. Average Mass Loss (g) of Second and Third Layer (Phase I)

	CC	35	50	60	70
28	9.8	8.4	7.8	8.8	11.7
56	6.4	7.0	4.6	8.4	8.3
90	5.1	4.3	3.2	5.8	5.2
120	4.2	3.0	2.9	4.9	4.5

Conversion: 1 lb = 453.6 g

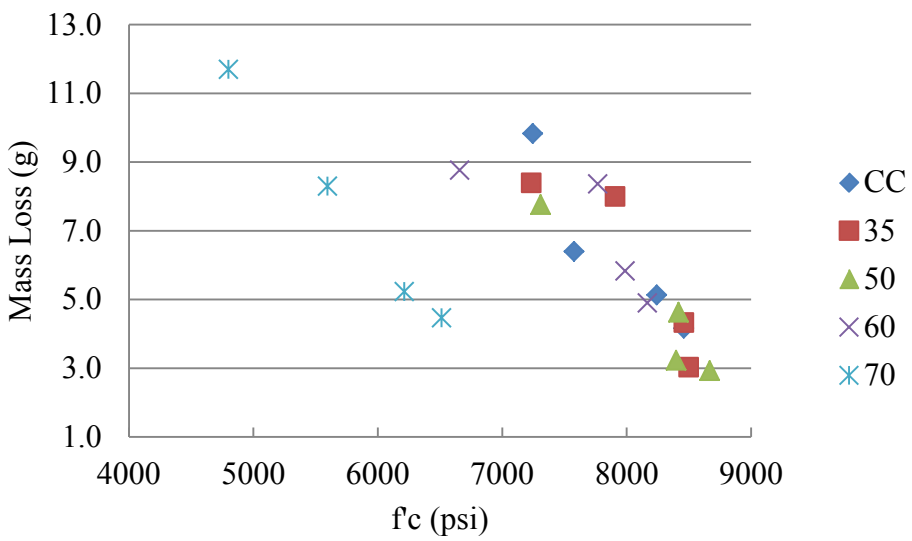

Conversion: 1,000 psi=6.895 MPa, 1 lb. = 453.6 g

Figure 4.17. Mass Loss vs. Compressive Strength for Phase I

The optimum replacement level seems to be the 50% mix. With the exception of 35% HVFAC at 56 days, Figure 4.18 shows that mass loss decreases until 50% replacement and then increased again.

An interesting occurrence is that 70% HVFAC actually performed as well or better than the 60% mix at ages later than 28 days and similar to that of the conventional by 90 days. By 56 days 60% HVFAC performs as well as the conventional mix at 28

days while 35% and 50% outperform the conventional at all ages (Exception: 35% at 56 days). Using the 28-day abrasion resistance would not be recommended for any replacement level. Increasing age led to a significant reduction in mass loss for each fly ash replacement percent.

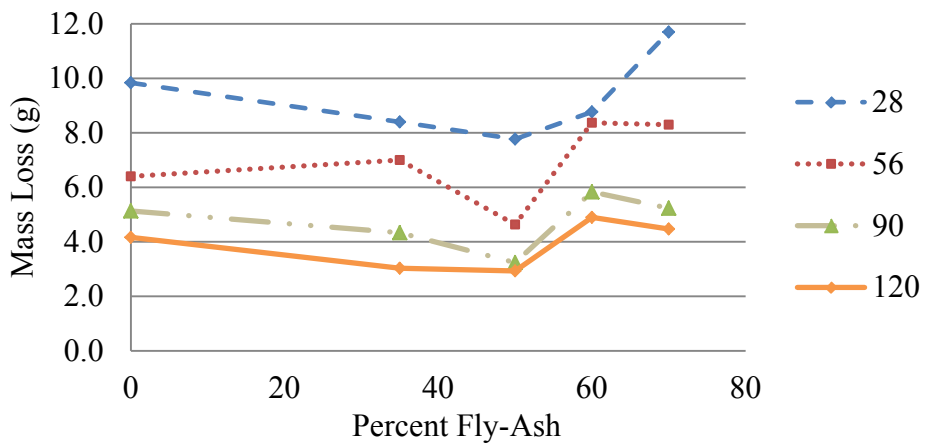

Conversion: 1 lb. = 453.6 g

Figure 4.18. Mass Loss vs. Percentage of Fly Ash

Table 4.8 shows the mass loss for Phase II specimens. The assumption was that the accelerated curing process would show similar mass loss results at 14 days as the traditional cured specimens at 28 days. However, this was not always the case.

Table 4.8. Average Mass Loss (g) of Second and Third Layer (Phase II)

	Phase I- 28d*	100-14d	100-28d	130-14d	130-28d	160-14d	160-28d
CC	9.8	13.2	10.0	20.3	11.8	12.3	10.4
35	8.4	12.4	11.5	16.1	12.3	17.8	13.7
50	7.8	17.9	14.7	19.6	10.4	12.9	9.3
60	8.8	12.9	10.5	15.4	11.2	26.1	15.2
70	11.7	28.2	21.0	28.9	26.1	26.2	21.5

Conversion: 1 lb. = 453.6 g. * Values are listed for comparison purposes

Table 4.8 gives a closer look between both phases. At all replacement rates the Phase II specimens performed worse at 14 and 28 than the 28-day Phase I specimens. Although they performed worse, the same general trend of a reduction in mass loss with an increase in age remained true even though by 14 days the compressive strengths ceased to show an increase. A visual representation is given in Figure 4.19 which shows that 70% HVFA is the most affected by temperature curing in reference to abrasion resistance.

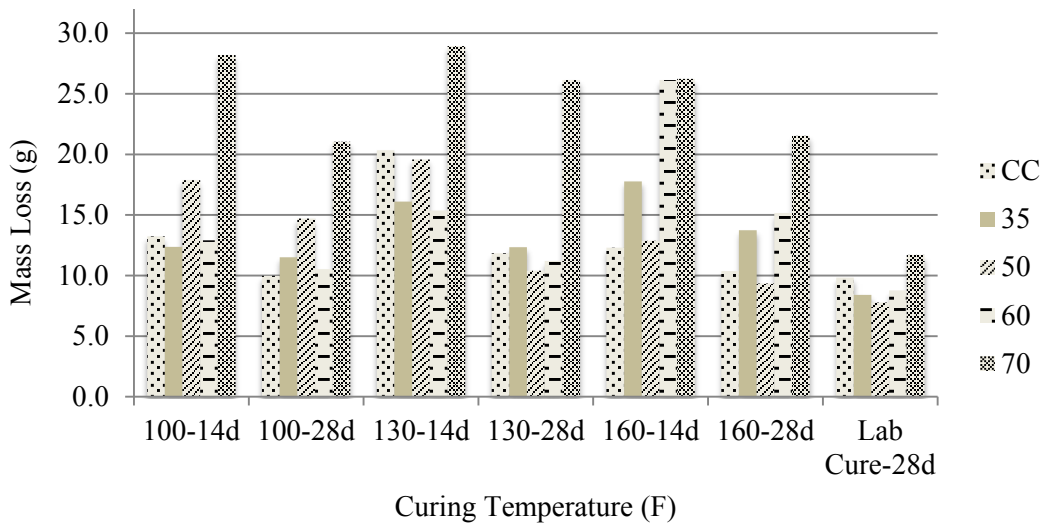

Conversion: 1°C=5/9(°F-32); 1 lb. = 453.6 g

Figure 4.19. CIP Deck Compressive Strength vs. Age

There is little correlation between percent fly ash and mass loss for Phase II. However, specimens cured at 100°F (37.8°C) performed best while the other two varied in performance. At all curing temperatures 70% HVFAC performed the worst. Reasons for poor performance by 70% include lack of and delayed hydration. Once again, temperature curing at high temperature seems to be detrimental to all mix designs.

Figure 4.20 continues to show that the curing method in Phase II was not very effective. The results were normalized between the two phases. No mix at any temperature performed better than the Phase I specimens. The conventional was the least affected by the temperature curing process. In most cases 100°F (37.8°C) showed the best results of phase II curing methods.

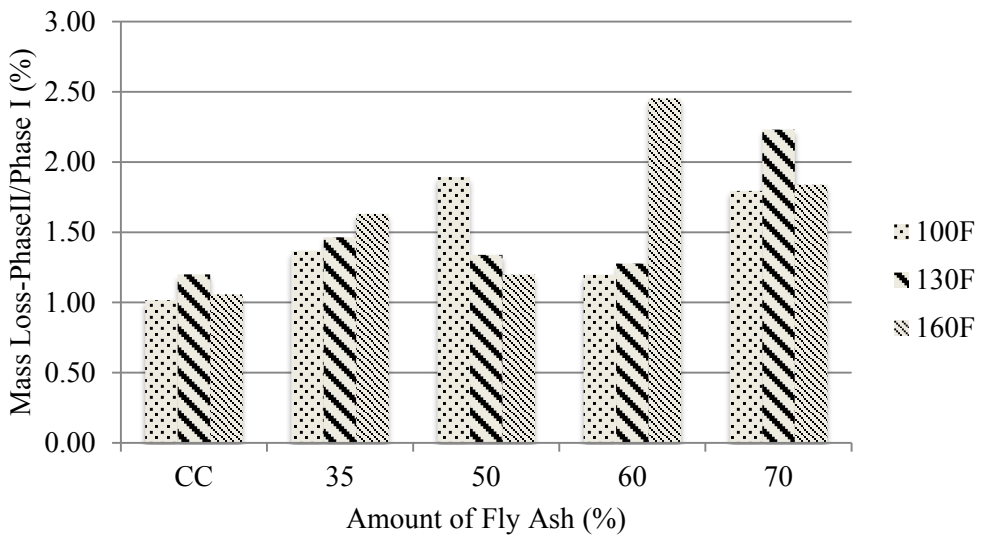

Figure 4.20. Normalized Mass Loss Phase II- 28 day

4.3.2. Freeze-Thaw Resistance

Resistance to freeze-thaw is important in concrete. The process of freezing and thawing can be detrimental to concrete. If not properly designed, the concrete will crack and spall leaving a vulnerable structure. Missouri sees many freeze-thaw cycles a year meaning freeze-thaw resistance in exterior concrete is of upmost concern.

Freeze and thaw durability factor (DF) was low (<35) for all mix designs (Table 4.9). This was to be expected as no air entrainment was added. The goal was to see the direct effect of the fly ash replacement level on the resistance to freezing and thawing of such concrete mixes and determine at what age each mix compares to the conventional mix at 28 days. Specifically, the DF was investigated in terms of RDM.

Table 4.9. Average Durability Factor (Phase I)

	28d	56d	90d	120d
CC	9.9	7.6	13.8	31.7
35	20	15	21.9	18.4
50	14	24	20.2	20.8
60	7.4	8.7	8.9	14.2
70	0	0	0	7.4

Literature review on the results of HVFAC on freeze-thaw resistance showed contradictory views; the same can be said for this experiment. Standard deviation fell within the acceptable ranges set forth by ASTM C666-03 Procedure A (Appendix C Table C.1). Except for the 35% HVFAC, the general trend was an increase in DF with an increase in age, although not significantly (Figure 4.21). Both the 35% mix and the 50% mix outperformed the conventional mix at every age except 120 days where the conventional mix DF increased rapidly. Within this experiment, the 35% mix showed no trend when compared to age of concrete.

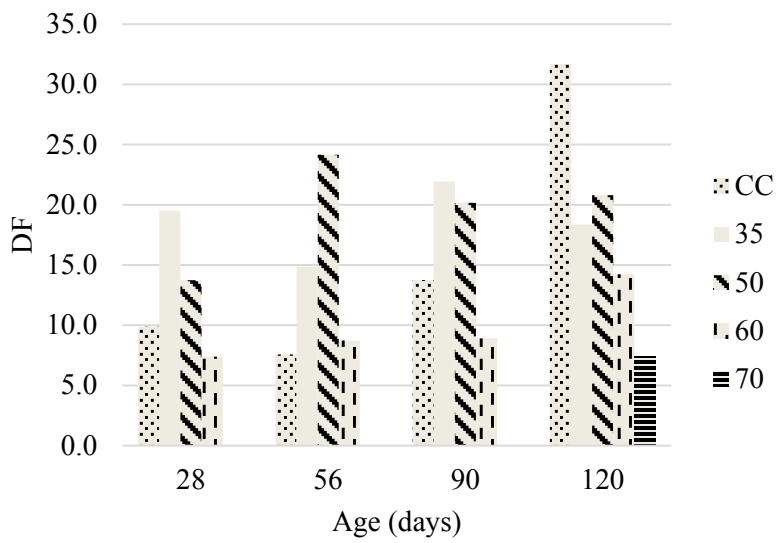

Conversions: 1 in = 25.4 mm, 1 kip = 4.448 kN

Figure 4.21. Durability Factor vs. Age (Phase I)

Naik and Singh (1994) reported that at replacement levels of 0-30% Class C fly ash the DF was identical and replacement above 30% saw a dramatic decline. However, in this experiment, as the replacement rate increased from 0- 50%, the DF continued to outperform the conventional mix except for 120 days. Above 50% replacement, the DF took a steep decline (Figure 4.22). The 70% mix did not obtain a DF until 120 days. Although this study examined non air-entrained HVFA concrete, an earlier study by Volz et al. (2012) found similar trends for air entrained HVFA concrete mixtures. Their study showed that "at 70% replacement and high cementitious content (730 lb./yd^3) concrete only had a DF of 2.1. Depending on the fly ash source, fly ash might have a high-carbon

content that makes it necessary to provide a higher content of air entrainment in the cases of high cement replacement levels".

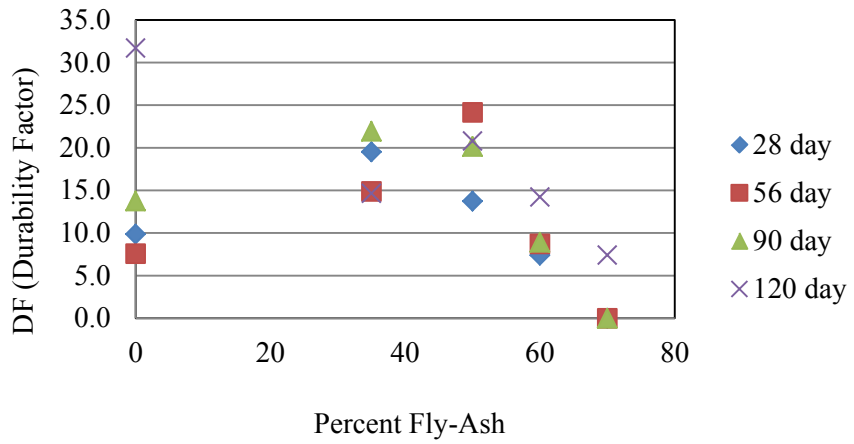

Figure 4.22. Durability Factor vs. Percentage of Fly Ash (Phase I)

Generally, as the compressive strength increased the DF also increased (Figure 4.23). However, this trend is more prevalent in the conventional mix. The compressive strength doesn't seem to have a significant effect on the DF of the HVFA concrete. The effect of compressive strength decreases as the percent of fly ash increases. At levels of 35 and 50 percent fly ash, the DF remains similar at 56 days of age and later.

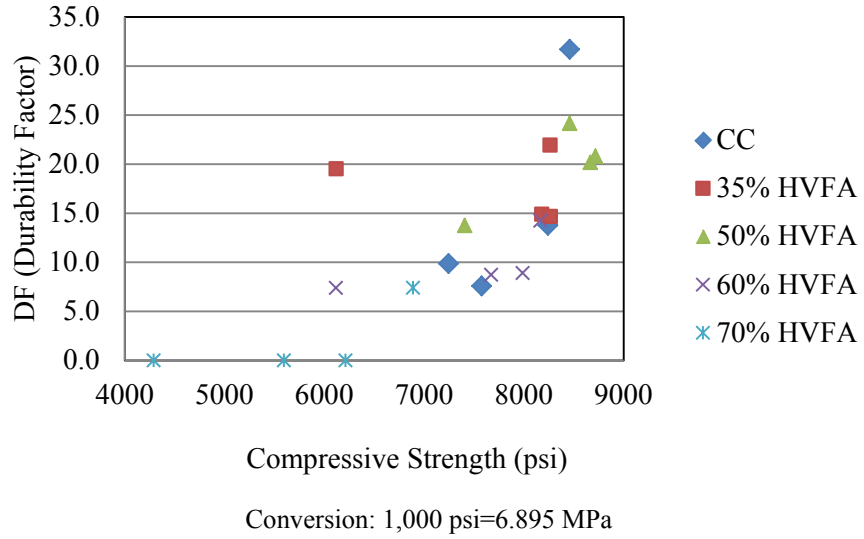

Figure 4.23. Durability Factor vs. Compressive Strength (Phase I)

Above 50% replacement, similar results were seen between 28 and 90 days of age. By 120 days, the 60% and 70% HVFAC saw a significant increase in their DF. Figure 4.22 agrees with Figure 4.23 as the concrete ages generally the DF increases. The optimum replacement level is 50% at 90 days and 120 days. At percentages above 50% the DF again decreases. When considering early ages, the optimum replacement level is 35%. At 70% replacement levels, the concrete never attains the DF equivalent to the conventional at 28 days. By 120 days, the 60% HVFAC acquires a DF greater than the conventional at 28 days, where as 35% and 50% HVFAC outperform the conventional mix.

Table 4.10. Average DF (Phase II)

	14d	28d
CCT100	14.7	10.6
CCT130	16.4	17.3
CCT160	9.2	7.1
35T100	0.0	0.0
35T130	0.0	0.0
35T160	0.0	0.0
50T100	25.8	9.5
50T130	19.5	16.8
50T160	9.5	6.2
60T100	1.3	5.7
60T130	4.5	11.6
60T160	0.0	0.0
70T100	0.0	0.0
70T130	0.0	0.0
70T160	0.0	0.0

Phase II specimens performed poorly (0<DF<26) (Table 4.10). Standard deviation and difference between two beams rarely met the requirements set forth by ASTM C666-03 (Table C.1). Many specimens failed post one cycle (36 freeze-thaw cycles). However,

the failure was not 60% reduction in RDM but rather too much surface deterioration where readings could not be taken. A full list of results is located in Appendix C.

Multiple specimens in Phase II did not achieve any DF. However, most specimens cured at 100°F (37.8°C) did. Unlike Phase I, all specimens except CCT130 and 60T100 did not improve from 14 to 28 days.

Although there was improvement in DF for CCT130 between 14 and 28 days it was not significant. Conventional specimens cured at 130°F (54.4°C) did however perform the best of the conventional specimens. Results varied greatly amongst Phase II specimens (Figure 4.24).

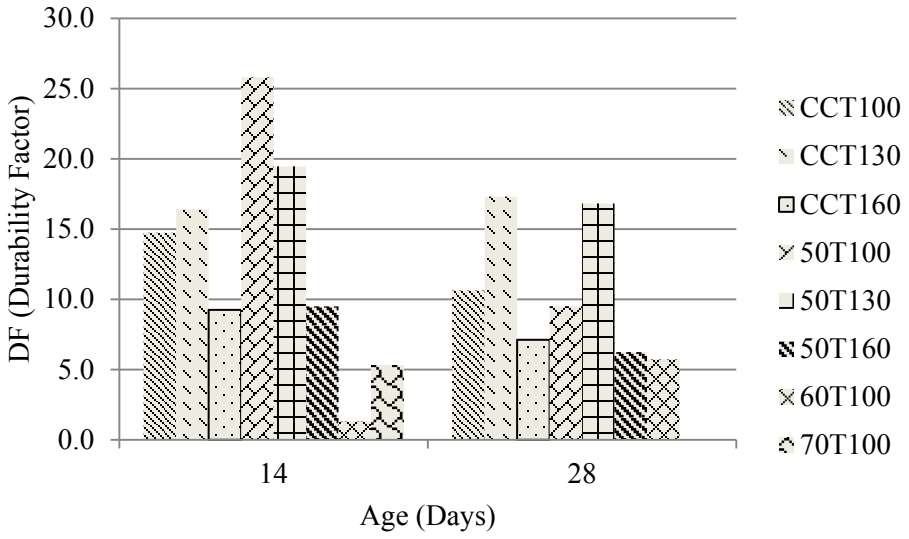

Figure 4.24. Durability Factor vs. Age (Phase II)

Even though results are scattered, a couple Phase II specimens did outperform their counterpart from Phase I (Table 4.11). At 14 days Phase II conventional concrete specimens cured at 100°F (37.8°C) and 130°F (54.4°C) outperform Phase I at 28, 56, and 90 days.

Conventional specimens cured at 160°F (71.1°C) did not perform better than Phase I specimens. At 100°F (37.8°C), Phase II 50% HVFAC at 14 days outperformed Phase I specimens at all ages. Phase II 50% HVFA specimens cured at 130°F (54.4°C)

also outperformed Phase I specimens but only at 28 days. Again, specimens (50% HVFAC) cured at 160°F (71.1°C) do not perform better than Phase I specimens.

Table 4.11. Phase I and Phase II Comparison

	14	28	56	90	120
CC	-	9.9	7.6	13.8	31.7
CCT100	14.7	10.6			
CCT130	16.4	17.3			
CCT160	9.2	7.1			
50%	-	13.7	24.2	20.2	20.8
50T100	25.8	9.5			
50T130	19.5	16.8			
50T160	9.5	6.2			

4.3.3. Chloride Ion Penetration

Many agree that as the percent fly ash increases the permeability decreases (Knutsson, 2010, Dhir, 1999, Myers and Carrasquillo 1998). Reasons for this include the bonding of fly ash with the chloride ions, the fly ash reactions produce denser hydration products, and the filler effect from the smaller particle size associated with fly ash.

However, there is an optimum replacement rate at which these expectations occur. Results pertaining to this experiment were anticipated to show similar results to those previously. For a complete collection of data consult Appendix D.

Phase I consisted of lab cured specimens post a 14-day moist cure period. These specimens were ponded with 3% NaCl solution for 3 months. After 3 months of ponding, specimens were drilled at 5 depths (Table 4.12). Based on the chloride content of the concrete at date of ponding, it seems there is a decrease in %Cl as the percent fly ash increases (Figure 4.25). This correlation agrees with Knutsson (2010) and Dhir (1999) hypothesis that the fly ash bonds CH from the cement to create more densified hydration products. However, there doesn’t seem to be a correlation between age and original chloride content.

Table 4.12. Ponding Sample Interval

Sampling Intervals (in)	
Location	Sample Range
1	Surface
2	3/8-3/4
3	1.0-1.4
4	1.6-2.0
5	2.2-2.5

Conversion: 1in=25.4mm

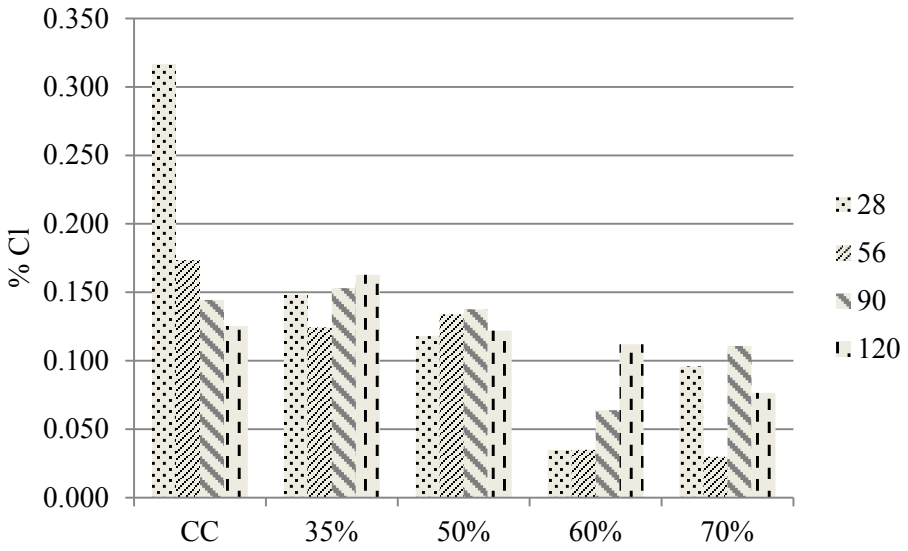

Figure 4.25. Chloride Content (%) vs. Percent Fly Ash

Generally, for all mixes in Phase I, the %Cl decreases as the depth of penetration increases (Figures 4.26 through 4.29). It is not the pores in concrete that make it permeable; rather it is the interconnectivity of those pores (Mindess et. al., 2003). Specimens were drilled in 3-4 locations and powders mixed together to gather an average value. If the pores connect in all directions, then a true representation may not be gathered at the drilling locations. With the exception of 56 days, 35% and 60% HVFAC continuously perform better than the conventional mix while 50% HVFAC performs very similar. Phase I specimens generally perform in the moderate range past location 2.

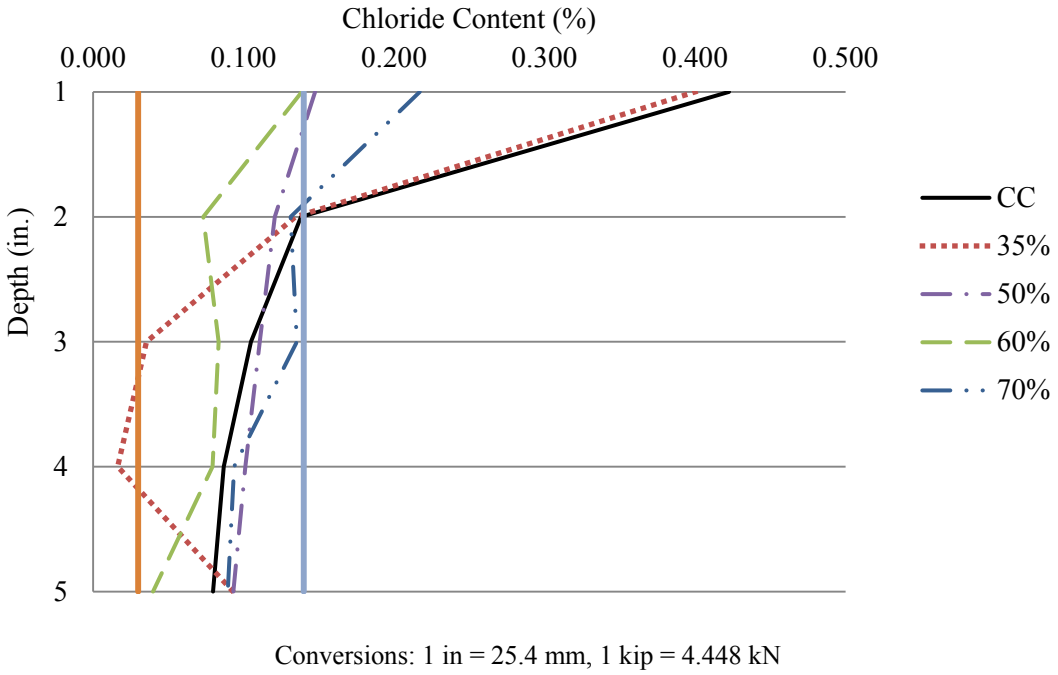

Figure 4.26. Chloride Profile at 28 Days (Phase I)

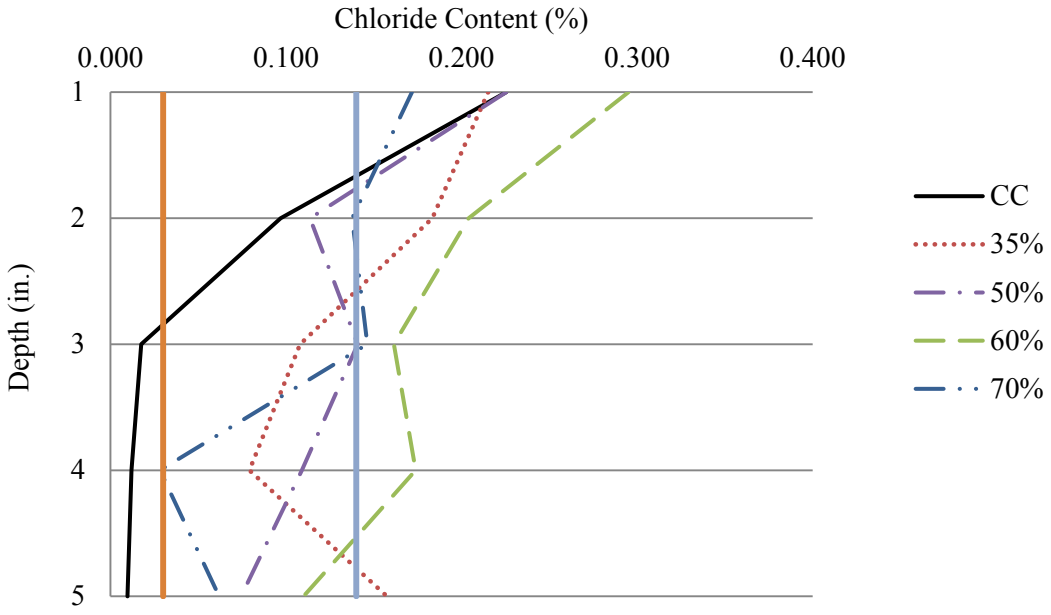

Figure 4.27. Chloride Profile at 56 Days (Phase I)

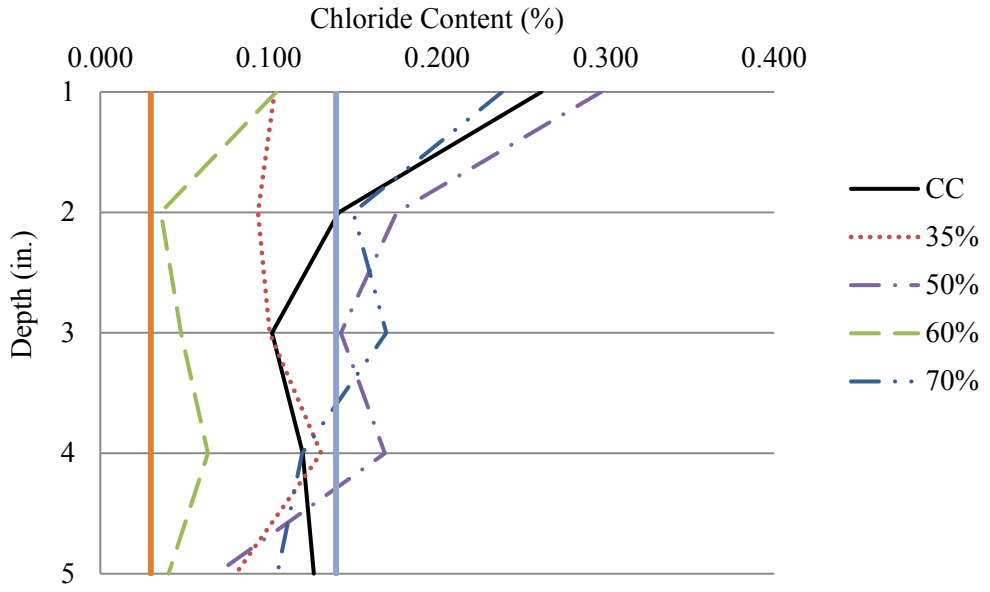

Figure 4.28. Chloride Profile at 90 Days (Phase I)

However, results were not very consistent throughout testing. HVFAC performed similarly or better than the conventional concrete at all ages suggesting that including fly ash up to 50% performs better in terms of permeability even at 28 days. Data was lost for conventional concrete at 120 days (Figure 4.29).

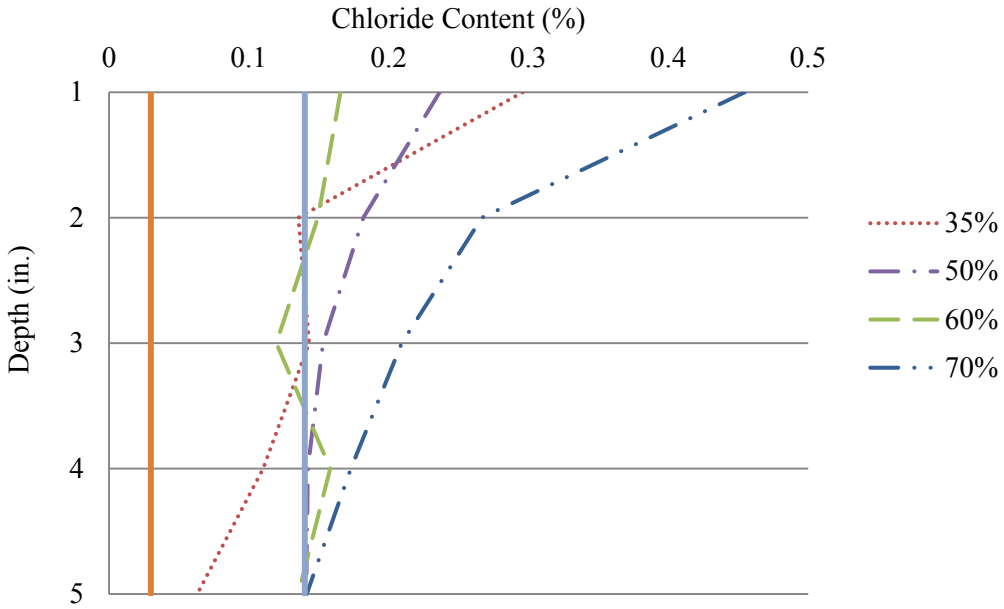

Figure 4.29. Chloride Profile at 120 Days (Phase I)

Refer to Appendix D for figures plotting Location vs. %Cl individually for each replacement level and age. Results were similar between 28 days and 120 days of age for each level of fly ash, except 60%, suggesting that the 28 day RCT values are sufficient for use in design.

Upon inspection of the surface of Phase II specimens, pores were observed. The rapid hydration and drying of surface water from the curing process is the culprit. This is detrimental to the overall permeability of these specimens. As mentioned, Phase II results show the same general trend as Phase I. As the depth of penetration increases, the %Cl decreases. As with the compressive strength trend of Phase II, the permeability results show a plateau. From the conventional mix to the 35% HVFAC mix there is an increase in %Cl at each location (Figures 4.30 and 4.31). However, the 28 day 35% HVFAC performs similar to that of the 14-day conventional mix. As the conventional mix ages from 14 to 28 days the %Cl actually increases at each location independent upon the temperature. The cause of this may be from the any excess water continuing to hydrate the concrete and leaving the specimen porous. Inversely, the 35% HVFAC shows a decrease in %Cl with age speculating that any excess water is continuing to hydrate the fly ash and create C-S-H like products to clog pours. Values between temperatures are very similar for each of these mixes.

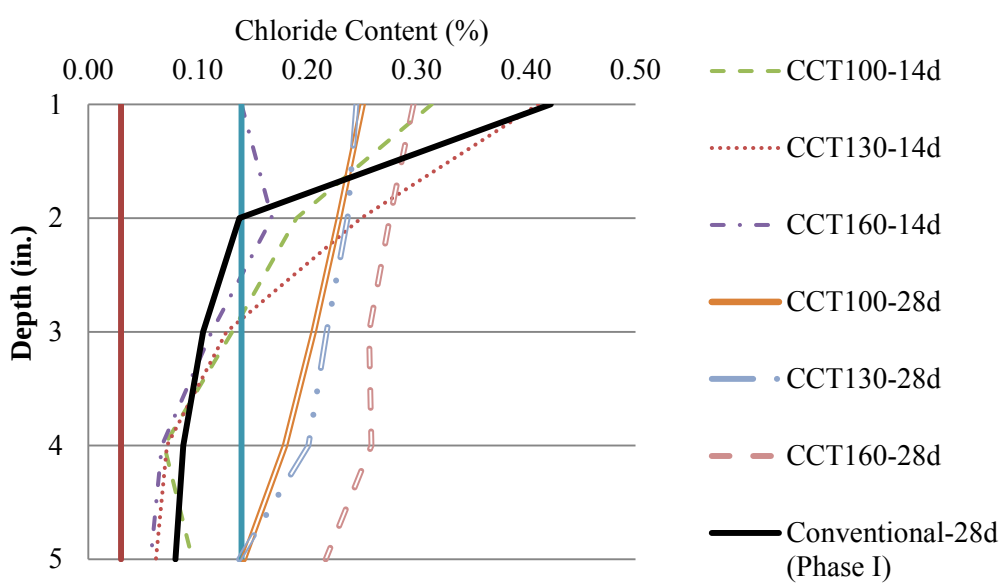

Figure 4.30. Conventional Concrete Chloride Profile (Phase II)

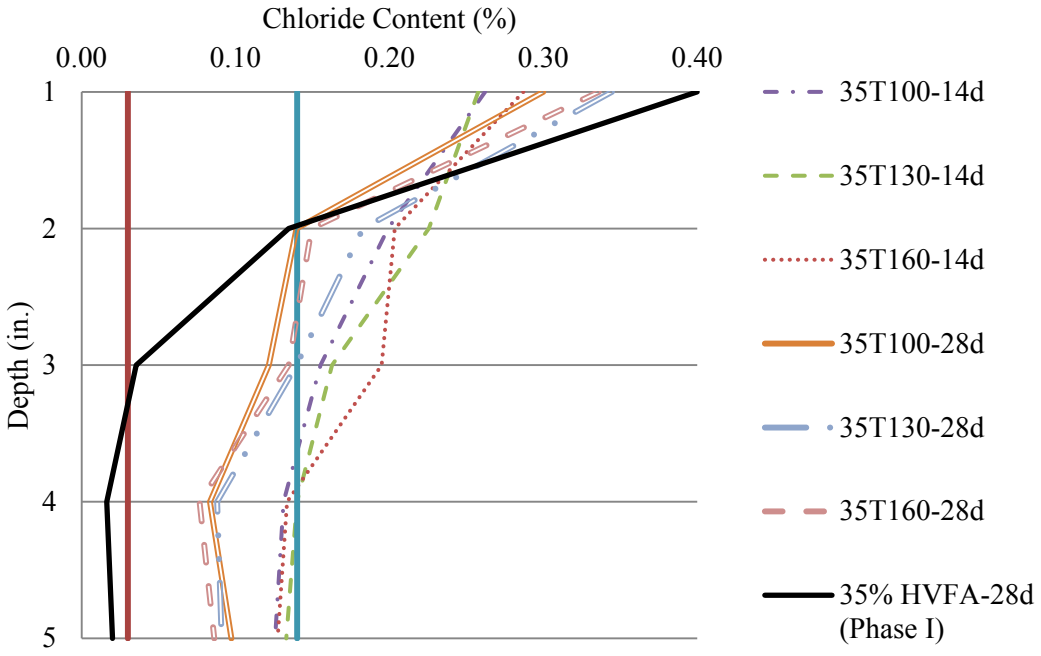

Figure 4.31. 35% HVFA Chloride Profile (Phase II)

Beyond 35% HVFAC, there is little fluctuation. At 50% (Figure 4.32), 60% (Figure 4.33) and 70% (Figure 4.34) HVFA the results are very similar.

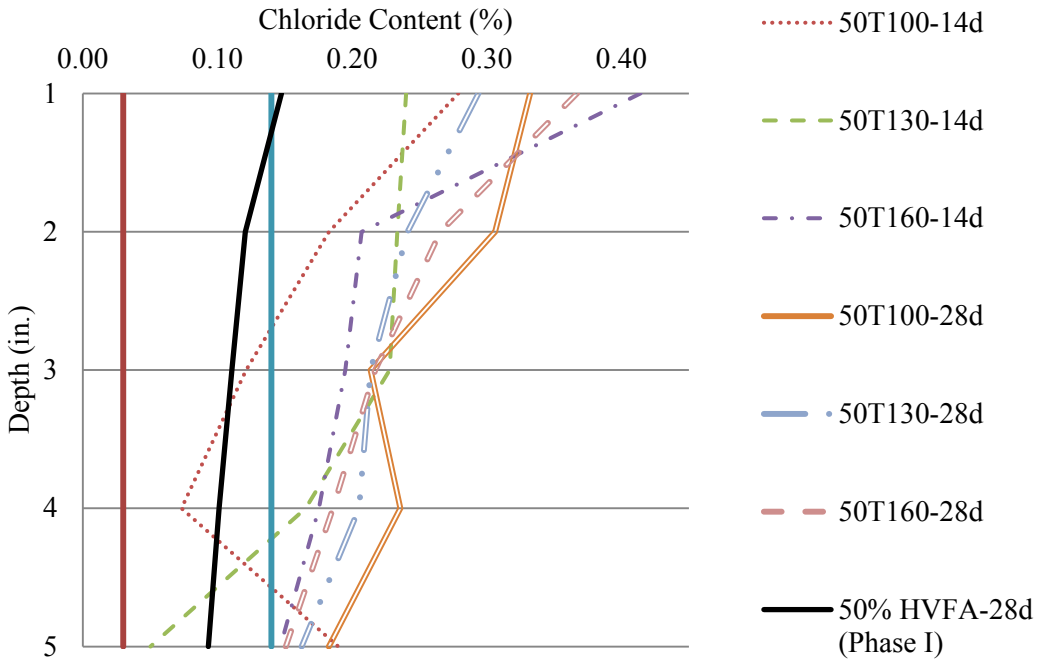

Figure 4.32. 50% HVFA Chloride Profile (Phase II)

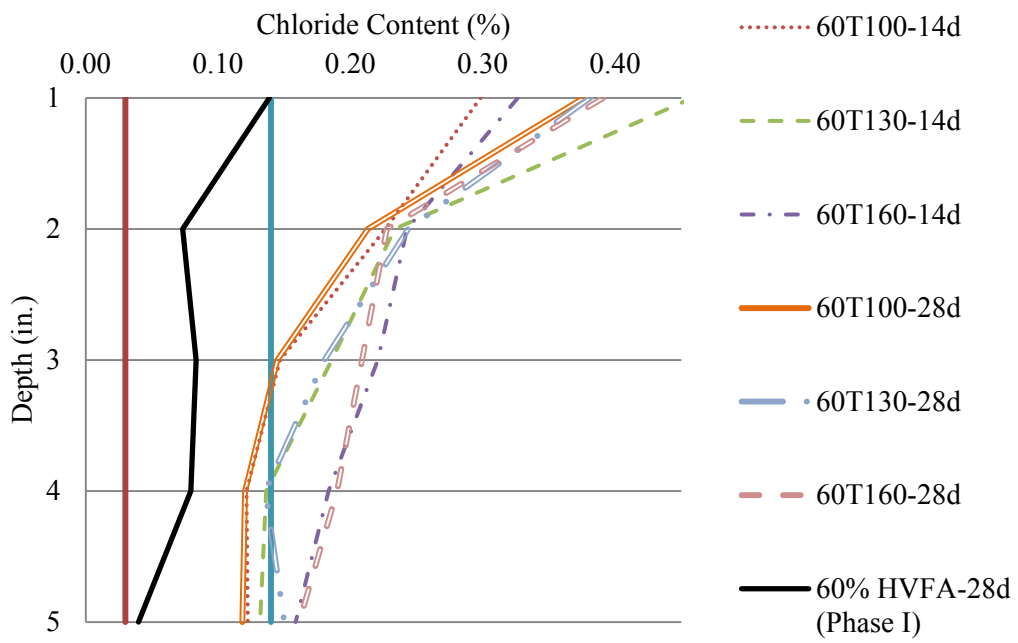

Figure 4.33. 60% HVFA Chloride Profile (Phase II)

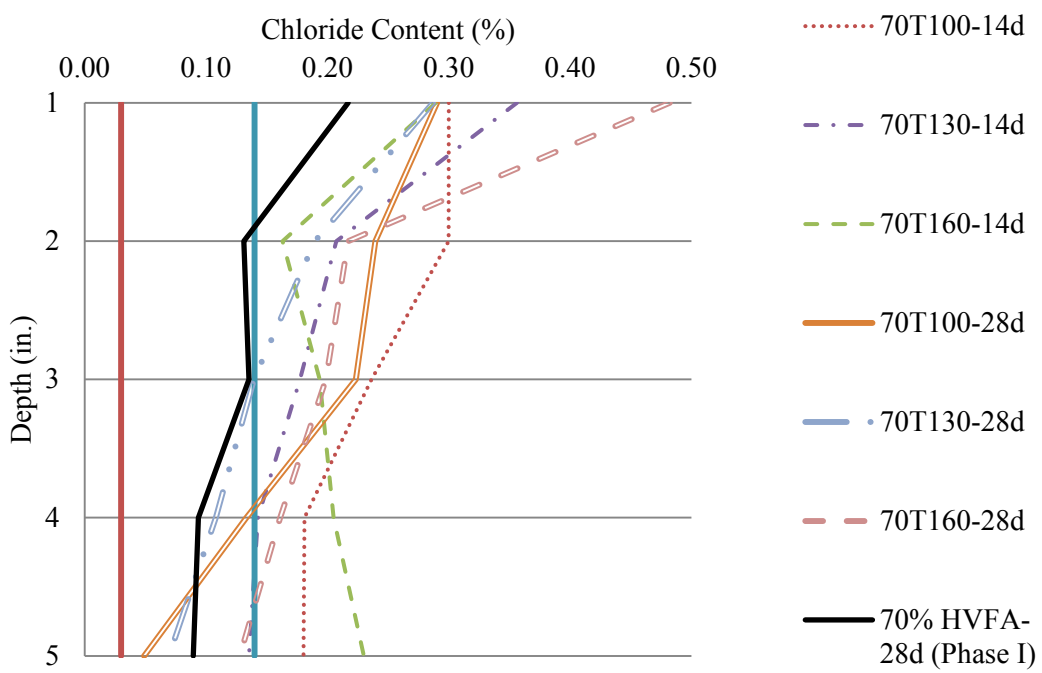

Figure 4.34. 70% HVFA Chloride Profile (Phase II)

Also with these mixes, the results do not vary much between 14 and 28 days. This correlates well with the compressive strength. It's speculated that hydration has ceased at

some time before 14 days with these mixes. Little correlation between curing temperature and %Cl is noticed. At 60% replacement level the specimens performed best at 100°F (37.8°C), the other mixes vary. In addition to these observations, it is also noticed that these three mixes generally fall above the high risk zone (%Cl > 0.14) at both ages and all three temperatures. At Location 5, results are borderline falling into the moderate range at 28 days and lower curing temperatures. All Phase II specimens performed poorly as none surpassed the negligible (%Cl < 0.03) mark for corrosion risk.

When compared to conventional concrete moist/lab cured, the temperature cured specimens showed greater chloride penetration at 14 and 28 days than the conventional concrete at 28 days with the exception of 28 days 70% HVFAC (70T130-28d and 70T130-28d) cured at 100°F (37.8°C) and 130°F (54.4°C). Overall, the 70% HVFAC performed closest to its Phase I counterpart due to a porous structure left from curing at such high temperatures. In addition, the high temperature curing did not protect the specimens from moisture loss, significantly affecting results.

5. CONCLUSIONS AND RECOMMENDATIONS

5.1. CONCLUSIONS

A push for sustainability and fiscal responsibility has emphasized the need for alternative materials to replace cement in concrete. The production of cement releases CO_2 into the atmosphere, while using fly ash instead deters landfill use and superior economically. Currently, American Society for Testing and Materials (ASTM) set test methods to determine concrete suitability for certain applications. These standards recommend using the 28 day properties of such concrete. With the implementation of fly ash, this may not always be the most beneficial due to delay in hydration causing a delay in the attainment of certain properties. This study investigated the compressive strength and durability characteristics of replacing cement with fly ash at many replacement levels (0, 35, 50, 60, and 70%). This was Phase I, in Phase II the same study was investigated with an accelerated curing method [cured at 100°F (37.8°C) 130°F (54.4° C) and 160°F (71.7°C)]. Specifically, investigated in this study was the age at which HVFA concrete needed to be before acquiring similar properties to that of the conventional concrete at 28 days. Considering this information, recommendations are made for amending ASTMs to allow for later age testing when determining concrete suitability.

For both phases, mechanical property tests consisted of compressive strength and modulus of elasticity. Furthermore, durability areas examined were abrasion, freeze-thaw, and permeability by RCT. Another component of research was the maturity method to estimate concrete compressive strength at any age.

5.1.1. Mix Design

Concrete mixes were designed using 750 pound per cubic yard cementitious materials. Since water to cement ratio largely affects the compressive strength and permeability of concrete, this value was set constant through all mixes at 0.40. To ensure a consistent slump, the mix designs varied in coarse and fine aggregates depending on the amount of fly ash. The five mix designs consisted of replacing cement with fly ash (by mass) at 0, 35, 50, 60 and 70%.

5.1.2. Fresh Properties

Refer to Table 4.1 for a complete summary of fresh properties. All concrete mixes reached a slump between 7 and 7 ¾ in. (177.80-196.85 mm). Concrete temperature at every level of fly ash replacement was higher than room temperature. Fly ash releases higher temperature during the mixing stage followed by a reduced temperature during hardening, cooling and densification stages. When fly ash was added, the difference in temperature increased during the mixing stage followed by a slower rate of heat generation in turn delaying hydration. Air content decreased as fly ash was added up to 50% before leveling out. Fly ash acts as filler packing air voids and decreasing air content. Mass and density across all mix designs were constant with HVFAC weighing slightly greater.

5.1.3. Compressive Strength (ASTM C39-14)

Past research has shown there is a delay in the hydration of HVFAC and this causes a delay in compressive strength gain. Although there is a delay in compressive strength, it has been discovered that there is an age where HVFAC is actually stronger than conventional concrete. In the area of compressive strength, for Phase I, the findings showed that by 56 days, mixtures up to 60% HVFAC were comparable, if not greater, in compressive strength to the conventional mix. In fact, the 35% and 50% HVFAC mixtures showed results comparable to that of the conventional mix at 28 days. The largest compressive strength gain was seen between 28 and 56 days considering HVFAC, and conventional concrete leveled off beginning at 28 days. All mixes gained a structural compressive strength of at least 2900 psi at some age except for 70% replacement mixes in Phase II. Although at a specific age each mix showed comparable results to the conventional mix, the 70% HVFAC never reached the compressive strength of any other mix at the respective age nor gained compressive strength similar to that of conventional concrete at 28 days.

Phase II specimens exhibited increased compressive strength from conventional curing methods within the first 3 days. Post 3 days there was a decrease in compressive strength from Phase I to Phase II. Within Phase II, the largest compressive strength gain was between 3 and 7 days at which point the compressive strengths generally plateaued.

As the curing temperature increased and moisture was lost, specimens plateaued earlier. As the specimens cured, water was wicked away from the surface leaving little water for HVFAC mixes to hydrate with.

5.1.4. Modulus of Elasticity (ASTM C469-14)

All concrete exhibited higher stiffness than predicted by ACI [Equation (2.1)] once the specimens gained 3,000 psi (20.68 MPa). Even for HVFAC the findings proved to be linear. Between 3,000 and 6,000 psi (20.68 MPa and 41.37 MPa) HVFAC gains stiffness per unit strength which exceeds the conventional mix. 70% HVFAC performs best within this range. Post 6,000 psi (41.37 MPa) HVFAC mixes tend to cease to increase in stiffness per unit strength while the conventional mix continues to gain stiffness. When considering mixes at or above 50% replacement, the MOE gained at 28 days is the stiffness expected at 120 days whereas the conventional and 35% HVFAC continues to gain stiffness as they age. At 28 days HVFAC shows a slightly increased MOE over the conventional even though HVFAC compressive strength is lower at this age.

5.1.5. Maturity Method (ASTM C1074-11)

The maturity method is a useful tool for estimating the concrete compressive strength at any age where the temperature history is recorded by non-destructive means. This method can also be used to estimate compressive strength at different curing temperatures as well. Knowing the concrete compressive strength at specific times is beneficial when determining a construction schedule. However, there are some disadvantages. The concrete must be cured in an environment where hydration can occur. This method does not take into account the effect of early-age heat generation on long-term compressive strength and must be accompanied by another means of indication of concrete compressive strength. Mortar cubes were made and tested to determine the datum temperatures and activation energy. Hydration of concrete can occur if cured at a temperature lower than the datum temperature. The datum temperature increased as the fly ash increased. Using Nurse-Saul's equation [Equation (3.3)], the maturity is computed and plotted against the compressive strength of the moist cured specimens. Using this

plot, the concrete compressive strength can be estimated at any time the temperature history of the in-place concrete is known. Inversely, the age of concrete at which a specific concrete compressive strength is required, such as formwork removal, can also be estimated based on the data and plots.

Maturity study results showed that HVFA concrete takes longer to hydrate in turn gaining compressive strength at a slower rate. Results showed that 70% HVFAC would take roughly 6 times longer to gain compressive strength than the conventional mix. Bridge A7957's specified target compressive strength was 3,000 psi (20.7 MPa) for 50% HVFAC. If 70% HVFA concrete had been used, over 25 days would have to pass before 70% HVFA reached the target strength, whereas 50% HVFA gains adequate compressive strength by day 4. In applications where time is a factor, it is not recommended to replace cement by fly ash with a percentage larger than 50%.

The maturity method also gave an indication about placing concrete in a variety of temperatures. As the temperature increased, the time to specific compressive strengths decreased. As the fly ash content increased the temperature during hydration was reduced. Again, 70% HVFAC is not recommended in application where early strength gain is necessary due to the delay in strength gain. Replacement levels of 35% to 60% perform similar between 65°F (18°C) and 95°F (35°C). Flash set is a concern when placing conventional concrete in temperatures above 80°F (27°C).

5.1.6. Abrasion Resistance (ASTM C944-12)

During Phase I, there was a correlation between compressive strength and mass loss. There was also a correlation between age and mass loss because the specimens gained compressive strength as they aged. As the specimens aged and gained compressive strength, the mass loss decreased. The optimum replacement level was 50%. There was a decreased mass loss up to 50% and a decrease beyond 50%. By 56 days, 70% HVFAC performed better than the conventional at 28 days, and by 90 days, 70% HVFAC performed similar to the conventional at 90 days and beyond. 35% and 50% HVFAC outperformed the conventional concrete at all ages. A significant decrease in mass loss was consistently seen up to 120 days of age at all levels of fly ash replacement.

In Phase II, compressive strength leveled out in all mixes prior to the first testing age of 14 days. However, the resistance to wear continued to increase at 28 days showing the bonds in the concrete were still increasing although the strength gain showed a reduction instead of increasing. Phase II specimens incurred issues with the surface layer being soft (high mass loss of the first trials). Standard deviation was above the allotted deviation set forth by ASTM C994-12. To compare results effectively, the first trial was omitted for Phase I and Phase II. By omitting trial one, all standard deviations and coefficients of variance fell within the acceptable range. No correlation between percentage of fly ash and mass loss was found during Phase II. Specimens cured at 100°F (37.8°C) performed best of phase II specimens, while specimens cured at the other two temperatures varied in performance. All specimens in Phase II performed worse than their Phase I counterparts.

5.1.7. Freeze-Thaw Resistance (ASTM C666-03 A)

No admixtures were used in this study. All specimens performed poorly in terms of durability factor (DF) during freeze-thaw testing as expected from the lack of air-entrainment. A slight increase in DF was seen with an increase in age and compressive strength. The compressive strength affected the conventional mix much greater than the HVFAC mixes. Replacement up to 50% showed an increase in DF until 120 days where conventional concrete shot past HVFAC mixes. At rates above 50%, a steep decrease in DF occurred. The 70% HVFAC performed the worst not showing a DF (<10) until 120 days. By 120 days, 60% HVFAC outperformed the conventional concrete at 28 days. Beginning at 28 days, the 35% and 50% HVFAC performed greater than the conventional concrete. Standard deviations of data met requirements set forth by ASTM C666-03 Procedure A.

Overall, between 28 and 56 days in ages, for the 35 and 50% HVFAC, there was a significant increase in DF prior to leveling off between 56 and 90 days. Fly ash levels greater than 50% showed similar results at each age of testing until 120 days where a significant increase occurred. DF for the conventional concrete increased up to 120 days.

Phase II specimens performed worse than Phase I. Data for this phase rarely fell within the acceptable range of standard deviation. Many Phase II specimens failed before

completing one set of 36 freeze-thaw cycles. However, these specimens did not necessarily fail due to falling below 60% initial relative dynamic modulus (RDM) rather they failed due to insubstantial surface area required for testing. A majority of Phase II specimens did not improve in terms of DF from 14 to 28 days. Lack of improvement could be caused from the lack of compressive strength gain during this period. During Phase II, 70% HVFAC never achieved a DF. 160°F curing temperature proved to be detrimental to all Phase II specimens. Phase II 14-day conventional concrete cured at 100°F (37.8°C) and 130°F (54.4°C) outperformed Phase I specimens at 28, 56, and 90 days. Phase II 50% HVFAC specimens cured at 100°F (37.8°C) performed better than the other Phase II samples at all ages. Curing temperature affected HVFA concrete greater than conventional concrete.

5.1.8. Chloride Ion Penetration (ASTM C1152-04)

Previous research showed that incorporating fly ash into the concrete mixture helped it become less permeable. The fly ash reacts with the CH to form denser hydration products. Fly ash also bonds to the chloride ions to combat penetration.

In both phases, the percentage of Cl content decreased as the depth increased. In Phase I, HVFAC mixes up to 60% performed similar if not better than the conventional mix beginning at 28 days. There seemed to be no correlation between age and permeability within the HVFAC mixes. However, as the conventional concrete aged the permeability decreased. The original chloride content decreased as the percentage of fly ash increased. Between ages of 28 and 120 days, each mix performed similar to itself at each location.

Upon inspection of Phase II specimens, the curing process left a porous structure. There was an increase in permeability from conventional concrete to 35% HVFAC. Above 35% HVFAC, the results remained very similar. The curing temperature and age (14 to 28 days) did not play a role in the percentage of Cl content. At both ages and all three temperatures, Phase II specimens consistently fall in the high risk zone (>0.14% Cl). Phase I 28-day conventional concrete showed lower permeability than Phase II specimens.

5.2. RECOMMENDATIONS

In reference to amending to the American Society for Testing and Materials (ASTM) test method, the followings modifications may be considered.

- In applications where structures will not undergo service conditioning for longer than 28 days, HVFAC is a suitable alternative to concretes without Class C fly ash replacement.
- Based on all results the maximum recommended replacement level is 50%.
- In terms of compressive strength, MOE, abrasion and freeze-thaw, the optimum replacement level was 50%.
- When considering chloride penetration, 50% performed similar to all the other replacement levels.

5.2.1. Phase I

When determining target compressive strength and modulus of elasticity, 56-day testing should be considered for HVFAC. The following recommendations should be considered:

- By 56 days, HVFAC performs similarly, if not better than conventional concrete. HVFAC mixes gained more strength between 28 and 56 days than conventional concrete.
- Beyond 56 days, the rate of compressive strength gain decreased.

When considering durability aspects, the results varied depending on the characteristic considered. The following aspects are to be taken into account:

- For abrasion resistance, 28 days is an adequate age to test HVFA concrete based on comparisons to the conventional mix. Both of these tests (abrasion and Freeze &Thaw) showed improved performance with the inclusion of fly ash up to 50% at 28 days although not significantly. These properties are partially reliant on the compressive strength whereas HVFAC approaches similar compressive strength to conventional concrete at 56 days. As the percent fly ash increases the effect of compressive strength decreases.

- Although 28-day abrasion resistance is adequate for HVFA concrete, it is recommended to use the resistance tested at 120 days of age. Concrete at all fly ash replacement levels showed a significant decrease in mass up to 120 days.

When considering freeze-thaw resistance, consider the following recommendations:

- The recommended age of testing is 56 days for a 50% fly ash replacement level.
- Above 50% fly ash replacement, it is necessary to wait 120 days until exposing HVFAC to freeze-thaw conditions. The conventional concrete consistently showed an increasing DF between 28 and 120 days of age.
- Chloride permeability by the rapid chloride test (RCT) showed scattered results. Beyond 28 days, results are unclear.
- There is little correlation between age and permeability. HVFAC performs similar to the conventional from 28 days on. When each HVFAC mixture's performance was evaluated individually, they performed similarly from 28 days to 120 days of age.

5.2.2. Phase II

The following recommendations were suggested:

- HVFA concrete should not be cured at temperatures greater than 100°F (37.8°C) and low relative humidity. High temperatures and low relative humidity are detrimental, in terms of mechanical and durability properties, to concrete and significantly affect HVFAC.
- Curing conventional concrete at high temperatures may cause flash or false set.
- Durability properties and later age strength may suffer as well.
- Future testing should explore curing HVFA concrete around 100°F (37.8°C) with high relative humidity so hydration continues.

5.3. FUTURE WORK

- Future work should focus on lowering the cement content and adjusting the mix constituents based on keeping a constant slump of 5 in.
- A 70% HVFAC replacement could be considered if admixtures are added to the mix design. Otherwise, 70% HVFAC mixtures should be omitted based on the results found in this study.
- Future studies should include investigation on the reliability of the maturity method in the field. From lab testing, the maturity method showed general expected trends found in the literature review.
- Future research should include verifying the estimation of concrete compressive strength at different temperatures.

APPENDIX A - COMPRESSIVE STRENGTH AND MOE

Table A.1: Compressive Strength and MOE. (a) Conventional Concrete; (b) Conventional Concrete Cured at 100°F (37.8°C)

Mix ID:	CC				
Age (days)	f'c (psi)	Avg. f'c (psi)	MOE (ksi)	Avg. MOE (psi)	ACI MOE (ksi)
3	4675	4623	4950	4925	3875
	4633		4900		
	4560				
7	5964	5822	5200	5225	43492
	5754		5250		
	5748				
14	6531	6674	5700	5625	46564
	6816		5550		
28	7235	7245	5300	5450	4852
	7267		5500		
	7233		5550		
			5450		
56	7618	7577	6150	6213	5159
	7577		6300		
	7536		6250		
			6150		
90	8011	8080	7100	7075	5557
	8086		7050		
	8144				
120	8037	8257	7100	7100	5524
	8374		7100		
	8361				

(a)

Mix ID:	CCT100				
Age (days)	f'c (psi)	Avg. f'c (psi)	MOE (ksi)	Avg. MOE (ksi)	ACI MOE (ksi)
2	5002	5259			
	5350				
	5424				
3	5416	5485	2600	3788	4221
	5610		2300		
	5428		5150		
			5100		
7	5519	5754	4550	4550	4324
	5989		4550		
14	6570	6408	5500	5188	4563
	6328		5450		
	6325		4950		
			4850		
28	6300	6477	5600	5600	4587
	6620		5600		
	6511				

(b)

Conversion 1,000 psi = 6.985 MPa

Table A.2: Compressive Strength and MOE. Conventional Concrete Cured at 130°F (54.4C); (b) Conventional Concrete Cured at 160°F (71.1°C)

Mix ID:	CCT130				
Age (days)	f'c (psi)	Avg. f'c (psi)	MOE (ksi)	Avg. MOE (ksi)	ACI MOE (ksi)
2	5247	5001			
	4709				
	5048				
3	5343	5373	5000	5000	4178
	5307		5000		
	5469				
7	5417	5745	4250	4538	4320
	5843		4200		
	5647		4850		
			4850		
14	6198	5908	5250	4850	4381
	5900		5150		
	5915		4550		
			4450		
28	6229	6487	5100	5125	4591
	6454		5150		
	6779				

(a)

Mix ID:	CCT160				
Age (days)	f'c (psi)	Avg. f'c (psi)	MOE (ksi)	Avg. MOE (ksi)	ACI MOE (ksi)
2	4886	4964			
	5269				
	4737				
3	5108	5239	4100	4075	4126
	-		4050		
	5369				
7	5537	5232	4650	4650	4123
	4927		4650		
14	5459	5382	5150	4738	4182
	5679		5150		
	5007		4350		
			4300		
28	5254	5704	4800	4875	4305
	6123		4950		
	5734				

(b)

Conversion 1,000 psi = 6.985 MPa

Table A.3: Compressive Strength and MOE. (a) 35% HVFA Concrete; (b) 35% HVFA Cured at 100°F (37.8°C)

Mix ID:	35% HVFA				
Age (days)	f'c (psi)	Avg. f'c (psi)	MOE (ksi)	Avg. MOE (ksi)	ACI MOE (ksi)
3	3001	3010	4850	4633	3127
	2833		4500		
	3196		4550		
			4350		
7	4432	4649	5150	5150	3886
	4510		5150		
	5004				
14	5335	5567	4400	4533	4253
	5798		4350		
			4850		
			5100		
28	6363	6120	5550	5563	4459
	5877		5600		
			5450		
			5650		
56	8263	8181	6250	6050	5155
	8344		6100		
	7935		5900		
			5950		
90	8205	8264	6000	6075	5182
	8291		6150		
	8295				
120	8205	8267	6700	6925	5183
	8416		7150		
	8179				

(a)

Mix ID:	35T100				
Age (days)	f'c (psi)	Avg. f'c (psi)	MOE (ksi)	Avg. MOE (psi)	ACI MOE (ksi)
2	4080	4064			
	4176				
	3937				
3	4567	4743	4350	4250	3926
	4827		4200		
	4836		4200		
5	5004	4973			
	4942				
7	5188	5254	5300	5300	4132
	5217		5300		
14	5583	5597	5650	5463	4264
	5700		5600		
	5507		5300		
			5300		
28	5742	5799	4750	5238	4341
	5856		4750		
	5795		5750		
			5700		

(b)

Conversion 1,000 psi = 6.985 MPa

Table A.4: Compressive Strength and MOE. (a) 35% HVFA Cured at 130F (54.4C); (b) 35% HVFA Cured at 160°F (71.1°C)

Mix ID:	35T130				
Age	f'c (psi)	Avg. f'c (psi)	MOE (ksi)	Avg. MOE (ksi)	ACI MOE (ksi)
2	4180	4133			
	4082				
	4138				
3	4721	4759	5300	5275	3932
	4796		5250		
5	4673	4726			
	4779				
7	5043	4941	4650	4650	4006
	4771		4650		
	5110				
14	4737	4905	5150	5150	3992
	4965		5150		
	5013				
28	5005	5151	5500	5550	4091
	5378		5600		
	5069				

(a)

Mix ID:	35T160				
Age	f'c (psi)	Avg. f'c (psi)	MOE (ksi)	Avg. MOE (ksi)	ACI MOE (ksi)
2	4621	4553			
	4575				
	4463				
3	4649	4683	4450	4475	3901
	4630		4500		
	4770				
5	4697	4595			
	4770				
7	4317	4669			3895
	4750				
	4939				
14	4648	4842	5000	4913	3966
	4939		4900		
	4939		4900		
			4850		
28	5228	4944	5150	5025	4008
	4693		5150		
	4910		4900		
			4900		

(b)

Conversion 1,000 psi = 6.985 MPa

Table A.5: Compressive Strength and MOE. (a) 50% HVFA Concrete; (b) 50% HVFA Cured at 100°F (37.8°C)

Mix ID:	50% HVFA				
Age (days)	f'c (psi)	Avg. f'c (psi)	MOE (ksi)	Avg. MOE (ksi)	ACI MOE (ksi)
3	3392	3403	4050	4050	3325
	3413		4050		
7	4721	4824	5150	5063	3959
	4927		5100		
			5000		
			5000		
14	6479	6499	5250	5250	4595
	6334		5250		
	6685		5250		
			5150		
28	7500	7408	6000	5913	4906
	7315		5800		
			5950		
			5900		
56	8322	8459	5950	6000	5242
	8425		6050		
	8630				
90	8805	8667	6050	6100	5307
	8534		6150		
	8662		6100		
120	8729	8717	5950	6038	5322
	8758		5950		
	8665		6200		
			6050		

(a)

Mix ID:	50T100				
Age (days)	f'c (psi)	Avg. f'c (psi)	MOE (ksi)	Avg. MOE (ksi)	ACI MOE (ksi)
2	3146	3443			33445937
	3181				
	4002				
3	4179	4054	4300	4300	3629
	3982		4300		
	4002				
7	4235	4787	5450	5375	3944
	4841		5400		
	4733		5350		
			5300		
14	4975	4970	4950	5050	4018
	5003		4950		
	4931		5150		
			5150		
28	4204	5103	5650	5500	4072
	5103		5350		

(b)

Conversion 1,000 psi = 6.985 MPa

Table A.6: Compressive Strength and MOE. (a) 50% HVFA Cured at 130°F (54.4°C); (b) 50% HVFA Cured at 160°F (71.1°C)

Mix ID:	50T130				
Age (days)	f'c (psi)	Avg. f'c (psi)	MOE (ksi)	Avg. MOE (ksi)	ACI MOE (ksi)
2	3603	3682			3459
	3732				
	3710				
3	3932	4110	4900	4900	3654
	3988		4900		
	4411				
7	3940	4103	4900	4900	3651
	4177		4900		
	4103				
14	4464	4523	5000	4900	3834
	4755		5000		
	4351		4800		
			4800		
28	4228	4669	4650	4675	3895
	4669		4700		

(a)

Mix ID:	50T160				
Age (days)	f'c (psi)	Avg. f'c (psi)	MOE (ksi)	Avg. MOE (ksi)	ACI MOE (ksi)
2	3975	3723			3478
	3465				
	3728				
3	3844	3997	2600	3513	3604
	4190		2450		
	3958		4500		
			4500		
7	4049	4045	4250	4100	3625
	4055		4250		
	4031		3950		
			3950		
14	3847	4122	4200	4213	3660
	3874		4150		
	4119		4250		
	4125		4250		
28	4045	4122.5	3450	3450	3660
	4200				

(b)

Conversion 1,000 psi = 6.985 MPa

Table A.7: Compressive Strength and MOE. (a) 60% HVFA Concrete (b) 60% HVFA Cured at 100°F (37.8°C)

Mix ID:	60% HVFA				
Age	f'c (psi)	Avg. f'c (psi)	MOE (ksi)	Avg. MOE (ksi)	ACI MOE (ksi)
3	2111	2143	1100	1100	2638
	2174		1100		
7	3678	3658	4650	4575	3447
	3638		4500		
14	4583	4723	5300	5275	3917
	4737		5250		
	4850		5150		
			5200		
28	6074	6117	5550	5550	4458
	6159		5550		
			5550		
			5650		
56	7710	7673	6000	5900	4993
	7464		5800		
	7844				
90	7997	7988	5900	5900	5094
	7866		5900		
	8100				
120	7802	8166	5950	5925	5151
	8525		5900		
	8172				

(a)

Mix ID:	60T100				
Age	f'c (psi)	Avg. f'c (psi)	MOE (ksi)	Avg. MOE (ksi)	ACI MOE (ksi)
2	2284	2378			
	2420				
	2430				
3	2925	3012	4050	3783	3128
	3156		4150		
	2955		3150		
5	3616	3412			
	3208				
7	3665	3508	3950	3063	3376
	3586		2900		
	3273		2650		
			2750		
18	4062	3831	4450	4450	3528
	3443		4450		
	3987				
28	3979	3802	5700	5650	3515
	3633		5600		
	3794				

(b)

Conversion 1,000 psi = 6.985 MPa

Table A.8: Compressive Strength and MOE. (a) 60% HVFA Cured at 130°F (54.4°C); (b) 60% HVFA Cured at 160°F (71.1°C)

Mix ID:	60T130				
Age	f'c (psi)	Avg. f'c (psi)	MOE (ksi)	Avg. MOE (ksi)	ACI MOE (ksi)
2	3212	3178			
	3012				
	3309				
3	3803	3741	4550	4600	3486
	3722		4650		
	3699				
5	3943	3780			
	3617				
7	3740	3748	2600	2850	3489
	3755		3100		
18	3658	3679	4750	4538	3457
	3708		4650		
	3672		4400		
			4350		
28	3728	3560	4650	4513	3401
	3297		4600		
	3654		4350		
			4450		

(a)

Mix ID:	60T160				
Age	f'c (psi)	Avg. f'c (psi)	MOE (ksi)	Avg. MOE (ksi)	ACI MOE (ksi)
2	2890	2891			
	2808				
	2976				
3	2767	2857	3850	4013	3047
	2827		3800		
	2977		4200		
			4200		
5	2801	2772			
	2742				
7	2822	2720	4050	3950	2973
	2687		3850		
	2652				
18	2847	2975	4000	3950	3109
	2971		3900		
	3108				
28	2945	2864	4100	4150	3051
	2925		4100		
	2723		4250		

(b)

Conversion 1,000 psi = 6.985 MPa

APPENDIX B - ABRASION RESISTANCE

Table B.1: Mass Loss (g) Results- 35% HVFA Concrete (Phase I)

Mix ID: 28d 35%									
10-Jan	Trial 1	Mass loss	Trial 2	Mass loss	Trial 3	Mass loss	Avg. loss	Stdv	CoV
W_0	12794.3	-	12781.7	-	12768.8	-			
W_1	12790.3	4.0	12777.2	4.5	12764.0	4.8	4.4	0.404	
W_2	12785.7	4.6	12772.9	4.3	12760.1	3.9	4.3	0.351	3.83
W_3	12781.7	4.0	12768.8	4.1	12755.8	4.3	4.1	0.153	3.17
						Total	12.8	0.15	GOOD

Mix ID: 56d 35%									
7-Feb	Trial 1	Mass loss	Trial 2	Mass loss	Trial 3	Mass loss	Avg. loss	Stdv	CoV
W_0	12761.6	-	12750.9	-	12739.9	-			
W_1	12759.0	2.6	12748.1	2.8	12736.8	3.1	2.8	0.252	
W_2	12754.8	4.2	12743.8	4.3	12732.7	4.1	4.2	0.100	38.86
W_3	12750.9	3.9	12739.9	3.9	12729.1	3.6	3.8	0.173	10.00
						Total	10.8	0.70	NO GOOD

Mix ID: 90d 35%									
13-Mar	Trial 1	Mass loss	Trial 2	Mass loss	Trial 3	Mass loss	Avg. loss	Stdv	CoV
W_0	13299.8	-	13293.5	-	13284.5	-			
W_1	13297.1	2.7	13289.5	4.0	13281.4	3.1	3.3	0.666	
W_2	13295.1	2.0	13286.7	2.8	13279.0	2.4	2.4	0.400	30.59
W_3	13293.5	1.6	13284.5	2.2	13277.0	2.0	1.9	0.306	21.54
						Total	7.6	0.68	GOOD

Mix ID: 120d 35%									
12-Apr	Trial 1	Mass loss	Trial 2	Mass loss	Trial 3	Mass loss	Avg. loss	Stdv	CoV
W_0	12907.7	-	12903.1	-	12898.5	-			
W_1	12905.9	1.8	12901.8	1.3	12897.0	1.5	1.5	0.252	
W_2	12904.2	1.7	12899.9	1.9	12895.2	1.8	1.8	0.100	16.00
W_3	12903.1	1.1	12898.5	1.4	12894.0	1.2	1.2	0.153	37.36
						Total	4.6	0.28	NO GOOD

Average Mass loss				
Age	28	56	90	120
	12.8	10.8	7.6	4.6

Including Layer 1			
Average Stdv		Average CoV	
0.59		18.83	<36%

Not Including Layer 1			
Average Stdv		Average CoV	
0.48		15.28	<36%

Table B.2: Mass Loss (g) Results-50% HVFA Concrete (Phase I)

Mix ID: 28d 50%									
31-Jan	Trial 1	Mass loss	Trial 2	Mass loss	Trial 3	Mass loss	Avg Loss	Stdv	CoV
W_o	12671.4	-	12659.3	-	12647.8	-	-		
W_1	12667.7	3.7	12655.3	4.0	12642.2	5.6	4.4	1.021	
W_2	12664.1	3.6	12651.7	3.6	12638.0	4.2	3.8	0.346	15.38
W_3	12659.3	4.8	12647.8	3.9	12634.8	3.2	4.0	0.802	-4.29
						Total Mass Loss	12.2	0.33	GOOD

Mix ID: 56d 50%									
27-Feb	Trial 1	Mass loss	Trial 2	Mass loss	Trial 3	Mass loss	Avg Loss	Stdv	CoV
W_o	13353.5	-	13346.7	-	13339.7	-	-		
W_1	13351.7	1.8	13344.2	2.5	13337.5	2.2	2.2	0.351	
W_2	13348.8	2.9	13341.7	2.5	13335.1	2.4	2.6	0.265	18.18
W_3	13346.7	2.1	13339.7	2.0	13333.1	2.0	2.0	0.058	24.46
						Total Mass Loss	6.8	0.30	GOOD

Mix ID: 90d 50%									
2-Apr	Trial 1	Mass loss	Trial 2	Mass loss	Trial 3	Mass loss	Avg Loss	Stdv	CoV
W_o	13090.3	-	13084.7	-	13079.2	-	-		
W_1	13087.9	2.4	13082.5	2.2	13076.7	2.5	2.4	0.153	
W_2	13086.4	1.5	13080.8	1.7	13075.0	1.7	1.6	0.115	36.67
W_3	13084.7	1.7	13079.2	1.6	13073.5	1.5	1.6	0.100	2.06
						Total Mass Loss	5.6	0.43	NO GOOD

Mix ID: 120d 50%									
2-May	Trial 1	Mass loss	Trial 2	Mass loss	Trial 3	Mass loss	Avg Loss	Stdv	CoV
W_o	13514.5	-	13509.9	-	13505.0	-	-		
W_1	13512.9	1.6	13508.3	1.6	13503.8	1.2	1.5	0.231	
W_2	13511.5	1.4	13506.3	2.0	13502.4	1.4	1.6	0.346	8.70
W_3	13509.9	1.6	13505.0	1.3	13501.3	1.1	1.3	0.252	18.18
						Total Mass Loss	4.4	0.13	GOOD

Average Mass loss				
Age	28	56	90	120
	12.2	6.8	5.6	4.4

Including Layer 1			
Average Stdv		Average CoV	
0.30		14.92	<36%

Not Including Layer 1			
Average Stdv		Average CoV	
0.29		10.10	<36%

Table B.3: Mass Loss (g) Results-60% HVFA Concrete (Phase I)

Mix ID: 120d 60%									
	Trial 1	Mass loss	Trial 2	Mass loss	Trial 3	Mass loss	Avg Loss	Stdv	CoV
W_o	12187.0	-	12173.0	-	12158.9	-	-		
W_1	12181.6	5.4	12167.8	5.2	12153.6	5.3	5.3	0.100	
W_2	12177.8	3.8	12163.5	4.3	12149.5	4.1	4.1	0.252	26.33
W_3	12173.0	4.8	12158.9	4.6	12144.8	4.7	4.7	0.100	14.45
						Total Mass Loss	14.1	0.62	GOOD

Mix ID: 120d 60%									
	Trial 1	Mass loss	Trial 2	Mass loss	Trial 3	Mass loss	Avg Loss	Stdv	CoV
W_o	12917.6	-	12906.3	-	12894.4	-	-		
W_1	12915.4	2.2	12902.1	4.2	12891.7	2.7	3.0	1.041	
W_2	12911.8	3.6	12898.2	3.9	12888.2	3.5	3.7	0.208	18.91
W_3	12906.3	5.5	12894.4	3.8	12883.4	4.8	4.7	0.854	24.70
						Total Mass Loss	11.4	0.84	GOOD

Mix ID: 120d 60%									
	Trial 1	Mass loss	Trial 2	Mass loss	Trial 3	Mass loss	Avg Loss	Stdv	CoV
W_o	13619.4	-	13610.3	-	13600.0	-	-		
W_1	13616.1	3.3	13606.5	3.8	13596.2	3.8	3.6	0.289	
W_2	13613.4	2.7	13603.9	2.6	13594.1	2.1	2.5	0.321	38.25
W_3	13610.3	3.1	13600.0	3.9	13591.0	3.1	3.4	0.462	30.86
						Total Mass Loss	9.5	0.61	NO GOOD

Mix ID: 120d 60%									
	Trial 1	Mass loss	Trial 2	Mass loss	Trial 3	Mass loss	Avg Loss	Stdv	CoV
W_o	12884.3	-	12876.1	-	12867.9	-	-		
W_1	12880.9	3.4	12872.5	3.6	12864.8	3.1	3.4	0.252	
W_2	12878.3	2.6	12869.6	2.9	12862.4	2.4	2.6	0.252	24.44
W_3	12876.1	2.2	12867.9	1.7	12859.5	2.9	2.3	0.603	14.97
						Total Mass Loss	8.3	0.56	GOOD

Average Mass loss				
Age	28	56	90	120
	14.1	11.4	9.5	8.3

Including Layer 1			
Average Stdv		Average CoV	
0.59		18.83	<36%

Not Including Layer 1			
Average Stdv		Average CoV	
0.48		15.28	<36%

Table B.4: Mass Loss (g) Results – Conventional Concrete (Phase II)

Mix ID: 14d CCT-100									
	Trial 1	Mass loss	Trial 2	Mass loss	Trial 3	Mass loss	Avg Loss	Stdv	CoV
W_o	13672.6	-	13650.5	-	13632.1	-	-		
W_1	13665.6	7.0	13644.1	6.4	13624.9	7.2	6.9	0.416	
W_2	13655.4	10.2	13638.0	6.1	13617.6	7.3	7.9	2.108	13.57
W_3	13650.5	4.9	13632.1	5.9	13612.3	5.3	5.4	0.503	37.78
						Total Mass Loss	20.1	1.26	NO GOOD

Mix ID: 28d CCT-100									
	Trial 1	Mass loss	Trial 2	Mass loss	Trial 3	Mass loss	Avg Loss	Stdv	CoV
W_o	13431.7	-	13404.2	-	13377.0	-	-		
W_1	13413.6	18.1	13387.2	17.0	13358.1	18.9	18.0	0.954	
W_2	13408.4	5.2	13382.1	5.1	13353.1	5.0	5.1	0.100	111.69
W_3	13404.2	4.2	13377.0	5.1	13347.8	5.3	4.9	0.586	4.68
						Total Mass Loss	28.0	7.52	NO GOOD

Mix ID: 14d CCT-130									
	Trial 1	Mass loss	Trial 2	Mass loss	Trial 3	Mass loss	Avg Loss	Stdv	CoV
W_o	14007.6	-	13976.7	-	13951.7	-	-		
W_1	13998.2	14.0	13968.8	7.9	13944.2	14.2	12.0	3.581	
W_2	13984.2	9.4	13960.5	8.3	13930.0	7.5	8.4	0.954	35.56
W_3	13976.7	7.5	13951.7	8.8	13921.8	8.2	8.2	0.651	2.82
						Total Mass Loss	28.6	2.17	GOOD

Mix ID: 28d CCT-130									
	Trial 1	Mass loss	Trial 2	Mass loss	Trial 3	Mass loss	Avg Loss	Stdv	CoV
W_o	13485.1	-	13458.7	-	13426.7	-	-		
W_1	13469.5	15.6	13439.6	19.1	13409.2	17.5	17.4	1.752	
W_2	13463.3	6.2	13432.3	7.3	13402.4	6.8	6.8	0.551	88.00
W_3	13458.7	4.6	13426.7	5.6	13397.4	5.0	5.1	0.503	28.73
						Total Mass Loss	29.2	6.68	NO GOOD

Mix ID: 14d CCT-160									
	Trial 1	Mass loss	Trial 2	Mass loss	Trial 3	Mass loss	Avg Loss	Stdv	CoV
Wo	13631.6	-	13612.5	-	13595.7	-	-		
W1	13625.4	11.9	13607.3	5.2	13590.4	5.3	5.6	3.840	
W2	13613.5	6.2	13601.7	5.6	13584.2	6.2	7.9	0.346	34.65
W3	13612.5	5.5	13595.7	6.0	13578.0	6.2	5.9	0.361	28.99
						Total Mass Loss	17.9	1.78	GOOD

Mix ID: 28d CCT-160									
	Trial 1	Mass loss	Trial 2	Mass loss	Trial 3	Mass loss	Avg Loss	Stdv	CoV
Wo	13302.7	-	13273.5	-	13248.1	-	-		
W1	13285.1	17.6	13257.5	16.0	13232.2	15.9	16.5	0.954	
W2	13278.9	6.2	13252.2	5.3	13226.8	5.4	5.6	0.493	98.19
W3	13273.5	5.4	13248.1	4.1	13222.1	4.7	4.7	0.651	17.36
						Total Mass Loss	26.9	6.55	NO GOOD

Average Mass loss			
Age	100	130	160
14	20.1	28.6	17.9
28	28.0	29.2	26.9

Including Layer 1			
Average Stdv		Average CoV	
4.33		41.84	>36%

Not Including Layer 1			
Average Stdv		Average CoV	
0.65		20.06	<36%

Table B.5: Mass Loss (g) Results – 35% HVFA Concrete (Phase II)

Mix ID: 14d 35T-100									
1-Feb	Trial 1	Mass loss	Trial 2	Mass loss	Trial 3	Mass loss	Avg. Loss	Stdv	CoV
W_o	13382.3	-	13349.7	-	13321.0	-			
W_1	13360.7	21.6	13333.9	15.8	13301.8	19.2	18.9	2.914	
W_2	13354.6	6.1	13324.5	9.4	13295.5	6.3	7.3	1.850	88.78
W_3	13349.7	4.9	13321.0	3.5	13288.6	6.9	5.1	1.709	35.04
						Total	**31.2**	7.40	NO GOOD

Mix ID: 28d 35T-100									
15-Feb	Trial 1	Mass loss	Trial 2	Mass loss	Trial 3	Mass loss	Avg. Loss	Stdv	CoV
W_o	13158.9	-	13132.6	-	13105.4	-			
W_1	13143.6	15.3	13118.7	13.9	13091.0	14.4	14.5	0.709	
W_2	13137.6	6.0	13110.7	8.0	13085.0	6.0	6.7	1.155	74.21
W_3	13132.6	5.0	13105.4	5.3	13080.8	4.2	4.8	0.569	31.88
						Total	**26.0**	5.15	NO GOOD

Mix ID: 14d 35T-130									
1-Feb	Trial 1	Mass loss	Trial 2	Mass loss	Trial 3	Mass loss	Avg. Loss	Stdv	CoV
W_o	13569.1	-	13533.3	-	13499.2	-			
W_1	13551.1	18.0	13515.3	18.0	13481.2	18.0	18.0	0.000	
W_2	13541.4	9.7	13507.8	7.5	13473.2	8.0	8.4	1.153	72.73
W_3	13533.3	8.1	13499.2	8.6	13466.8	6.4	7.7	1.153	8.70
						Total	**34.1**	5.76	NO GOOD

Mix ID: 28d 35T-130									
15-Feb	Trial 1	Mass loss	Trial 2	Mass loss	Trial 3	Mass loss	Avg. Loss	Stdv	CoV
W_o	13250.9	-	13214.2	-	13178.2	-			
W_1	13229.0	21.9	13191.0	23.2	13156.1	22.1	22.4	0.700	
W_2	13218.8	10.2	13182.6	8.4	13150.6	5.5	8.0	2.371	94.41
W_3	13214.2	4.6	13178.2	4.4	13146.7	3.9	4.3	0.361	60.54
						Total	**34.7**	9.56	NO GOOD

Mix ID: 14d 35T-160									
1-Feb	Trial 1	Mass loss	Trial 2	Mass loss	Trial 3	Mass loss	Avg. Loss	Stdv	CoV
Wo	13078.3	-	13040.9	-	12997.5	-			
W1	13058.5	19.8	13016.4	24.5	12975.2	22.3	22.2	2.352	
W2	13051.1	7.4	13007.2	9.2	12965.2	10	8.9	1.332	85.84
W3	13040.9	10.2	12997.5	9.7	12958.4	6.8	8.9	1.836	0.38
						Total	**40.0**	7.69	NO GOOD

Mix ID: 28d 35T-160									
15-Feb	Trial 1	Mass loss	Trial 2	Mass loss	Trial 3	Mass loss	Avg. Loss	Stdv	CoV
Wo	13366.5	-	13332.8	-	13304.4	-			
W1	13345.6	20.9	13319.0	13.8	13286.5	17.9	17.5	3.564	
W2	13337.9	7.7	13311.6	7.4	13278.0	8.5	7.9	0.569	76.12
W3	13332.8	5.1	13304.4	7.2	13272.7	5.3	5.9	1.159	29.13
						Total	**31.3**	6.24	NO GOOD

Average Mass loss			
Age	100	130	160
14	31.2	34.1	40.0
28	26.0	34.7	31.3

Including Layer 1			
Average Stdv		Average CoV	
5.25		54.81	>36%

Not Including Layer 1			
Average Stdv		Average CoV	
1.27		27.61	<36%

Table B.6: Mass Loss (g) Results – 50% HVFA Concrete (Phase II)

Mix ID: 14d 50T-100									
	Trial 1	Mass loss	Trial 2	Mass loss	Trial 3	Mass loss	Avg Loss	Stdv	CoV
W_0	13726.0	-	13698.0	-	13671.2	-	-		
W_1	13716.2	9.8	13689.1	8.9	13662.9	8.3	9.0	0.755	
W_2	13706.3	9.9	13679.8	9.3	13653.5	9.4	9.5	0.321	5.76
W_3	13698.0	8.3	13671.2	8.6	13645.4	8.1	8.3	0.252	13.43
						Total Mass Loss	26.9	0.60	GOOD

Mix ID: 28d 50T-100									
	Trial 1	Mass loss	Trial 2	Mass loss	Trial 3	Mass loss	Avg Loss	Stdv	CoV
W_0	13040.1	-	13002.8	-	12964.1	-	-		
W_1	13020.9	19.2	12982.0	20.8	12948.9	15.2	18.4	2.884	
W_2	13009.9	11.0	12970.6	11.4	12944.2	4.7	9.0	3.758	68.29
W_3	13002.8	7.1	12964.1	6.5	12940.8	3.4	5.7	1.986	45.80
						Total Mass Loss	33.1	6.60	NO GOOD

Mix ID: 14d 50T-130									
	Trial 1	Mass loss	Trial 2	Mass loss	Trial 3	Mass loss	Avg Loss	Stdv	CoV
W_0	13285.0	-	13252.5	-	13224.8	-	-		
W_1	13273.5	11.5	13242.2	10.3	13215.4	9.4	10.4	1.054	
W_2	13261.1	12.4	13230.6	11.6	13202.4	13.0	12.3	0.702	17.01
W_3	13252.5	8.6	13224.8	5.8	13195.1	7.3	7.2	1.401	52.13
						Total Mass Loss	30.0	2.57	NO GOOD

Mix ID: 28d 50T-130									
	Trial 1	Mass loss	Trial 2	Mass loss	Trial 3	Mass loss	Avg Loss	Stdv	CoV
W_0	13589.6	-	13560.1	-	13537.8	-	-		
W_1	13572.1	17.5	13547.6	12.5	13522.7	15.1	15.0	2.501	
W_2	13566.3	5.8	13541.8	5.8	13517.4	5.3	5.6	0.289	90.97
W_3	13560.1	6.2	13537.8	4.0	13513.3	4.1	4.8	1.242	16.67
						Total Mass Loss	25.4	5.69	NO GOOD

Mix ID: 14d 50T-160									
	Trial 1	Mass loss	Trial 2	Mass loss	Trial 3	Mass loss	Avg Loss	Stdv	CoV
Wo	13643.6	-	13604.1	-	13563.0	-	-		
W1	13630.3	13.3	13589.9	14.2	13548.0	15.0	14.2	0.850	
W2	13617.3	13.0	13575.9	14.0	13534.7	13.3	13.4	0.513	5.31
W3	13604.1	13.2	13563.0	12.9	13522.7	12.0	12.7	0.624	5.61
						Total Mass Loss	40.3	0.73	GOOD

Mix ID: 28d 50T-160									
	Trial 1	Mass loss	Trial 2	Mass loss	Trial 3	Mass loss	Avg Loss	Stdv	CoV
Wo	13309.3	-	13276.9	-	13236.6	-	-		
W1	13289.1	20.2	13253.7	23.2	13215.5	21.1	21.5	1.539	
W2	13282.5	6.6	13243.4	10.3	13206.2	9.3	8.7	1.914	84.45
W3	13276.9	5.6	13236.6	6.8	13199.3	6.9	6.4	0.723	30.33
						Total Mass Loss	36.7	8.12	NO GOOD

Average Mass loss			
Age	100	130	160
14	26.9	30.0	40.3
28	33.1	25.4	36.7

Including Layer 1			
Average Stdv		Average CoV	
3.23		36.31	>36%

Not Including Layer 1			
Average Stdv		Average CoV	
1.14		27.33	<36%

Table B.7: Mass Loss (g) Results – 60% HVFA Concrete (Phase II)

Mix ID: 14d 60T-100									
	Trial 1	Mass loss	Trial 2	Mass loss	Trial 3	Mass loss	Avg. Loss	Stdv	CoV
W_0	13322.4	-	13292.3	-	13269.7	-			
W_1	13307.0	15.4	13279.7	12.6	13258.3	11.4	13.1	2.053	
W_2	13297.9	9.1	13273.9	5.8	13251.00	7.3	7.4	1.652	55.84
W_3	13292.3	5.6	13269.7	4.2	13244.3	6.7	5.5	1.253	29.46
						Total	26.0	3.97	NO GOOD

Mix ID: 28d 60T-100									
4-Feb	Trial 1	Mass loss	Trial 2	Mass loss	Trial 3	Mass loss	Avg. Loss	Stdv	CoV
W_0	13507.9	-	13483.8	-	13455.9	-			
W_1	13494.2	13.7	13467.2	16.6	13442.3	13.6	14.6	1.704	
W_2	13488.3	5.9	13460.0	7.2	13437.4	4.9	6.0	1.153	83.68
W_3	13483.8	4.5	13455.9	4.1	13432.4	5.0	4.5	0.451	27.85
						Total	25.2	5.46	NO GOOD

Mix ID: 14d 60T-130									
	Trial 1	Mass loss	Trial 2	Mass loss	Trial 3	Mass loss	Avg. Loss	Stdv	CoV
W_0	13078.0	-	13039.3	-	13011.4	-			
W_1	13055.3	22.7	13027.5	11.8	12992.5	18.9	17.8	5.533	
W_2	13046.2	9.1	13020.2	7.3	12984.10	8.4	8.3	0.907	73.15
W_3	13039.3	6.9	13011.4	8.8	12978.5	5.6	7.1	1.609	15.18
						Total	33.2	5.87	NO GOOD

Mix ID: 28d 60T-130									
4-Feb	Trial 1	Mass loss	Trial 2	Mass loss	Trial 3	Mass loss	Avg. Loss	Stdv	CoV
W_0	13183.1	-	13156.7	-	13132.8	-			
W_1	13168.8	14.3	13144.7	12	13119.6	13.2	13.2	1.150	
W_2	13161.5	7.3	13139.2	5.5	13114.5	5.1	6.0	1.172	75.26
W_3	13156.7	4.8	13132.8	6.4	13110	4.5	5.2	1.021	13.10
						Total	24.4	4.38	NO GOOD

Mix ID: 14d 60T-160									
	Trial 1	Mass loss	Trial 2	Mass loss	Trial 3	Mass loss	Avg. Loss	Stdv	CoV
Wo	13485.0	-	13462.8	-	13438.1	-			
W1	13475.8	9.2	13450.7	12.1	13429.7	8.4	9.9	1.947	
W2	13468.1	7.7	13444.8	5.9	13423.1	6.6	6.7	0.907	38.08
W3	13462.8	5.3	13438.1	6.7	13416.7	6.4	6.1	0.737	9.33
						Total	22.8	2.02	NO GOOD

Mix ID: 28d 60T-160									
4-Feb	Trial 1	Mass loss	Trial 2	Mass loss	Trial 3	Mass loss	Avg. Loss	Stdv	CoV
Wo	13021.7	-	13003.2	-	12984.4	-			
W1	13013.3	8.4	12993.3	9.9	12974.2	10.2	9.5	0.964	
W2	13009.1	4.2	12987.8	5.5	12969.7	4.5	4.7	0.681	66.98
W3	13003.2	5.9	12984.4	3.4	12965.2	4.5	4.6	1.253	2.86
						Total	18.8	2.79	NO GOOD

Average Mass loss			
Age	100	130	160
14	26.0	33.2	22.8
28	25.2	24.4	18.8

Including Layer 1			
Average Stdv		Average CoV	
2.80		40.90	>36%

Not Including Layer 1			
Average Stdv		Average CoV	
1.07		16.29	<36%

Table B.8: Mass Loss (g) Results – 70% HVFA Concrete (Phase II)

Mix ID: 14d 70T-100									
	Trial 1	Mass loss	Trial 2	Mass loss	Trial 3	Mass loss	Avg Loss	Stdv	CoV
W_0	13383.7	-	13341.5	-	13300.2	-	-		
W_1	13370.3	13.4	13328.3	13.2	13287.1	13.1	13.2	0.153	
W_2	13355.8	14.5	13314.2	14.1	13273.2	13.9	14.2	0.306	6.81
W_3	13341.5	14.3	13300.2	14.0	13259.4	13.8	14.0	0.252	0.95
						Total Mass Loss	41.4	0.50	GOOD

Mix ID: 28d 70T-100									
	Trial 1	Mass loss	Trial 2	Mass loss	Trial 3	Mass loss	Avg Loss	Stdv	CoV
W_0	13262.9	-	13210.0	-	13164.4	-	-		
W_1	13233.8	29.1	13184.0	26.0	13139.9	24.5	26.5	2.346	
W_2	13222.2	11.6	13175.2	8.8	13128.5	11.4	10.6	1.562	85.82
W_3	13210.0	12.2	13164.4	10.8	13120.2	8.3	10.4	1.976	1.58
						Total Mass Loss	47.6	9.25	NO GOOD

Mix ID: 14d 70T-130									
	Trial 1	Mass loss	Trial 2	Mass loss	Trial 3	Mass loss	Avg Loss	Stdv	CoV
W_0	13257.2	-	13212.2	-	13168.9	-	-		
W_1	13241.6	15.6	13197.2	15.0	13153.0	15.9	15.5	0.458	
W_2	13229.3	12.3	13183.2	14.0	13139.9	13.1	13.1	0.850	16.53
W_3	13212.2	17.1	13168.9	14.3	13123.9	16.0	15.8	1.411	18.43
						Total Mass Loss	44.4	1.46	GOOD

Mix ID: 28d 70T-130									
	Trial 1	Mass loss	Trial 2	Mass loss	Trial 3	Mass loss	Avg Loss	Stdv	CoV
W_0	13123.4	-	13058.8	-	13005.0	-	-		
W_1	13095.0	28.4	13027.5	31.3	12972.8	32.2	30.6	1.986	
W_2	13077.0	18.0	13016.3	11.2	12961.4	11.4	13.5	3.870	77.43
W_3	13058.8	18.2	13005.0	11.3	12953.1	8.3	12.6	5.076	7.14
						Total Mass Loss	56.8	10.15	NO GOOD

Mix ID: 14d 70T-160									
	Trial 1	Mass loss	Trial 2	Mass loss	Trial 3	Mass loss	Avg Loss	Stdv	CoV
Wo	12902.5	-	12842.9	-	12778.0	-	-		
W1	12877.5	25.0	12802.2	40.7	12744.6	33.4	33.0	7.856	
W2	12864.5	13.0	12789.9	12.3	12731.9	12.7	12.7	0.351	89.13
W3	12842.9	21.6	12778.0	11.9	12724.7	7.2	13.6	7.343	6.86
						Total Mass Loss	59.3	11.51	NO GOOD

Mix ID: 28d 70T-160									
	Trial 1	Mass loss	Trial 2	Mass loss	Trial 3	Mass loss	Avg Loss	Stdv	CoV
Wo	12877.3	-	12845.0	-	12812.7	-	-		
W1	12866.3	11.0	12833.9	11.1	12802.9	9.8	10.6	0.723	
W2	12853.3	13.0	12821.7	12.2	12790.3	12.6	12.6	0.400	16.93
W3	12845.0	8.3	12812.7	9.0	12780.8	9.5	8.9	0.603	34.06
						Total Mass Loss	32.2	1.83	GOOD

Average Mass loss			
Age	100	130	160
14	41.4	44.4	59.3
28	47.6	56.8	32.2

Including Layer 1			
Average Stdv		Average CoV	
4.53		30.14	<36%

Not Including Layer 1			
Average Stdv		Average CoV	
2.00		11.50	<36%

APPENDIX C - FREEZE-THAW

Table C.1: Durability Factor Precision for two or more Beams [Adapted from ASTM C666-03]

Range of Average DF	Std. dev.	Acceptable Range
0 to 5	0.6	1.6
5 to 10	1.1	3.1
10 to 20	4.2	11.8
20 to 30	5.9	16.7
30 to 50	9.0	25.4
50 to 70	10.8	30.6
70 to 80	8.2	23.1
80 to 90	4.0	11.3
90 to 95	1.5	4.2
Above 95	0.8	2.2

Table C.2: Results and Precision – Phase I

	28					56					90					120				
Mix No.	a	b	Avg. DF	std	Diff.	a	b	Avg. DF	std	Diff.	a	b	Avg. DF	std	Diff.	a	b	Avg. DF	std	Diff.
CC	9.6	10.1	**9.9**	0.4	0.5	7.3	7.9	**7.6**	0.4	0.6	16.4	11.1	**13.8**	3.8	5.3	33.4	29.9	**31.7**	2.5	3.5
35	18.8	20.3	**19.5**	1.0	1.5	13.9	15.9	**14.9**	1.4	2.0	21.5	22.4	**21.9**	0.6	0.9	18.4	11.0	**14.7**	5.2	7.4
50	17.5	10.0	**13.7**	5.3	7.5	25.1	23.2	**24.2**	1.3	1.9	22.8	17.5	**20.2**	3.7	5.3	15.5	26.1	**20.8**	7.4	10.5
60	7.7	7.1	**7.4**	0.4	0.5	8.7	-	**8.7**	-	-	8.7	9.1	**8.9**	0.3	0.4	18.4	10.1	**14.2**	5.9	8.3
70	0.0	0.0	**0.0**	-	0.0	0.0	0.0	**0.0**	-	0.0	0.0	0.0	**0.0**	-	0.0	-	7.4	**7.4**	-	-

Table C.3: Results and Precision (Phase II)

	14day					28day				
	a	b	Avg DF	Stdev	Diff.	a	b	Avg DF	Stdev	Diff.
CCT100	19.9*	9.6	14.7	7.3	10.3	11.2	10.1	10.6	0.8	1.1
CCT130	21.5	11.3	16.4	7.2	10.2	22.5	12.1	17.3	7.4	10.5
CCT160	11.8	6.7	9.2	3.6	5.1	7.1	7.1	7.1	0.0	0.1
35T100	*	*	*	-	-	*	*	*	-	-
35T130	*	*	*	-	-	*	*	*	-	-
35T160	*	*	*	-	-	*	*	*	-	-
50T100	18.1	33.5	25.8	10.9	15.4	10.4	8.6	9.5	1.3	1.8
50T130	18.9	20.0	19.5	0.7	1.0	22.0	11.7	16.8	7.3	10.3
50T160	7.7	11.4*	9.5	2.6	3.7	6.2*	6.2*	6.2	0.0	0.0
60T100	1.5*	1.1*	1.3	0.3	0.4	0.0	11.4	5.7	8.1	11.4
60T130	*	*	*	-	-	11.6	11.6	11.6	0.1	0.1
60T160	*	*	*	-	-	*	*	*	-	-
70T100	*	*	*	-	-	0.0	10.6	*	7.5	10.6
70T130	*	*	*	-	-	11.7	*	*	-	11.7
70T160	*	*	*	-	-	*	*	*	-	-

*Specimens failed due to falling below 60% RDM while other specimens failed from destruction of surface area

APPENDIX D - CHLORIDE CONTENT

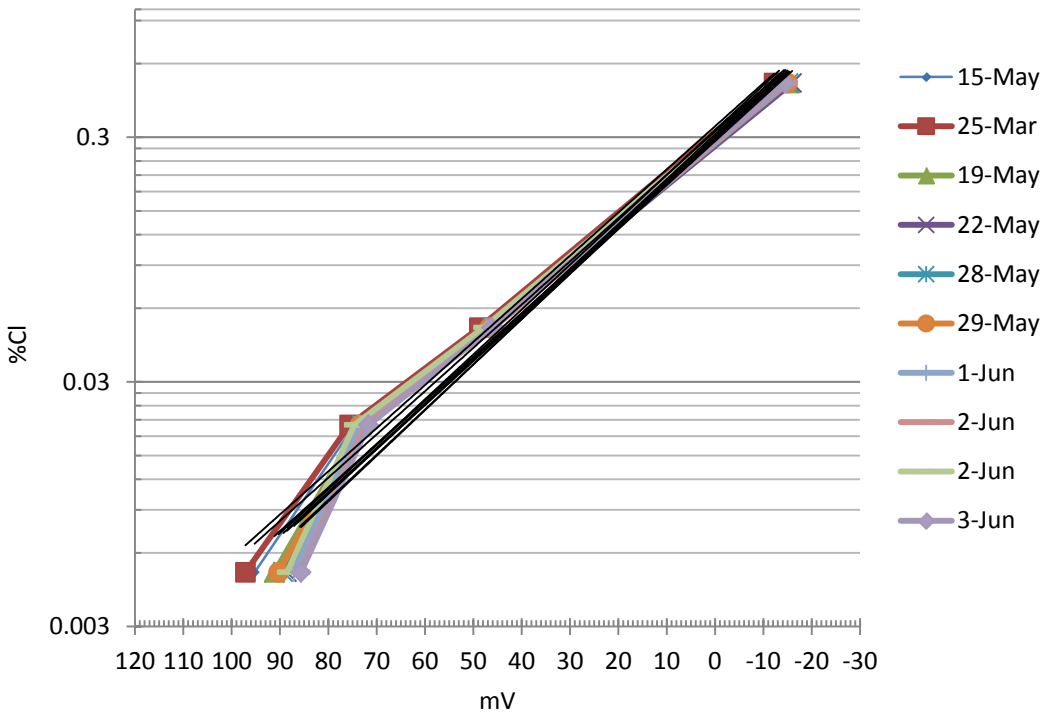

Figure D.1: Calibration Curves

Table D.1: Original Chloride Contents (%) -Phase I

	CC	35	50	60	70
28	0.317	0.148	0.118	0.035	0.096
56	0.174	0.124	0.134	0.035	0.030
90	0.144	0.153	0.138	0.064	0.111
120	0.125	0.163	0.122	0.112	0.077

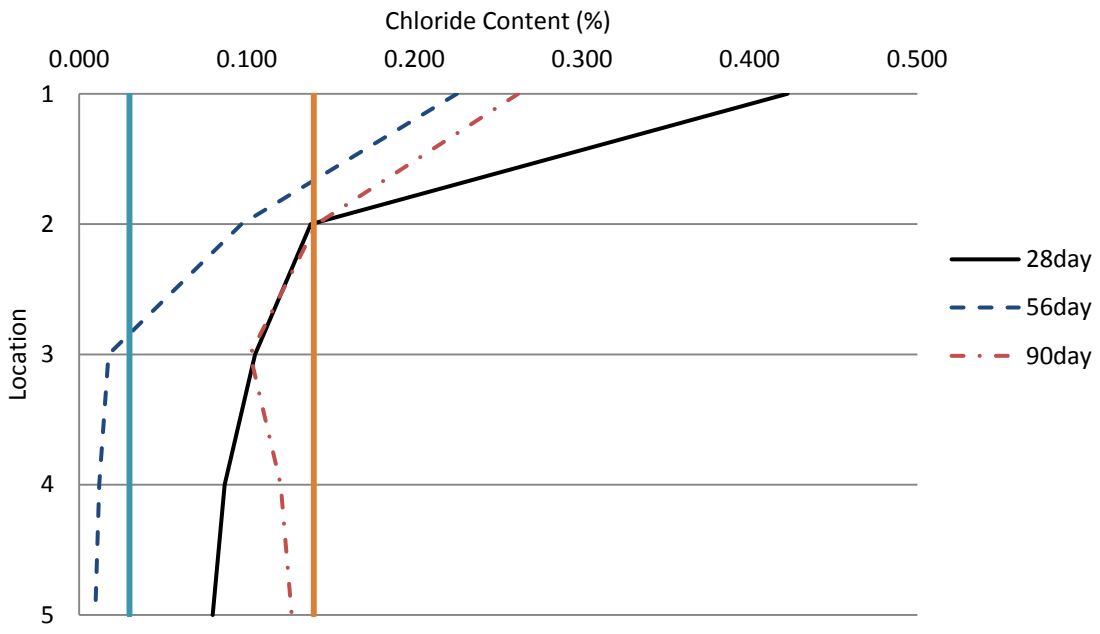

Figure D.2: Conventional Concrete Chloride Profile (Phase I)

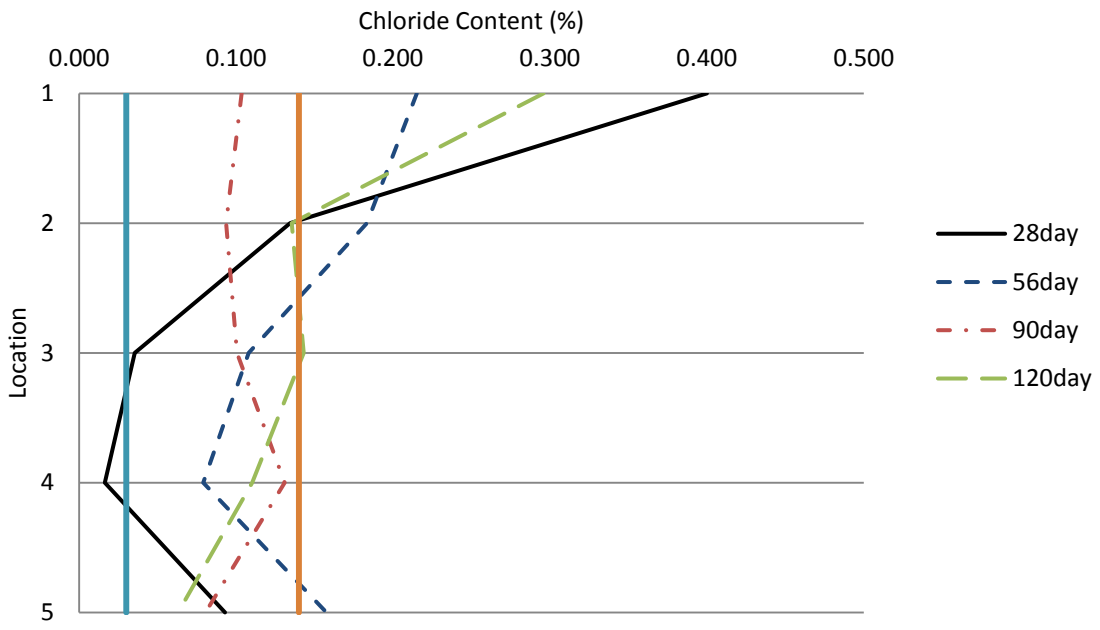

Figure D.3: 35% HVFA Concrete Chloride Profile (Phase I)

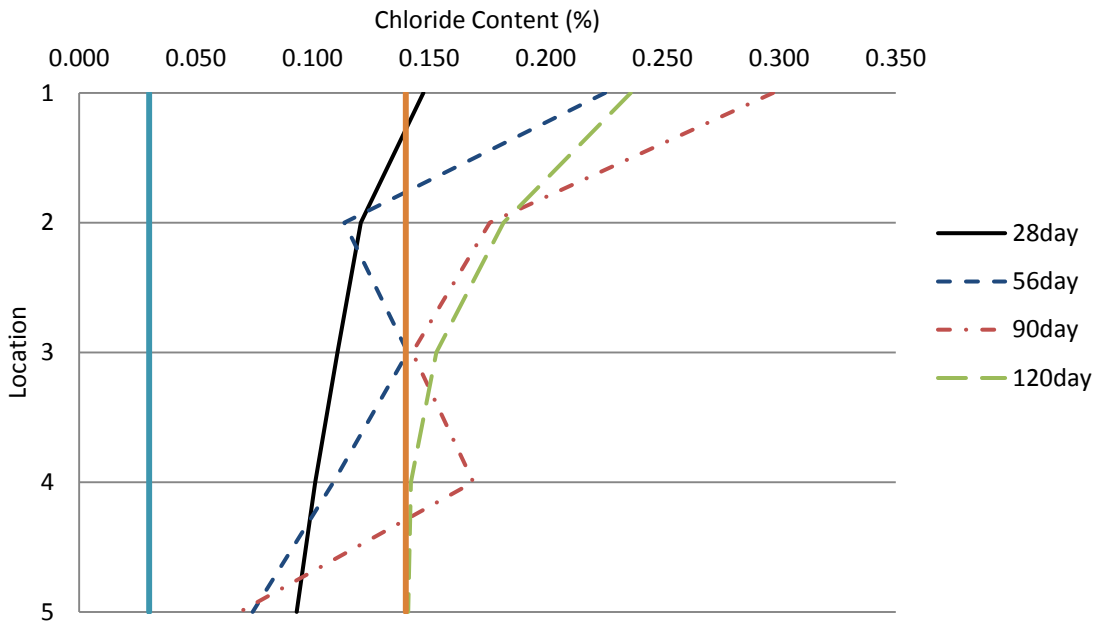

Figure D.5: 50% HVFA Concrete Chloride Profile (Phase I)

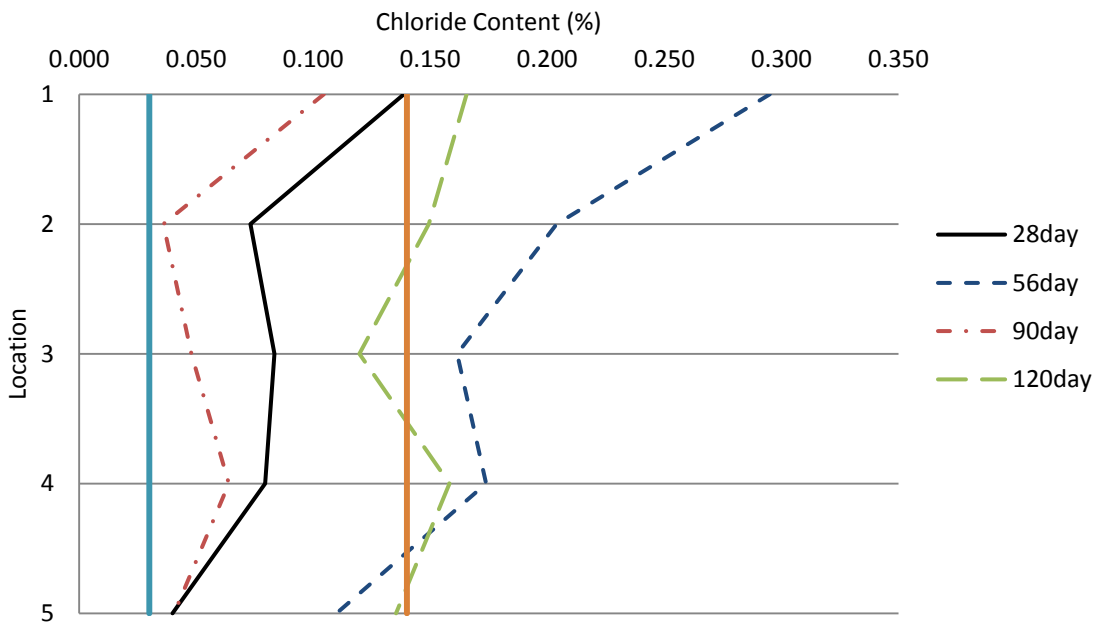

Figure D.5: 60% HVFA Concrete Chloride Profile (Phase I)

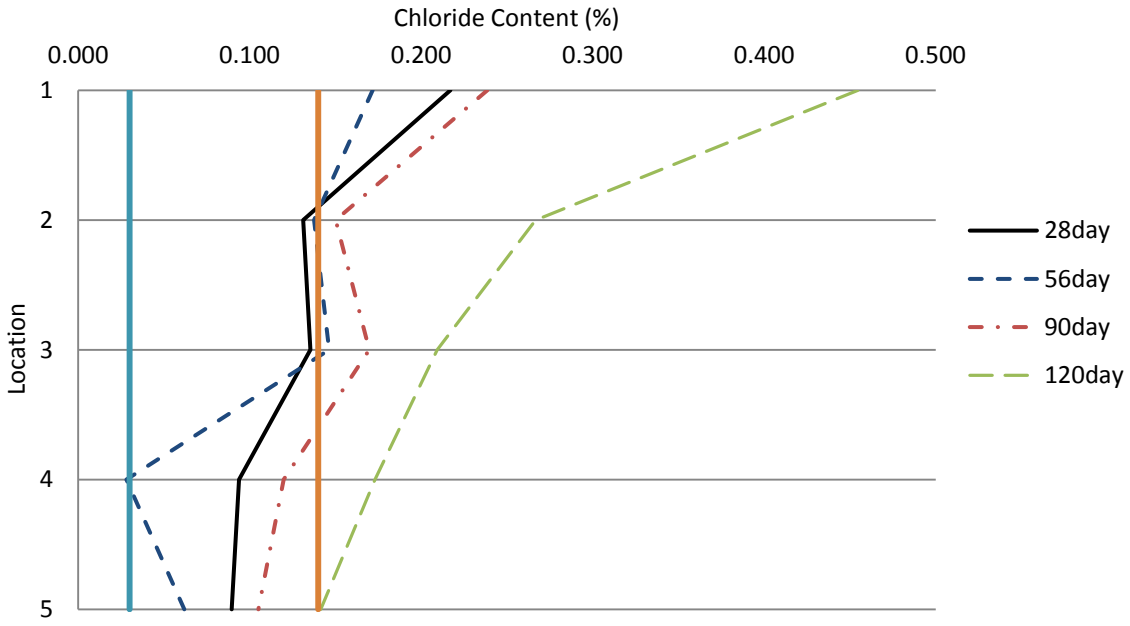

Figure D.6: 70% HVFA Concrete Chloride Profile (Phase I)

Table D.1: Original Chloride Contents (%) (Phase II)

	14d	28d
CCT100	0.058	0.143
CCT130	0.067	0.164
CCT160	0.047	0.112
35T100	0.234	0.084
35T130	0.203	0.118
35T160	0.157	0.144
50T100	0.148	0.174
50T130	0.177	0.144
50T160	0.179	0.155
60T100	0.109	0.154
60T130	0.128	0.124
60T160	0.099	0.133
70T100	0.149	0.142
70T130	0.126	0.123
70T160	0.120	0.142

Table D.2: Original RCT Results Conventional HVFA (Phase I)

Conventional				
Age	Location	Test Date	mV	% Cl
28 days	original	1-Jun	-0.6	0.317
	1	2-Jun	-8.2	0.423
	2	2-Jun	17.8	0.138
	3	2-Jun	24.2	0.105
	4	2-Jun	28.6	0.087
	5	2-Jun	30.6	0.080
56 days	original	2-Jun	12.5	0.174
	1	24-Mar	8.3	0.225
	2	24-Mar	28.9	0.097
	3	24-Mar	70.6	0.018
	4	24-Mar	79.9	0.012
	5	24-Mar	85.2	0.010
90 days	original	1-Jun	18.1	0.144
	1	29-May	3.3	0.262
	2	29-May	18.3	0.142
	3	29-May	26.3	0.102
	4	29-May	22.3	0.120
	5	29-May	21.0	0.127
120 days	original	15-May	23.8	0.125
	1	N/A: Data Lost		
	2			
	3			
	4			
	5			

Table D.3: Original RCT Results 35% HVFA (Phase I)

35% HVFA				
Age	Location	Test Date	mV	% Cl
28 days	original	19-May	22.4	0.118
	1	24-Mar	-11.7	0.400
	2	24-Mar	20.9	0.134
	3	24-Mar	53.4	0.035
	4	24-Mar	72.3	0.016
	5	24-Mar	29.9	0.093
56 days	original	15-May	24.0	0.124
	1	19-May	7.7	0.215
	2	19-May	11.6	0.183
	3	19-May	24.5	0.108
	4	19-May	32.1	0.079
	5	19-May	15.3	0.158
90 days	original	28-May	15.7	0.153
	1*	28-May	25.0	0.104
	2*	28-May	27.4	0.094
	3	28-May	25.7	0.101
	4	28-May	19.4	0.131
	5	28-May	31.0	0.080
120 days	original	19-May	14.5	0.163
	1	28-May	0	0.296
	2	28-May	18.6	0.135
	3	28-May	17.3	0.143
	4	28-May	23.5	0.110
	5	28-May	36.8	0.063

* Indicates samples less than the specified 1.5 g

Table D.4: Original RCT Results 50% HVFA (Phase I)

50% HVFA				
Age	Location	Test Date	mV	% Cl
28 days	original	19-May	16.8	0.148
	1	29-May	17.3	0.148
	2	29-May	22.2	0.121
	3	29-May	24.3	0.111
	4	29-May	26.5	0.101
	5	29-May	28.5	0.093
56 days	original	15-May	22.2	0.134
	1	24-Mar	8.3	0.225
	2	1-Jun	23.8	0.114
	3	1-Jun	18.7	0.141
	4	1-Jun	24.8	0.109
	5	1-Jun	33.9	0.074
90 days	original	28-May	18.6	0.138
	1	19-May	-0.2	0.297
	2	19-May	12.6	0.176
	3	19-May	17.7	0.143
	4	19-May	13.6	0.169
	5	19-May	35.5	0.069
120 days	original	19-May	23.6	0.112
	1	29-May	5.8	0.236
	2	29-May	12.2	0.182
	3	29-May	16.4	0.153
	4	29-May	18.2	0.142
	5	29-May	18.4	0.141

Table D.5: Original RCT Results 60% HVFA (Phase I)

60% HVFA				
Age	Location	Test Date	mV	% Cl
28 days	original	15-May	55.1	0.035
	1	19-May	18.4	0.139
	2	19-May	34.0	0.073
	3	19-May	30.8	0.083
	4	19-May	32.0	0.079
	5	19-May	48.8	0.040
56 days	original	24-Mar	53.8	0.035
	1	29-May	0.4	0.295
	2	29-May	9.4	0.204
	3	29-May	15.1	0.161
	4	29-May	13.3	0.174
	5	15-May	27.0	0.110
90 days	original	19-May	37.3	0.064
	1	28-May	25.3	0.105
	2	28-May	51.3	0.036
	3	28-May	44.3	0.048
	4	28-May	37.3	0.064
	5	28-May	48.4	0.041
120 days	original	19-May	21.6	0.122
	1*	1-Jun	14.1	0.165
	2	1-Jun	16.6	0.149
	3	1-Jun	22.0	0.120
	4	1-Jun	15.2	0.158
	5	1-Jun	19.0	0.135

* Indicates samples less than the specified 1.5 g

Table D.5: Original RCT Results 70% HVFA (Phase I)

70% HVFA				
Age	Location	Test Date	mV	% Cl
28 days	original	19-May	27.4	0.096
	1*	1-Jun	8.4	0.217
	2	2-Jun	21.3	0.131
	3*	29-May	19.4	0.135
	4	2-Jun	29.3	0.094
	5	2-Jun	30.4	0.090
56 days	original	24-Mar	57.6	0.030
	1*	28-May	13.2	0.172
	2	28-May	18.6	0.138
	3*	28-May	17.1	0.146
	4*	28-May	57.3	0.028
	5	28-May	38.1	0.062
90 days	original	19-May	23.9	0.111
	1	22-May	4.7	0.239
	2	22-May	16.0	0.150
	3	22-May	13.0	0.170
	4	22-May	21.5	0.120
	5	22-May	24.7	0.105
120 days	original	19-May	32.9	0.077
	1	1-Jun	-9.2	0.455
	2	1-Jun	3.5	0.267
	3	15-May	11.3	0.209
	4	1-Jun	13.8	0.173
	5	1-Jun	18.6	0.141

* Indicates samples less than the specified 1.5 g

Table D.6: Conventional Concrete RCT Data (Phase II)

CCT-100				
Age	Loc.	Test Date	mV	% Cl
14 days	Orig.	24-Mar	41.4	0.058
	1	29-May	-1.1	0.314
	2	29-May	11.1	0.190
	3	29-May	20.1	0.132
	4	29-May	35.7	0.069
	5	29-May	28.0	0.095
28 days	Orig.	15-May	20.6	0.143
	1	22-May	3.5	0.251
	2	22-May	5.7	0.229
	3	22-May	8.3	0.206
	4	22-May	11.6	0.180
	5	28-May	17.5	0.142

CCT-130				
Age	Loc.	Test Date	mV	% Cl
14 days	Orig.	24-Mar	37.8	0.067
	1	1-Jun	-6.8	0.411
	2	1-Jun	5.1	0.249
	3	1-Jun	21.3	0.126
	4	1-Jun	34.7	0.072
	5	1-Jun	38.3	0.062
28 days	Orig.	15-May	17.2	0.164
	1*	28-May	4.5	0.245
	2	28-May	5.3	0.237
	3	28-May	7.3	0.218
	4	28-May	9.2	0.201
	5	28-May	18.2	0.138

CCT-160				
Age	Loc.	Test Date	mV	% Cl
14 days	Orig.	24-Mar	46.5	0.047
	1	28-May	24.9	0.140
	2	22-May	13.3	0.168
	3	22-May	23.0	0.113
	4	22-May	35.6	0.067
	5	22-May	39.6	0.057
28 days	Orig.	15-May	26.5	0.112
	1	28-May	-0.1	0.297
	2	28-May	1.7	0.276
	3	28-May	3.4	0.257
	4	28-May	3.2	0.259
	5	28-May	7.4	0.217

Table D.7: 35% HVFA Concrete RCT Data (Phase II)

35T-100				
Age	Loc.	Test Date	mV	% Cl
14 days	Orig.	15-May	8.6	0.234
	1	2-Jun	2.9	0.262
	2	2-Jun	9.3	0.199
	3	2-Jun	15.1	0.155
	4	2-Jun	19.0	0.131
	5	2-Jun	20.0	0.126
28 days	Orig.	19-May	30.5	0.084
	1	1-Jun	0.7	0.300
	2	1-Jun	18.9	0.140
	3	1-Jun	22.2	0.122
	4	1-Jun	31.2	0.083
	5	1-Jun	27.5	0.097

35T-130				
Age	Loc.	Test Date	mV	% Cl
14 days	Orig.	15-May	12	0.203
	1	2-Jun	3.3	0.258
	2	2-Jun	6.4	0.226
	3	2-Jun	14	0.163
	4	2-Jun	17.5	0.140
	5	2-Jun	18.7	0.133
28 days	Orig.	19-May	22.4	0.118
	1	1-Jun	-2.6	0.345
	2	1-Jun	12.5	0.183
	3	1-Jun	18.9	0.140
	4	1-Jun	29.9	0.088
	5	1-Jun	29.1	0.091

35T-160				
Age	Loc.	Test Date	mV	% Cl
14 days	Orig.	15-May	18.3	0.157
	1	3-Jun	1.2	0.287
	2	3-Jun	9.2	0.203
	3	3-Jun	10.2	0.195
	4	3-Jun	19.0	0.133
	5	3-Jun	20.1	0.127
28 days	Orig.	19-May	17.5	0.144
	1	1-Jun	-2.0	0.336
	2	1-Jun	17.3	0.149
	3	1-Jun	19.8	0.134
	4	1-Jun	33.2	0.077
	5	1-Jun	30.4	0.086

Table D.8: 50% HVFA Concrete RCT Data (Phase II)

50T-100				
Age	Loc.	Test Date	mV	% Cl
14 days	Orig.	29-May	17.3	0.148
	1	22-May	0.9	0.279
	2	22-May	11.2	0.183
	3	22-May	21.2	0.121
	4	22-May	33.5	0.073
	5	22-May	10.3	0.190
28 days	Orig.	29-May	13.3	0.174
	1	2-Jun	-2.6	0.332
	2	2-Jun	-0.7	0.306
	3	15-May	10.8	0.214
	4	15-May	8.4	0.236
	5	2-Jun	11.3	0.183

50T-130				
Age	Loc.	Test Date	mV	% Cl
14 days	Orig.	29-May	12.8	0.177
	1	19-May	13.2	0.240
	2	19-May	5.7	0.234
	3	19-May	6.3	0.228
	4	19-May	14.1	0.165
	5	19-May	43.2	0.050
28 days	Orig.	29-May	17.9	0.144
	1	1-Jun	1.2	0.294
	2	1-Jun	5.9	0.241
	3	15-May	10.8	0.214
	4	15-May	11.8	0.205
	5	1-Jun	15.3	0.162

50T-160				
Age	Loc.	Test Date	mV	% Cl
14 days	Orig.	29-May	12.6	0.179
	*1	28-May	-8	0.414
	2	28-May	8.5	0.207
	3	2-Jun	9.8	0.195
	4	2-Jun	14.4	0.175
	5	28-May	16.7	0.147
28 days	Orig.	29-May	16.1	0.155
	1	22-May	-5.8	0.367
	2	22-May	2.1	0.265
	3	22-May	7.0	0.217
	4	22-May	10.8	0.186
	5	22-May	15.9	0.151

Table D.9: 60% HVFA Concrete RCT Data (Phase II)

60T-100				
Age	Loc.	Test Date	mV	% Cl
14 days	Orig.	15-May	27.3	0.109
	1	3-Jun	0.3	0.298
	2	3-Jun	6.7	0.227
	3	3-Jun	16.8	0.147
	4	3-Jun	21.2	0.121
	5	3-Jun	21.0	0.122
28 days	Orig.	15-May	18.8	0.154
	1	2-Jun	-5.5	0.376
	2	2-Jun	7.7	0.213
	3	2-Jun	16.7	0.145
	4	2-Jun	21.0	0.120
	5	2-Jun	21.4	0.118

60T-130				
Age	Loc.	Test Date	mV	% Cl
14 days	Orig.	15-May	23.3	0.128
	1	3-Jun	-9.7	0.459
	2	3-Jun	6.0	0.233
	3	3-Jun	11.3	0.186
	4	3-Jun	18.5	0.136
	5	3-Jun	19.3	0.132
28 days	Orig.	15-May	24.1	0.124
	1	2-Jun	-5.8	0.381
	2	2-Jun	4.6	0.244
	3	2-Jun	11.6	0.180
	4	2-Jun	18.2	0.136
	5	2-Jun	12.6	0.150

60T-160				
Age	Loc.	Test Date	mV	% Cl
14 days	Orig.	15-May	29.5	0.099
	1	3-Jun	-1.8	0.327
	2	3-Jun	5.1	0.243
	3	3-Jun	7.3	0.221
	4	3-Jun	11.6	0.184
	5	3-Jun	15.0	0.159
28 days	Orig.	15-May	22.4	0.133
	1	2-Jun	-6.4	0.391
	2	2-Jun	6.2	0.227
	3	2-Jun	8.2	0.209
	4	2-Jun	10.4	0.190
	5	2-Jun	14.2	0.161

Table D.10: 70% HVFA Concrete RCT Data (Phase II)

70T-100				
Age	Loc.	Test Date	mV	% Cl
14 days	Orig.	2-Jun	18.3	0.149
	1	19-May	10.1	0.300
	2	19-May	-0.4	0.300
	3	19-May	5.4	0.236
	4	19-May	11.9	0.181
	5	19-May	12.0	0.180
28 days	Orig.	2-Jun	19.5	0.142
	1	22-May	-0.1	0.290
	2	22-May	4.6	0.240
	3	22-May	6.3	0.223
	4	22-May	18.9	0.133
	5	22-May	43.3	0.049

70T-130				
Age	Loc.	Test Date	mV	% Cl
14 days	Orig.	2-Jun	22.3	0.126
	1	29-May	-4.2	0.356
	2	29-May	9.0	0.207
	3	29-May	12.8	0.177
	4	29-May	18.1	0.143
	5	29-May	19.4	0.135
28 days	Orig.	2-Jun	22.8	0.123
	1	22-May	0.2	0.287
	2	22-May	10.3	0.190
	3	22-May	17.8	0.139
	4	22-May	24.0	0.108
	5	22-May	34.8	0.069

70T-160				
Age	Loc.	Test Date	mV	% Cl
14 days	Orig.	2-Jun	23.4	0.120
	1	2-Jun	0.6	0.289
	2	15-May	17.4	0.163
	3	15-May	13.2	0.194
	4	15-May	11.8	0.205
	5	15-May	9.0	0.230
28 days	Orig.	2-Jun	19.5	0.142
	1	1-Jun	-10.6	0.482
	2	1-Jun	8.4	0.217
	3	1-Jun	10.5	0.199
	4	1-Jun	15.5	0.161
	5	1-Jun	21.0	0.128

REFERENCES

"751.4 Reinforced Concrete Design Properties." *Engineering Policy Guide RSS*. MoDOT, 10 Dec. 2013. Web. 05 June 2015.

Acquaye, Lucy. Effect of High Curing Temperatures on the Strength, Durability and Potential of Delayed Ettringite Formation in Mass Concrete Structures. Diss. University of Florida, 2006. Print.

American Coal Ash Association (ACAA), 2013 "Production & Use Reports." *Publications*. Web.

ASTM C 39. (2014) Standard Test Method for Compressive Strength of Cylindrical Concrete Specimens. West Conshohocken, PA: ASTM International.

ASTM C 70. (2013) Standard Test Method for Surface Moisture in Fine Aggregate. West Conshohocken, PA: ASTM International.

ASTM C 109. (2013) Standard Test Method for Compressive Strength of Hydraulic Cement Mortars (Using 2-in. or [50-mm] Cube Specimens). West Conshohocken, PA: ASTM International.

ASTM C 138. (2014) Standard Test Method for Density (Unit Weight), Yield, and Air Content (Gravimetric) of Concrete. West Conshohocken, PA: ASTM International.

ASTM C 143. (2010). *Standard Test Methods for Slump of Hydraulic Cement Concrete*. West Conshohocken, PA: ASTM International.

ASTM C 192. (2014) Standard Practice for Making and Curing Concrete Test Specimens in the Laboratory. West Conshohocken, PA: ASTM International.

ASTM C 231. (2014) Standard Test Method for Air Content of Freshly Mixed Concrete by the Pressure Method. West Conshohocken, PA: ASTM International.

ASTM C 469. (2014) Standard Test Method for Static Modulus of Elasticity and Poisson's Ratio of Concrete in Compression. West Conshohocken, PA: ASTM International.

ASTM C 618. (2012) Standard Specification for Coal Fly-ash and Raw or Calcined Natural Pozzolan for Use in Concrete. West Conshohocken, PA: ASTM International.

ASTM C 666. (2003) Standard Test Method for Resistance of Concrete to Rapid Freezing and Thawing. West Conshohocken, PA: ASTM International.

ASTM C 944. (2012) Standard Test Method for Abrasion Resistance of Concrete or Mortar Surfaces by the Rotating-Cutter Method. West Conshohocken, PA: ASTM International.

ASTM C 1074. (2011) Standard Practice for Estimating Concrete Strength by the Maturity Method. West Conshohocken, PA: ASTM International.

ASTM C 1543. (2010) Standard Test Method for Determining the Penetration of Chloride Ion into Concrete by Ponding. West Conshohocken, PA: ASTM International.

Atis, Cengiz Duran. "High Volume Fly-ash Abrasion Resistant Concrete," Journal of Materials in Civil Engineering - 14(3):274 - PDF (ASCE). Journal Of Materials In Civil Engineering May-June 2002. Web.

Barrow, R.S., Hadchiti, K.M., Carrasquillo, P.M., and Carrasquillo, R.L., "Temperature Rise and Durability of Concrete Containing Fly-ash," Proceedings of the CANMET/ACI Third International Conference on the Use of Fly-ash, Silica Fume, Slag and Natural Pozzolans in Concrete, Trondheim, Norway, Vol. 1, 1989, pp. 331-348.

Bilodeau A. and Malhotra V.M., "Concrete Incorporating High Volumes of ASTM Class F Fly-ashes Mechanical Properties and Resistance to Deicing Salt Scaling and to Chloride-Ion Penetration," Proceedings of the Fourth International Conference on the Use of Fly-ash, Silica Fume, Slag and Natural Pozzolans in Concrete, Istanbul, Turkey, V.M. Malhotra, Ed., 1 (ACI Special Publication SP-132), 319-349 (1992).

Blomberg, Jason M., P.E. Laboratory Testing Of Bridge Deck Mixes. Tech. No. Rdt 03-004. 044th Ed. Vol. Ri101. Jefferson City: Missouri Department of Transportation Research, Development, and Technology, 2003. Print. Research Investigation.

Davis, Drew A. Effects of High Volume Fly-ash and Powder Activators on Plastic And Hardened Concrete Properties. Thesis. Missouri University of Science and Technology, 2012. N.P. Print.

Dhir, R.K., Jones, M.R. (1999): Development of Chloride–Resisting Concrete Using Fly-ash. *Fuel*, Vol. 78, No. 2 1999, pp. 137-142.

Federal Highway Administration. “Fly-ash.” *Fly-ash*. United States Department of Transportation, 7 Apr. 2007. <http://www.fhwa.dot.gov/infrastructure/materialsgrp/flyash.htm>.

G.M. Campbell, R.J. Detwiler “Development of mix designs for strength and durability of steam-cured concrete,” Concr. Int., 7 (1993), pp. 37–39.

Gebler, Steven H., and Paul Klieger. “Effect of Fly-ash on the Durability of Air-Entrained Concrete.” *International Concrete Abstracts Portal.* American Concrete Institute, 1 Feb. 1986. Web.

Gjorv, O. E., Tan, K., and Monteiro, P. J. M., "Effect of Elevated Curing Temperature on the Chloride Permeability of High-Strength Lightweight Concrete," *Cement, Concrete, and Aggregates,* CCAGPD, Vol. 16, No. 1, June 1994, pp. 57-62.

Goto, S., and Roy, D.M., *Diffusion of Ions through Hardened Cement Pastes*, Cement and Concrete Research, Vol. 11, 751-759, 1981.

Hadchti, K. M., and Carrasquillo, R. L. (1988). ‘‘Abrasion resistance and scaling resistance of concrete containing fly-ash.’’ Research Rep.481–3, Center for Transportation Research, Bureau of Engineering Research, Univ. of Texas at Austin, Austin, Tex.

Haque, M. N., Kayyali, O. A., and Gopalan, M. K., “Fly-ash Reduces Harmful Chloride Ions in Concrete,” *ACI Materials Journal*, Vol. 89, No. 3, May–June 1992, pp. 238–241.

Headwaters Resources. Fly-ash Increases Resistance to Freezing & Thawing. South Jordan: Headwaters Resources, n.d. Technical Bulletins. Web. <http://flyash.com/resource-library/tech-bulletins/>.

Helmuth, R., *Fly-ash in Cement and Concrete,* Portland Cement Association, Skokie, IL, 1987.

Kaburu, Allan Mugambi, J. W. Kaluli, and C. K. Kabubo. "Use of the Maturity Method in Quality Control of Concrete: A Review." *Proceeding of the Sustainable Research and Innovation (SRI) Conference* 6-8 May 2015: 264-66. Web.

Kjellsen, K.O., Detwiler, R.J., Gjorv, O.E., Pore Structure of Plain Cement Pastes Hydrated at Different Temperatures, Cem. Concr. Res. 20(6) (1990) 927–933.

Kaur, I., Umer, F., and Harshdeep, S., “Mechanical Properties of High Volume Fly-Ash (HVFA) Concrete Subjected to Elevated Temperatures Up to 120°C.” *Proceeding of the National Conference on Geo Technical and Geo Environmental Aspects of Wastes and Their Utilization in Infrastructure Projects (GGWUIP 2013)* February 2013.

Khayat, Kamal H., Dr. *Sustainability in Concrete.* Ppt. ed. N.p.: n.p., 2014. Print.

Knutsson, Anna. "Freeze/Thaw Durability of Concrete with Fly-ash." (2010): 22-42.

Chalmers University of Technology. Web. <http://publications.lib.chalmers.se/records/fulltext/135847.pdf>.

Krivenko, Pavel V., and Della Roy. "Durability of Alkali-Activated Cements and Concretes." *Alkali-Activited Cements and Concretes*. By Caijun Shi. New York: Taylor & Francis, 2006. 76. Print.

Lamond, Joseph F., and J.H. Pielert. “Chapter 24: Chemical Resistance of Concrete.” *Significance of Tests and Properties of Concrete and Concrete-making Materials.* Philadelphia, PA: ASTM, 2006. 257-61. Print.

Langan, B. W., M. A. Ward, and K. Weng. "Effect of Silica Fume and Fly-ash on Heat of Hydration of Portland Cement." Cement and Concrete Research, 15 Feb. 2002. Web.

Langan B.W., Joshi R.C. and Ward M.A., "Strength and Durability of Concrete Containing 50% Portland Cement Replacement by Fly-ash and Other Materials," Canadian Journal of Civil Engineering, 17, 19-27 (1990).

Liu, Baoju, Youjun Xie, and Jian Li. "Influence of Steam Curing on the Compressive Strength of Concrete Containing Supplementary Cementing Materials." Cement and Concrete Research 35.5 (2005): 994-98. Science Direct. Web.

Malhotra, V. M. "Global Warming, and Role of Supplementary Cementing Materials and Superplasticizers in Reducing Greenhouse Gas Emissions from the Manufacturing

of Portland Cement." *IJSTRUCTE International Journal of Structural Engineering* 1.2 (2010): 116. Web.

Malhotra, V.M., Ramezanianpour (1994): *Fly-ash in concrete*. CANMET, Ottawa, 307 pp.

Mehta, P. Kumar, and Paulo J. M. Monteiro. *Concrete: Microstructure, Properties, and Materials.* New York: McGraw-Hill, 2006. Print.

Mindess, S., Young, J. F., & Darwin, D. (2003). Concrete. Prentice Hall.

Mohamed, Heba A. "Effect of Fly-ash and Silica Fume on Compressive Strength of Self-Compacting Concrete under Different Curing Conditions." *Ain Shams Engineering Journal 2.2* (2011): 79-86. Print.

Mohsen, J.P., Roach, B.L., and Kessinger, D.T. (2004). "Maturity Method Applied to Highway Construction," *Transportation Research Record*, Washington, D.C., pp. 79-85.

Myers, J. J. (2000). *The Use of Maturity Method as a Quality Control Tool for High Performance Concrete Bridge Decks*. PCI / FHWA / FIB International Symposium on High Performance Concrete.

Myers, J.J., and Carrasquillo (1998), R.L. Production and Quality Control of High Performance Concrete in Texas Bridge Structures. Center for Transportation Research Bureau of Engineering Research, the University of Texas at Austin, Report No. 9-580/589-1.

Myers, J.J., Hernandez, E.S., Griffin, A., and Alghazali, H. (2014), *Self-Consolidating Concrete (SCC) and High-Volume Fly Ash Concrete (HVFAC) for Infrastructure Elements: Implementation*. Washington: U.S. U.S. Department of Transportation. August 2014. Report NUTC315. Project No. 00040350.

Naik, T.R., and Singh, S.S., "Effects of Inclusion of Fly-ash on Abrasion Resistance of Concrete," *Proceedings of the Second CANMET/ACI Conference on Durability of Concrete*, Montreal, Canada, Supplementary Paper, August 1991, pp. 683-707.

Naik, T.R., and Ramme, B.W., "Freezing and Thawing Durability of High-Lime Content Class C Fly-ash Concrete," *Proceedings of the Second CANMET/ACI International Conference on Durability of Concrete*, Montreal, Quebec, Canada, V.M. Malhotra, Ed. August 1991, pp. 615-641.

Naik, Tarun R., and Shiw S. Singh. Performance of High-Volume Class C Fly-ash Concrete Systems Under Freezing and Thawing Environment. Rep. No. Rep-225. N.P.: Department of Civil Engineering and Mechanics College of Engineering and Applied Science. University of Wisconsin - Milwaukee, 1994. Print.

Naik, Tarun R., Shiw S. Singh, and Mohammad M. Hossain. Abrasion Resistance of High-Strength Concrete Made with Class C Fly-ash. Rep. N.p.: Center for By-Products Utilization U of Wisconsin-Milwaukee, n.d. Print.

"National Oceanic and Atmospheric Administration " *NOAA*. N.p., n.d. Web. 4 June 2015. <http://www.noaa.gov/>.

Neville, A.M (2003): *Properties of Concrete*. Pearson Education Limited, Edinburgh, 844 pp.

Ozyildirim, Celik, Ph.D. Effects of Temperature on The Development of Low Permeability in Concretes. Publication. Vtrc Ed. Vol. 98. Charlottesville: n.p., 1998. Print. R14.

Papenfus, Dr. *Abrasion Wear, Abrasion Resistance, and Related Strength Characteristics in Concrete, with Special Reference to Concrete Pavers*. Thesis. University of Witwatersand, Johannesburg, 2002. N.p.: n.p., n.d. *Dams for Africa*. Web.

Pitroda, Jayeshkumar R., and F. S. Umrigar, Dr. "Evaluation of Modulus of Elasticity of Concrete with Partial Replacement of Cement by Thermal Industry Waste (Fly-ash) and Paper Industry Waste (Hypo Sludge)." *International Journal of Engineering Science and Innovative Technology (IJESIT)* 2.1 (2013): 133-38. Web.

Portland Cement Association. "Durability." *Concrete Thinking for a Sustainable World* <http://www.concretethinker.com/solutions/durability.aspx>.

Portland Cement Association, *Survey of Mineral Admixtures and Blended Cements in Ready Mixed Concrete,* Portland Cement Association, 2000, 16 pages.

Portland Cement Association, *Survey of Mineral Admixtures and Blended Cements in Ready Mixed Concrete,* Portland Cement Association, 1988.

Rohne, Ryan J., and Bernard Igbafen Izevbekhai. *Demonstration of Concrete Maturity Test Process on TH-694/ TH-35E Interchange – Unweave the Weave*. Rep. no. MN/RC 2009-26. St. Paul: Minnesota Department of Transportation Research Services Section, 2009. *Local Road Research Board*. Web.

Shamsai, Abolfazl, Saber Peroti, Kamal Rahmani, and Loghman Rahemi. "Effect of Water-Cement Ratio on Abrasive Strength, Porosity and Permeability of Nano-Silica Concrete." *World Applied Sciences Journal* 17.8 (2012): 929-33. Web.

Sustainable Sources. "Flyash Concrete." N.p., 2014. <http://flyash.sustainablesources.com/#Define>.

Tanesi, Jussara, Benjamin Graybeal, P.E., and Marcia Simon, P.E. Durability of Ultra-High Performance Concrete. U.S.A.: Federal Highway Administration, 2004 Print.

Tattersall, G.H., and P.F.G. Banfill, *The Rheology of Fresh Concrete*, Pitman Advanced Publishing Program, Vol. xii, p. 356, 1983.

Upadhyaya, Sushant. "Step by Step Procedure for Optimizing the Design of HVFA Mixtures." *Early Age Strength Prediction for High Volume Fly-ash Concrete Using Maturity Modeling*. Ann Arbor: ProQuest LLC, 2009. 105-115. Print.

Ukita K., Shigematsu S., and Ishii M., "Improvement in the Properties of Concrete Utilizing Classified Fly-ash," Proceedings of the Third International Conference on the Use of Fly-ash, Silica Fume, Slag and Natural Pozzolans in Concrete, Trondheim, Norway, V.M. Malhotra, Ed., 1 (ACI Special Publication SP-114), 219-240 (1989).

Verbeck, George J.; Helmuth, Richard H.; "Structures and Physical Properties of Cement Paste," Proceedings of the 5th International Symposium of the Chemistry of Cement, Tokyo 1968, pp. 1-32.

Volz, J., Myers, J., Richardson, D., Arezoumandi, M., Beckemeier, K., Davis, D., Tucker, B. (2012). *Design and Evaluation of High-Volume Fly Ash (HVFA) Concrete Mixes* (Report cmr 13-008). Missouri University of Science and Technology, Rolla, Missouri.

W. Ma, C. Liu, P.W. Brown, S. Komarneni, Pore structure of fly-ashes activated by $Ca(OH)_2$ and $CaSO_42H_2O$, Cem. Concr. Res. 25 (2) (1995) 425–427.

Y. Maltais, J. Marchand, Influence of curing temperature on cement hydration and mechanical strength development of fly-ash mortars, Cem. Concr. Res. 27 (7) (1997) 1009–1020.

Yazıcı Halit, Serdar Aydın, Hüseyin Yiğiter, and Bülent Baradan. "Effect of Steam Curing on Class C High-volume Fly-ash Concrete Mixtures." *Cement and Concrete Research* 35.6 (2005): 1122-1127. *Science Direct*. Web.